universität wien

MASTERARBEIT / MASTER'S THESIS

Titel der Masterarbeit / Title of the Master's Thesis

„Focused genetic and pharmacologic targeting of hyperactive JAK/STAT targets reveals new therapy options in T-ALL "

verfasst von / submitted by

Valerie Magdalena Klaus, B.Sc.

angestrebter akademischer Grad / in partial fulfilment of the requirements for the degree of

Master of Science (MSc)

Wien, 2023/ Vienna, 2023

Studienkennzahl lt. Studienblatt / degree programme code as it appears on the student record sheet:	UA 066 830
Studienrichtung lt. Studienblatt / degree programme as it appears on the student record sheet:	Masterstudium Molecular Microbiology, Microbial Ecology and Immunobiology
Betreut von / Supervisor:	Univ.-Prof. Dipl.-Ing. Dr.rer.nat. Richard Moriggl

Acknowledgements

I would like to express my heartfelt thanks to Prof. Dr. Richard Moriggl for the opportunity to work on this interesting project. I am very grateful for the support, feedback, and scientific input that he and his lab members provided me.

My gratitude also goes to Dr. Heidi Neubauer for allowing me to work on the project and for her time, feedback, and expertise throughout.

A monumental thank you to my supervisor Christina Wagner. Words truly cannot express how eternally grateful I am for your time, support, and trust in me. Thank you for your patience when teaching me new methods and techniques and for answering all my questions. Thank you for encouraging me to follow my ideas and helping me build confidence in myself and my abilities. Lastly, I thank you for all the talks; you have truly been the best supervisor!

I would also like to thank Gabriele Manhart and the entire Grebien Lab for allowing me to work in their lab, teaching me new techniques and methods and always helping in times of need.

Thank you also to the entire laboratory team. I really enjoyed working with all of you, and I am very grateful to you for always lending a helping hand.

I also would also like to thank Prof. Dr. Thomas Decker from the University of Vienna for his role as an expert during the master's thesis registration process.

Finally, I would like to thank my family for always supporting me, encouraging me and cheering me on. Without your love and support, this milestone would not have been possible.

Table of contents

1 Introduction

1.1 JAK/STAT pathway

1.1.1 JAKs and STATs

Cells depend on stimuli from their environment for development and survival. Information from the environment must pass through the cell membrane to elicit an appropriate response such as a change in enzymatic or ion channel activity or a change in gene expression. Most stimuli, such as cytokines, cannot pass through the cell membrane unhindered and thus must rely on a complex network of signal transduction pathways (Berg et al., 2008).

The Janus kinase (JAK)/Signal transducer and activator of transcription (STAT) pathway is a key pathway downstream of cytokine signalling (Berg et al., 2008). The cytokine superfamily consists among others of interferons, interleukins, and colony-stimulating factors (Imada & Leonard, 2000; Leonard & O'Shea, 1998). Cytokine signalling is important for biological responses linked to cell growth, differentiation, apoptosis, haematopoiesis, and immune response (Berg et al., 2008). Interleukin-2 (IL-2), for instance, signals through the JAK/STAT pathway to alter the gene programme and determine T-cell fate (Ross & Cantrell, 2018).

The cytokine signal is transmitted through the membrane via transmembrane proteins (cytokine receptors) that are associated with JAKs. As tyrosine kinases, the JAKs can transmit information by means of phosphorylation (Berg et al., 2008). The JAK family comprises four members: JAK1, JAK2, JAK3, and TYK2 (Leonard & O'Shea, 1998). The signal is further transduced through the kinase activity of the JAKs to the STAT proteins. The STAT protein family has seven members: STAT1, STAT2, STAT3, STAT4, STAT5A, STAT5B, and STAT6. The STAT proteins are transcription factors (TF) that translocate to the nucleus to prompt a change in gene expression upon activation (Imada & Leonard, 2000; Leonard & O'Shea, 1998).

1.1.1.1 Structure of JAK

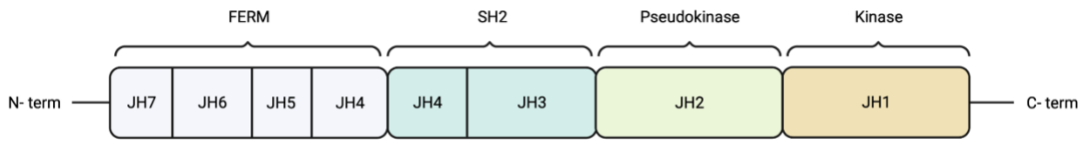

Figure 1: *Structure of the JAK family of protein tyrosine kinases. (Figure created with BioRender.com)*

Seven JAK homology (JH) domains compose the structure of the JAKs (**Figure 1**). The parallel of the tandem of pseudokinase (JH2) and kinase (JH1) domains to the roman "two-faced" god gives rise to the name of the Janus kinase family of protein tyrosine kinases (Leonard & O'Shea, 1998). The JH1 at the carboxyl terminus has a tyrosine kinase activity. The adjacent JH2 domain is homologous to a protein kinase however its function has not yet been entirely resolved (Berg et al., 2008; Bousoik & Montazeri Aliabadi, 2018). Nevertheless, evidence suggests that this pseudokinase has ATP-binding activity (Min et al., 2015), a low-level kinase activity (Ungureanu et al., 2011), and also an auto-inhibitory activity to negatively regulate the JH1 domain (Saharinen et al., 2000). The Src homology 2 (SH2) domain (JH3 and 4) enables the JAKs to bind the phosphotyrosine on other proteins (Berg et al., 2008). Lastly, the four-point-one, ezrin, radixin, moesin (FERM) domain helps to anchor the JAKs to the cytoplasmic site of the receptor and can be found at the amino terminus of the protein (Berg et al., 2008; Bousoik & Montazeri Aliabadi, 2018).

1.1.1.2 Structure of STAT

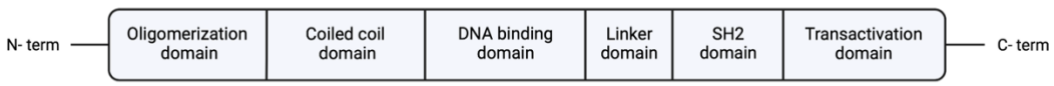

Figure 2: *Structure of the STAT proteins. (Figure created with BioRender.com)*

The STAT proteins consist of six functional domains (**Figure 2**). Like the JAKs, the STAT proteins have an SH2-domain which is important for their association with the cytokine receptors but also for homo- or heterodimerization (Imada & Leonard, 2000). Differences within the SH2-domain account for STATs binding to different cytokine receptors (Mikita et al., 1998). A conserved tyrosine between the SH2-domain and the transactivation domain (TAD) at the carboxyl terminus can be subjected to phosphorylation and is needed for the parallel dimerization and activation of STAT proteins (Awasthi et al., 2021; Leonard & O'Shea, 1998). The TAD and the DNA binding domains are important for the STAT's activity to modulate gene expression. The DNA binding domain of the STAT proteins recognizes and interacts with specific DNA sequences: the IFN-stimulated response elements (ISRE; Horvath & Darnell, 1997) and γ-IFN activated sequences (GAS) motifs (Lew et al., 1991). The TAD is required for transcriptional activation; however, the different STAT proteins show subtle differences within this domain (Leonard & O'Shea, 1998). The TAD of STAT2, for instance, interacts with transcriptional co-activators to modulate gene expression (Bhattacharya et al., 1996; M. Huang et al., 2002). The TAD of STAT1, STAT3, and STAT4, on the other hand, have a conserved serine residue whose phosphorylation is important for the protein's activity (Cho et al., 1996; Wen et al., 1995). The coiled coil domain promotes the binding to other TF and co-activators but is also involved in the nuclear translocation of the STAT proteins via a nuclear localization signal (NLS; Awasthi et al., 2021). Lastly, the oligomerization domain at the amino terminus of the proteins is implicated in the oligomerization of STAT dimers to form homo- and heterotetramers which was shown for all STAT proteins except STAT2 (Delgoffe & Vignali, 2013a; Imada & Leonard, 2000; Mitchell & John, 2005).

1.1.2 Signal transduction in the JAK/STAT pathway

A schematic description of the JAK/STAT pathway is illustrated in **Figure 3**. The docking of cytokines to the membrane-associated receptors induces receptor dimerization. Through dimerization, the receptor-associated JAKs come into proximity, allowing cross-phosphorylation. The kinase domain of the JAKs allows the

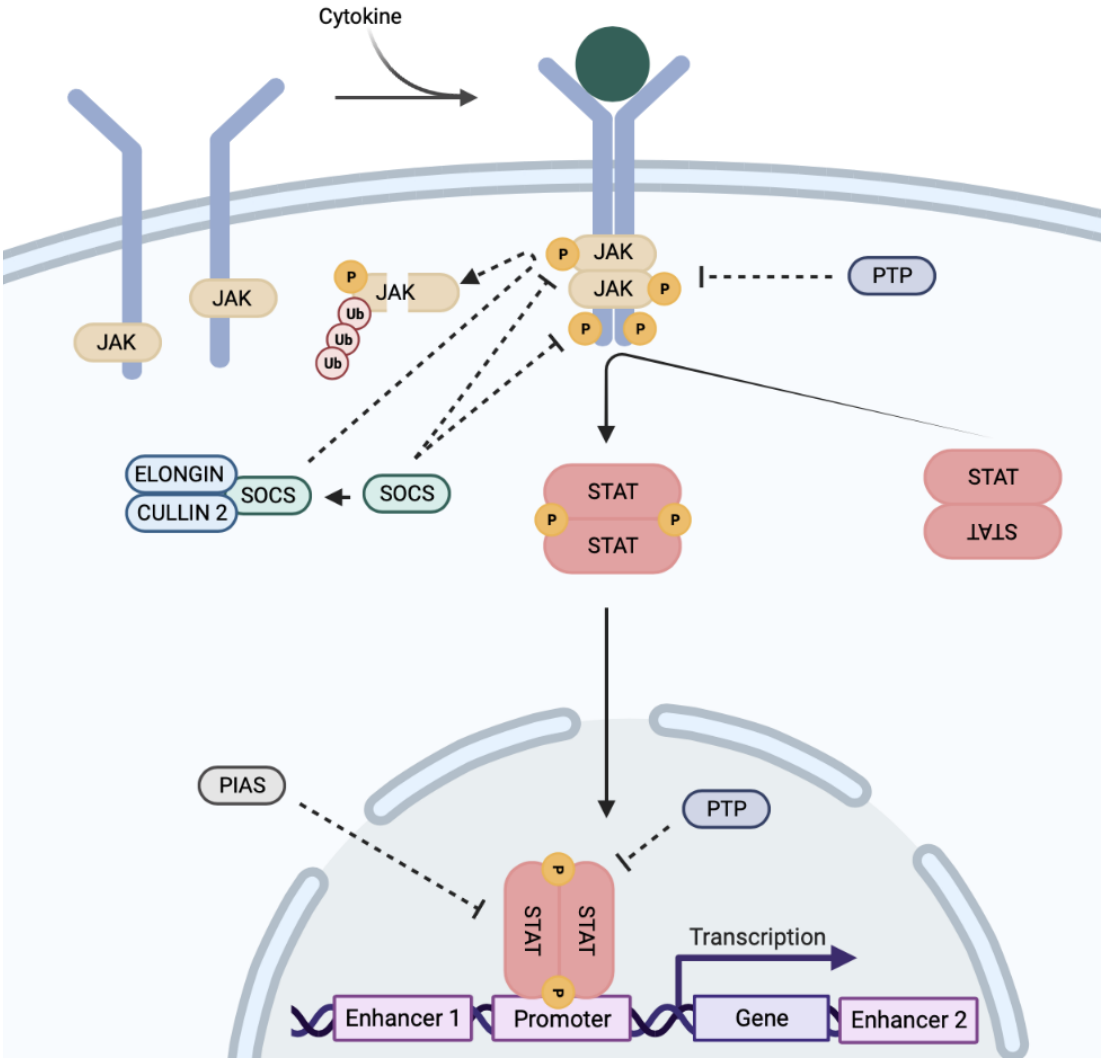

Figure 3: *Cytokine signals from the extracellular environment activate the JAK/STAT pathway through interaction with membrane-associated receptors. Receptor-associated JAKs transduce the signal through tyrosine phosphorylation to STAT TFs. Activated STATs form parallel dimers then translocate to the nucleus upon phosphorylation to modulate gene expression. Protein tyrosine phosphatases (PTP), PIAS and SOCS proteins are negative regulators of the JAK/STAT pathway. (Figure created with BioRender.com)*

transfer of a phosphoryl group to a tyrosine residue (Berg et al., 2008). Tyrosine residues in the cytoplasmic side of the receptor are phosphorylated by activated JAKs, creating a docking site for the STAT proteins (Bousoik & Montazeri Aliabadi, 2018). STATs can bind the phosphorylated tyrosine on the receptor with their SH2-domain (Imada & Leonard, 2000). Upon docking to the receptors, the JAKs phosphorylate a

conserved tyrosine residue of the STATs. Inactivated STATs dimers have an anti-parallel conformation but phosphorylation of the STAT proteins allows parallel homo- or heterodimerisation by bivalent interactions (Bousoik & Montazeri Aliabadi, 2018). Whether a homo- or heterodimerization occurs is dependent on the specificity of the SH2-domain and the microenvironment (Leonard & O'Shea, 1998). Over 50 different cytokines signal through the JAK/STAT pathway which, however, consists of a limited number of signalling proteins. The variation between homo- or heterodimerization might be a possible mechanism to increase the number of combinations and thus modify signals (Delgoffe & Vignali, 2013). Parallel-dimerized and activated STAT proteins translocate to the nucleus via importins to modulate gene expression (Bousoik & Montazeri Aliabadi, 2018).

Homeostasis within the cell must be ensured and therefore several mechanisms negatively regulate the activity of the JAK/STAT pathway. Firstly, protein inhibitors of activated STAT (PIAS) and suppressors of cytokine signalling (SOCS) proteins can inhibit STAT signalling directly through a negative feedback loop (Bousoik & Montazeri Aliabadi, 2018; Imada & Leonard, 2000; Leonard & O'Shea, 1998). SOCS proteins are direct target genes of activated STAT TFs and thus STAT activity leads directly to the expression of inhibitory factors. The SOCS proteins possess an SH2-domain with which they bind to phosphorylated JAKs and cytokine receptors; hence, physically blocking further signal transduction. Additionally, SOCS proteins can form a complex with CULLIN 2 and the ELONGIN BC complex which facilitates ubiquitin-dependent degradation of JAKs (Rawlings et al., 2004). PIAS proteins have a carboxyl domain and a conserved SAF-A/Acinus/PIAS (SAP) domain which allows binding to activated STAT TFs and inhibiting their DNA binding activity (Rawlings et al., 2004). A second method for PIAS to inhibit STAT activity is the recruitment of transcriptional co-repressors, such as histone deacetylase 1, to STAT target genes. Also, PIAS proteins have a small ubiquitin-like modifier (SUMO)-E3-ligase activity, that helps to regulate sub-nuclear protein localization, protein-protein interactions, protein stability, and transcription factor activity (Heppler & Frank, 2017). Another reported mechanism for JAK/STAT signal regulation is the ubiquitin/proteasome-mediated degradation of

STAT1 (T. K. Kim & Maniatis, 1996). Furthermore, truncated forms lacking a C-terminal region for STAT1 and STAT5 have been revealed that act as dominant suppressors (Caldenhoven et al., 1996; D. Wang et al., 1996). Lastly, dephosphorylation of the respective activation residues by phosphatases also results in the loss of JAK/STAT signalling (Haspel et al., 1996). For instance, the receptor tyrosine phosphatase CD45 can inhibit signalling by dephosphorylating the JAKs (Hermiston et al., 2003). Furthermore, the protein tyrosine phosphatase (PTP) SHP-2 dephosphorylates STAT5 but also STAT3 (Y. Chen et al., 2003; M. Kim et al., 2018; C. L. Yu et al., 2000). Moreover, STAT3 can also be dephosphorylated by PTP receptor-type D or T (PTPRD, PTPRT; M. Kim et al., 2018). Dual-specificity phosphatases (DUSP), on the other hand, can dephosphorylate serin and tyrosine residues; STAT5 can be regulated by DSUP4 while STAT3 can be regulated by DSUP3 (Hsiao et al., 2015; B. R. Kim et al., 2020).

1.2 Characteristics and Functions of STAT5

The STAT5 proteins are implicated in the proliferation, differentiation, and apoptosis of hematopoietic cells (Nosaka et al., 1999). Cytokine signals activating JAK1, JAK2 and JAK3 can transmit their signal to the STAT5 proteins by phosphorylating either tyrosine residue 694 on STAT5A or tyrosine residue 699 on STAT5B (Bousoik & Montazeri Aliabadi, 2018; Brachet-Botineau et al., 2020; Schaller-Schönitz et al., 2014). Upon activation, the STAT5 proteins translocate to the nucleus to modulate gene expression; targeting genes such as *MYC*, *BCL2L1*, and *PIM1* (Lord et al., 2000; Nosaka et al., 1999).

The STAT5A and STAT5B proteins are over 90% conserved at the amino acid level and share many functions but also have distinct roles (Hennighausen & Robinson, 2008). The conserved nature of the STAT5 proteins suggests possible redundant roles; in fact, a chromatin immunoprecipitation assay with sequencing (ChIP seq) experiment in $CD4^+$ T-cells revealed overlapping binding profiles. However, the ChIP

seq data also showed distinct binding sites for STAT5A and STAT5B (Kanai et al., 2014). Subtle differences in the DNA-binding, the C- and N-terminal domains or interactions with co-activators may cause the distinct binding properties of the two proteins. Complete knock-out of *Stat5a* and *Stat5b* in mice is embryonic lethal. However, few mice survive the complete knock-out of both Stat5 proteins, and the surviving mice failed to develop $CD8^+$ or γδ T-cells, indicating the critical role of Stat5 in T-cell development and homeostasis (Hoelbl et al., 2006). A single intact allele of either *Stat5a* or *Stat5a* rescues mice from embryonic lethality, indicating a compensatory role of the two proteins, as suggested by the ChIP seq data. One-allele *Stat5a* and *Stat5b* deficient ($Stat5a^{+/-}Stat5b^{+/-}$) and two-allele *Stat5b* deficient ($Stat5a^{+/+}Stat5b^{-/-}$) mice showed a decreased white blood cell count (Villarino et al., 2016), while mice with a two-allele *Stat5a* knock-out ($Stat5a^{-/-}Stat5b^{+/+}$) lacked hematopoietic deficiencies (X. Liu et al., 1997; Villarino et al., 2016). Stat5b deficiency in mice led to lower levels of $CD8^+$, $CD4^+$ as well as $CD4^+$ regulatory T-cells, implying and reinforcing the more dominant role of STAT5B in effector and regulatory T-cell immunity (Villarino et al., 2016). STAT5A, on the other hand, has a more important role in mammary gland development (X. Liu et al., 1997; Udy et al., 1997).

1.2.1 JAK1/3 and STAT5 in T-cell development

T-cells undergo a maturation process from hematopoietic stem cells (HSC) to mature T-cells that can participate in the immune response (**Figure 4**). Checkpoints and several selection processes thereby ensure the correct development of antigen receptors and T-cells. Maturation and migration of T-cells are governed by extracellular signals such as cytokines and chemokines leading to the activation of transcriptional factors within the cell. HSCs differentiate into common lymphoid progenitors in the bone marrow which migrate with the help of chemokines to the thymus where the maturation process takes place. Activation of the transcriptional regulators NOTCH1 and GATA3 leads to the commitment of the common lymphoid progenitor to the T-cell lineage. Moreover, the expression of CD44 and CD25 on the cell surface marks the transition from committed T-cell progenitors to pro T-

lymphocytes. Pro T-lymphocytes express neither CD4 nor CD8 (double negative), and this stage is characterized by the rearrangement of the β-chain of the TCR. Successful TCRβ$^+$ T-cells are selected, and a checkpoint must be passed before the recombination and selection of the TCR α- chain can begin in CD4$^+$ CD8$^+$ (double positive) cells. T-cells have to pass a second checkpoint with a successfully arranged TCRαβ complex before functional TCRs are selected. A second T-lymphocyte lineage can develop from the T-cell progenitor distinguished by the TCRγδ instead of the TCRαβ complex. During the following TCR selection process, double positive (DP) T-cells transition into single positive (SP) T-cells: cells recognizing the major histocompatibility complex (MHC) class I differentiate to CD8$^+$ CD4$^-$ T-cells, and cells recognizing MHC class II differentiate to CD4$^+$ CD8$^-$ T-cells. Additionally, cells recognizing self-antigen either die or differentiate into regulatory T-cells. Lastly, mature T-cells leave the thymus to circulate in the peripheral tissues (Abbas et al., 2021).

During the maturation process in the thymus, a diverse repertoire of antigen receptors must be generated by creating a large pool of T-cells. Thymic stromal cells secrete interleukin-7 (IL-7) to promote T-cell proliferation. Mature T-cells in the peripheral tissues, on the other hand, can be activated upon antigen recognition, leading to the expression of the cytokine interleukin-2 (IL-2) as well as its receptor. The binding of IL-2 or IL-7 to its receptor activates the JAK/STAT pathway leading to an altered transcriptional program promoting cell growth, survival, proliferation, and differentiation (Abbas et al., 2021). Both cytokines stimulate the activation of JAK1 and JAK3, leading to downstream activation of the STAT5 proteins (Miyazaki et al., 1994; Russell et al., 1994). Burchill et al. showed that activated STAT5 leads to increased levels of pro T-cells in the thymus as well as of mature αβ, γδ and NK T-cells (Burchill et al., 2003). Furthermore, mice with an inactivating Stat5b mutation showed normal lymphoid development but decreased levels of single positive CD4$^+$ and CD8$^+$ T-cells as well as decreased levels of peripheral T-cells. Additionally, these T-cells showed the morphology of activated T-cells, a phenotype consistent with mice lacking the IL-2 receptor. This indicates the importance of the IL-2/JAK1/3/STAT5-

axis for the proliferation and survival of T-cells (Moriggl et al., 1999). Studies also revealed MYC, which promotes proliferation, and BCL-xL, which has anti-apoptotic functions, as STAT5 targets, supporting the above findings (De Groot et al., 2000; Lord et al., 2000).

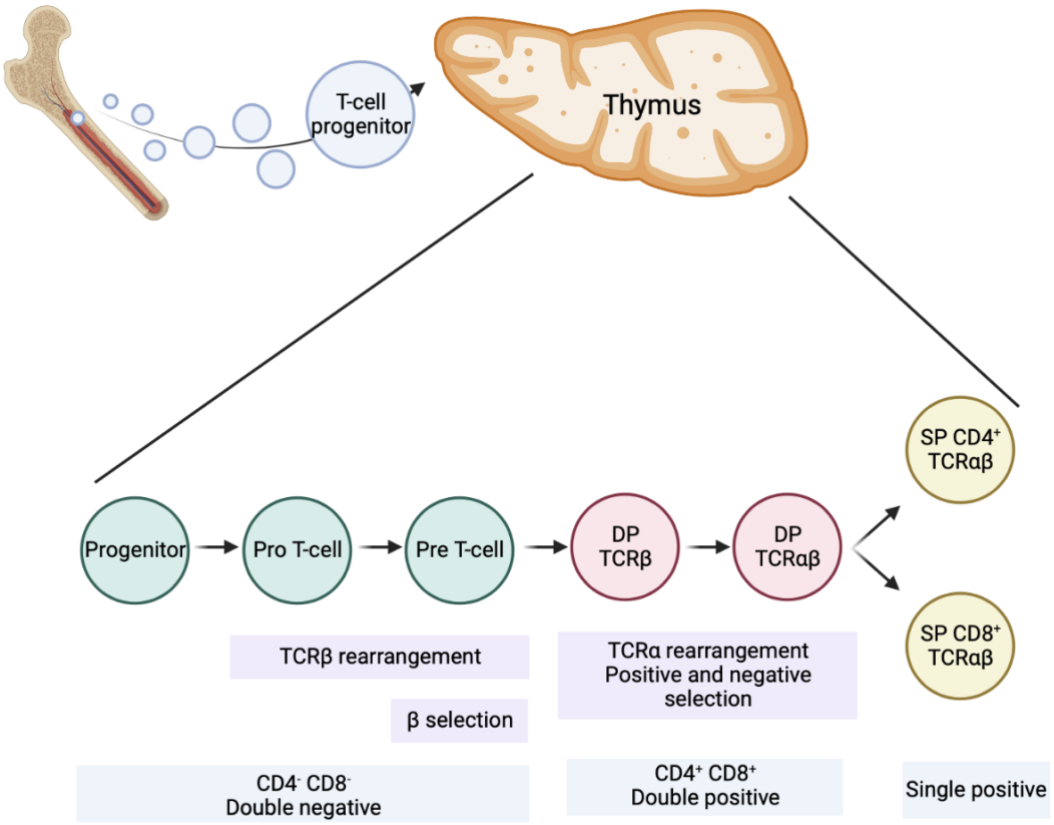

Figure 4: *T-cell maturation begins in the bone marrow with hematopoietic stem cells (HSC) which mature to T-cell progenitors that migrate to the thymus. In the thymus, several checkpoints and selection steps ensure the correct formation and functionality of the T-cell receptor (TCR). Naive single positive $CD4^+$ or $CD8^+$ T-cells leave the thymus to circulate the peripheral tissues (Figure created with BioRender.com).*

1.2.2 STAT5 hyperactivation in cancer

The JAK/STAT pathway is involved in a great number of biological functions, among them proliferation, cell survival and apoptosis; hence, abnormal activity of the pathway

often leads to diseases such as cancer (Berg et al., 2008). Continuous hyperactivation of STAT5 is associated with cell survival, self-renewal and proliferation (Bar-Natan et al., 2012), processes defined as hallmarks of cancer as described by Hanahan & Weinberg (Hanahan & Weinberg, 2011). The hyperactivation of STAT5 can either be due to upstream deregulation of JAK signalling, or other oncogenic kinases, or due to mutations within *STAT5B* itself (Bandapalli et al., 2014; Rane & Reddy, 2000). Mutations in the *JAK1* and *JAK3* genes were documented for several hematologic malignancies with a high prevalence in T-cell acute lymphoblastic leukaemia (T-ALL; Flex et al., 2008; Vicente et al., 2015). Sequencing of T-ALL samples showed that JAK3 is mutated in 16% of cases and the most frequently found mutation was the gain of function (GOF) mutation $JAK3^{M511I}$. The GOF mutation leads to hyperactivation of the JAK3 protein and thus to increased downstream STAT5 signalling. This hyperactivation of JAK3 is further increased by the accumulation of a second mutation such as $JAK3^{A572T}$ (Degryse et al., 2018). However, STAT5 signalling is also activated by other oncogenic kinases such as BCR-ABL and FLT3- internal tandem duplication (ITD). *BCR-ABL* is a chimeric fusion gene leading to the expression of a constitutively active tyrosine kinase able to phosphorylate and thus activate STAT5. The oncogenic kinase BCR-ABL is linked to acute lymphoblastic leukaemia (ALL) but also chronic myeloid leukaemia (CML), and the activation of STAT5 is thereby crucial to uphold BCR-ABL-driven leukaemias (Hoelbl et al., 2010). FLT3 is also a tyrosine kinase and ITD mutations in this kinase are found in 20% of acute myeloid leukaemia (AML) patients (Choudhary et al., 2007). The oncogenic activation of FLT3 due to ITD mutations also leads to the JAK-independent activation of STAT5 (Nakao et al., 1996). In summary, several oncogenic factors upstream of STAT5 can lead to its hyperactivation to promote cancer. But, as mentioned above, also mutations within the *STAT5* gene can lead to its continuous activation.

Several mutations in the STAT5B protein's SH2-domain have been identified, among them the GOF mutation $STAT5B^{N642H}$ which has been associated with STAT5B hyperactivation. This mutation has been detected in patients suffering from different hematopoietic malignancies such as T-ALL and T-cell prolymphocytic leukaemia (T-

PLL; Pham et al., 2018; Shahmarvand et al., 2018). A study by Pham et al. demonstrated that this mutation drives aggressive $CD8^+$ T-cell lymphoma/leukaemia in a transgenic mouse model, and *in vivo* mouse transplant experiments revealed that the $STAT5B^{N642H}$ mutation also drives γδ T-cell transformation (de Araujo et al., 2019; Pham et al., 2018). Moreover, in humans the presence of this mutation is associated with higher relapse rates in T-ALL patients (Bandapalli et al., 2014). STAT5A, on the other hand, is very infrequently mutated in leukaemias with only two reported cases (Brachet-Botineau et al., 2020). Additionally, it was demonstrated that STAT5B, and not STAT5A, is required for BCR-ABL-driven leukaemia (Kollmann et al., 2019). However, a genetically engineered GOF mutation $STAT5A^{S710F}$ is able to induce a peripheral T-cell lymphoma-like phenotype in mice (Maurer et al., 2020; Moriggl et al., 2005; Onishi et al., 1998).

1.3 T-cell leukaemia and lymphoma

Leukaemias are cancers affecting white blood cells originating in the bone marrow. Leukaemias are divided into fast (acute) and slow (chronic) growing cancers. The main forms of leukaemia are AML, CML, ALL, and chronic lymphocytic leukaemia (CLL). Leukaemias make up about 3% of cancers, but about 33% of childhood cancers are leukaemias with ALL being the most common form (Buratovic & Jackson-Grusby, 2016). Lymphomas, on the other hand, are cancers originating in the lymphatic system. Lymphomas are also divided into two groups: Hodgkin's lymphomas differ from Non-Hodgkin's lymphomas by the presence of large and abnormal lymphocytes called Reed-Sternberg cells (Buratovic & Jackson-Grusby, 2016).

T-cell leukaemias and lymphomas are specifically derived from T-cells and include diseases such as cutaneous T-cell lymphoma (CTCL), peripheral T-cell lymphomas (PTCL), anaplastic large cell lymphoma (ALCL), and T-ALL (Varghese & Alsubait, 2022). The cause for T-cell transformation remains unknown for the most part;

however, hyperactivation of core cancer pathways such as JAK/STAT and NOTCH1 have been implicated in the development of T-cell cancers (Aifantis et al., 2008; Flex et al., 2008; Moriggl et al., 2005; Vainchenker & Constantinescu, 2013; Varghese & Alsubait, 2022; Vicente et al., 2015).

1.3.1 T-ALL

T-ALL accounts for 15% of childhood cases and about 25% of adult cases of ALL (Aifantis et al., 2008; Raetz & Teachey, 2016). T-ALL arises from maturational arrest of immature precursor T-cells, called thymocytes (**Figure 4**), and subsequent proliferation and survival of the transformed cells (Kroeze et al., 2020). T-ALL subtypes can be distinguished by the developmental stage at which the maturational arrest takes place. Several classification systems have been suggested and are in development; one classification is based on the presence of cytoplasmic (cy) or surface (s) CD3, or CD1a markers, leading to three T-ALL subtypes: early ($sCD3^-$, $CD1a^-$), thymic ($sCD3^{-/+}$, $CD1a^+$), and mature ($sCD3^+$, $CD1a^-$) T-ALL. Common mutations found in T-ALL can occur and co-occur with different prevalence in the different subtypes of T-ALL (Hoelzer et al., 2009; Shiraz et al., 2021; **Figure 5**). The transformation of the T-cells to form T-ALL has been linked to mutations in key thymocyte regulators such as NOTCH1, and the JAK/STAT pathway (Flex et al., 2008; Vainchenker & Constantinescu, 2013; Vicente et al., 2015; Weng et al., 2004). Abnormal NOTCH1 signalling has been detected in all T-ALL subtypes and was detected in more than 50% of T-ALL patients (Weng et al., 2004). Thymocytes express the NOTCH1 receptor which is stimulated by the ligands Delta-like and Jagged, expressed by the thymic cells. NOTCH1 stimulation is needed for the differentiation of T-cell progenitor cells to mature T-cells. In the absence of NOTCH1, progenitors differentiate into B-cells by default (Koch et al., 2008). High NOTCH1 expression is also detected in pre T-cells during TCR β-chain selection as well as for the subsequent checkpoint to transition to DP T-cells (E. Y. Huang et al., 2003). Activating mutations in the *NOTCH1* gene lead to constant signalling in T-ALL (Weng et al., 2004). A target gene of the NOTCH1 signalling pathway is *MYC*, a factor

involved in self-renewal, and differentiation of hematopoietic stem cells and in T-cell activation. MYC expression is increased in developing thymocytes and high levels of MYC are needed for the proliferation of leukemic T-cells in T-ALL (Palomero et al., 2006; R. Wang et al., 2011; A. Wilson et al., 2004).

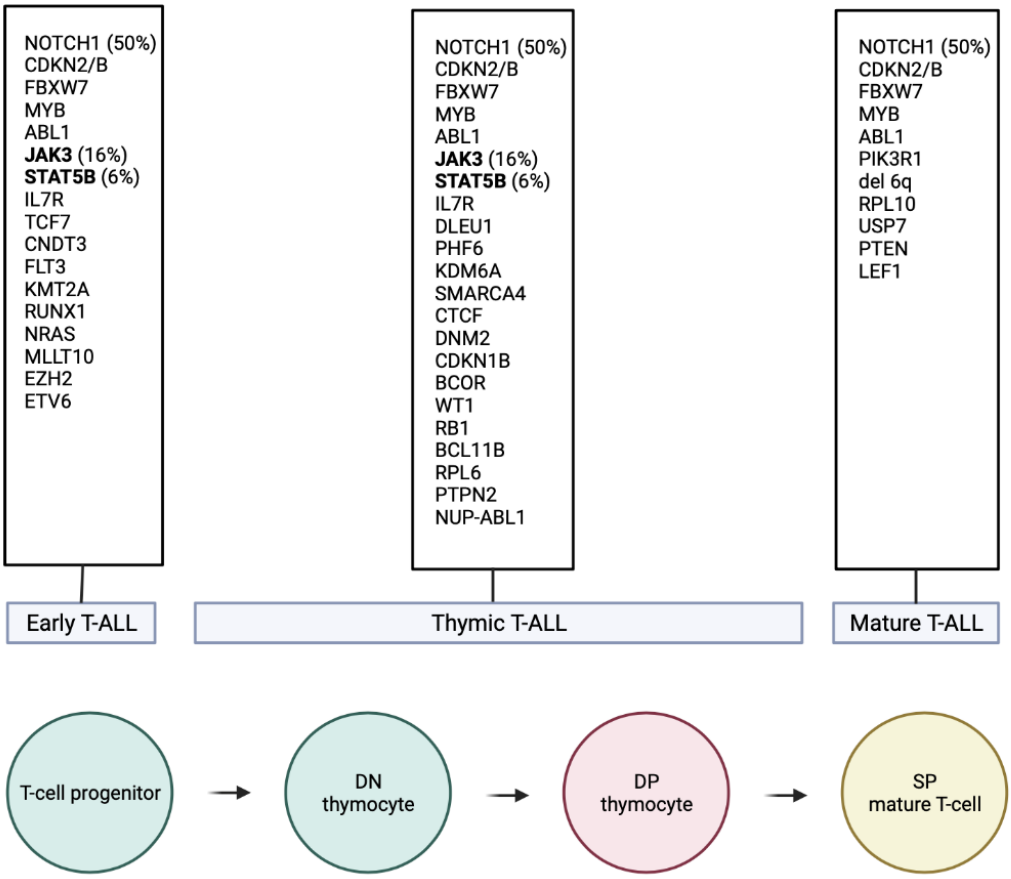

Figure 5: *T-ALL can be divided into subtypes: early (sCD3$^-$, CD1a$^-$), thymic (sCD3$^{-/+}$, CD1a$^+$) and mature (sCD3$^+$, CD1a$^-$) T-ALL. Several mutations leading to the transformation of immature T-cells have been identified, occurring and co-occurring in the subtypes. JAK3 and STAT5B mutations (bold font) are predominantly found in early and thymic T-ALL (Figure created with BioRender.com).*

High JAK3/STAT5B signalling is common in early and thymic T-ALL (**Figure 5**). As mentioned above, immature T-cells proliferate in the thymus when stimulated by IL-7 while mature T-cells proliferate upon stimulation with IL-2, and abnormal proliferation

is a hallmark of cancer (Abbas et al., 2021; Hanahan & Weinberg, 2011). Associated with the IL-7 or IL-2 receptors are the kinases JAK1 and JAK3 which are responsible to transduce the signal by phosphorylating downstream factors such as STAT5 (Miyazaki et al., 1994; Russell et al., 1994). 16% of T-ALL samples show a JAK3 mutation with a higher prevalence in early T-ALL of over 50% (Degryse et al., 2018; Vicente et al., 2015). The GOF mutation JAK3^{M511I} was thereby the most frequent, present in nearly 10% of samples (Vicente et al., 2015). The GOF mutation JAK3^{M511I} leads to continuous JAK3-signalling and downstream activation of factors such as STAT5 (Degryse et al., 2018). The *EZH2* gene, which encodes an H3K27-specific histone methyltransferase, can be mutated in early T-ALL but is also connected to JAK3. EZH2 as well as EED and SUZ12 are components of the polycomb repressive complex 2 (PRC2). Phosphorylation of EZH2 by JAK3 leads to its dissociation from PRC2 which in turn will decrease the levels of the polycomb heterochromatin marker H3K27me3, switching EZH2 to a transcriptional activator resulting in increased cell proliferation (W. Kim et al., 2013; Qi et al., 2012; Yan et al., 2016). Mutations in the *STAT5B* gene itself can also increase its transcriptional activity; the STAT5B^{N642H} mutation induces a 47-fold increase in transcriptional activity and has a prevalence of about 6% in T-ALL (Bandapalli et al., 2014; Kontro et al., 2013). Similar to NOTCH1 signalling, STAT5B activation also leads to the expression of MYC but also other pro-proliferation and pro-survival factors in leukemic cells (Lord et al., 2000). A more in-depth knowledge of hyperactive STAT5B target genes is needed to better understand the mechanisms of how T-cells transform due to JAK3/STAT5B deregulation. Insights into the mechanism might lead to new treatment options.

Typical treatment options for newly diagnosed T-ALL patients involve chemotherapy regimens for 2 - 3 years (Fattizzo et al., 2020; Raetz & Teachey, 2016). Patients treated with chemotherapy show a 5-year survival rate of above 70% (Möricke et al., 2016). In addition to chemotherapy, cranial radiation therapy (CRT) is also used to treat T-ALL. However, secondary malignancies due to CRT pose an additional burden on patients and thus efforts to eliminate this approach are underway, hence it is only used for high-risk patients (Fattizzo et al., 2020; Raetz & Teachey, 2016). Less than

20% patients relapse which mostly occurs within 2 years of diagnosis. The relapse rate depends on the treatment option and correlates with a lower survival rate of 25% (Fattizzo et al., 2020; Raetz & Teachey, 2016). Also, the STAT5B^{N642H} mutation correlates with a higher relapse rate (Bandapalli et al., 2014). Currently, hematopoietic cell transplantation is the only therapy strategy available for relapsed T-ALL patients. However, agents targeting the key disease drivers such as NOTCH1 or the JAK/STAT pathway are being investigated (Fattizzo et al., 2020; Raetz & Teachey, 2016). Overall, T-ALL is a rare disease for which no target therapies currently exist for patient treatment.

1.4 Preliminary data for the project

Hyperactivation of the STAT5 TF (via direct or upstream mutations) will lead to aberrant gene transcription and the potential activation of various oncogenic downstream pathways driving cancer. Understanding and mapping transcriptional changes induced by JAK/STAT hyperactivation may allow us to identify new vulnerabilities and therapeutic targets. Therefore, these changes were previously investigated in the lab by performing RNA sequencing (RNA seq) on cell lines modelling GOF JAK/STAT mutations.

1.4.1 Ba/F3 RNA seq

The murine pro-B cell line Ba/F3 is dependent on the cytokine murine interleukin-3 (mIL-3) and is therefore suitable and commonly used for the study of cytokine-induced pathways like the JAK/STAT pathway. Ba/F3 cell lines stably expressing the GOF mutations STAT5B^{N642H}, JAK3^{M511I}, or STAT5A^{S710F} were previously established in our lab and used to explore the transcriptional changes induced by these GOF mutations via RNA seq. The GOF mutations STAT5B^{N642H} or JAK3^{M511I} are often found in patients suffering from T-cell neoplasias (Pham et al., 2018; Vicente et al., 2015). The genetically engineered GOF STAT5A^{S710F} mutation, on the other hand, induces a

peripheral T-cell lymphoma-like phenotype in mice (Maurer et al., 2020; Moriggl et al., 2005; Onishi et al., 1998). Christina Wagner, MSc (University of Veterinary Medicine Vienna) starved the Ba/F3 GOF cell lines, the respective wild-type (wt) controls and the empty vector control (pMSCV) for 18 h of mIL-3, followed by a 1 h restimulation with 10 ng/ml mIL-3 to activate the JAK/STAT pathway. Additionally, the Ba/F3 cell lines carrying STAT5B^{N642H}, JAK3$^{M511I/wt}$, and STAT5A^{S710F} were transformed to be cytokine-independent through long-term culture without mIL-3. The RNA seq was then performed by the Next Generation Sequencing Facility at Vienna BioCenter Core Facilities (VBCF), a member of the Vienna BioCenter (VBC), Austria. Christina Wagner used the RNA seq data to determine a list of differently expressed JAK3/STAT5 target genes as hallmark examples of JAK/STAT hyperactivation that are common between the GOF mutants and could explain cancer initiation or progression. Genes that were commonly upregulated by comparing the GOF vs. pMSCV and the transformed vs. pMSCV cells resulted in 332 potential target genes.

1.4.2 TCL38 RNA seq

The RNA seq data from the Ba/F3 cell lines were integrated with RNA seq data of 38 human T-cell cancer lines (TCL38), of which some also show JAK/STAT pathway hyperactivation, to find human-relevant target genes. The TCL38 cell lines include CTCL, ALCL, γδ T-cell lymphoma (γδ TCL), NK/T-cell lymphoma (NK TCL), Peripheral T-cell lymphoma not otherwise specified (PTCL-NOS), T-cell large granular lymphocytic leukaemia (T-LGLL) and T-ALL cell lines. RNA seq was performed on the TCL38 cell line panel as well as on healthy control CD3$^+$ T-cells by the sequencing facility and the group of Marco Herling at the University Hospital of Cologne.

1.4.3 Target gene list

Overlapping differentially expressed genes from the GOF Ba/F3 and TCL38 RNA seq datasets uncovered 160 potential target genes. The target gene list was reduced to

46 genes by prioritizing genes that were implicated in other cancers or that could be targeted by inhibitors (**Table 4**, Materials & Methods). These genes are interesting to further interrogate as potential vulnerabilities in T-cell cancer driven by hyperactive JAK/STAT signalling (**Figure 6**).

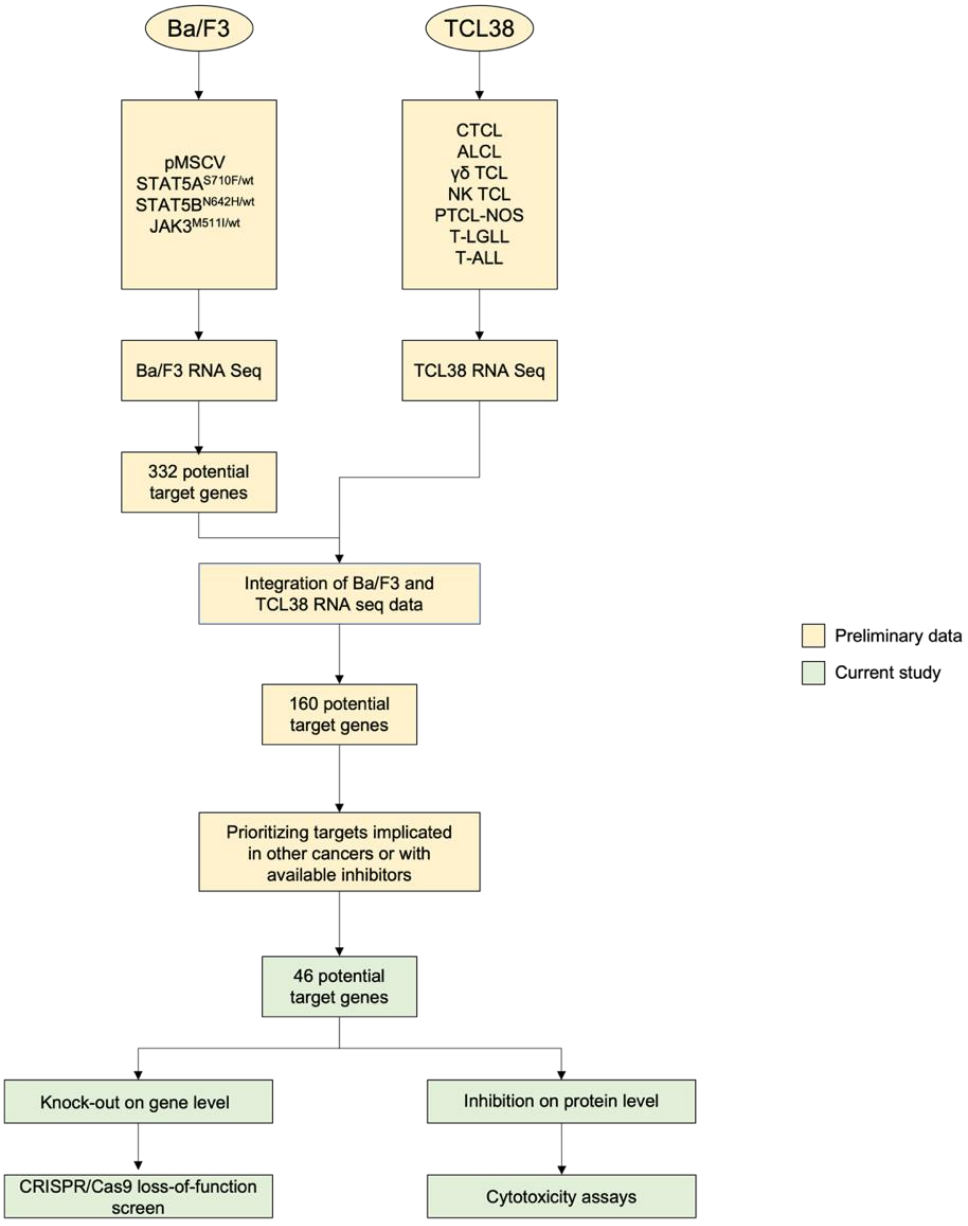

Figure 6: *Workflow from the Ba/F3 and TCL38 cell lines to the RNA seq data integration and finally to determining the 46 target genes that became the subject of the CRISPR/Cas9 loss-of-function screen and the cytotoxicity assays.*

1.5 Aim of the thesis

The preliminary data revealed 46 target genes relevant to hyperactive JAK/STAT signalling in T-cell cancer. We hypothesize that JAK/STAT-induced genes from this target gene list are essential for oncogenicity in T-cells due to JAK/STAT hyperactivation. This project aims to interrogate these targets by genetic and pharmacologic disruption of genes and proteins respectively to identify targetable vulnerabilities in T-ALL.

The 46 target genes will be explored using a focused Clustered Regularly Interspaced Short Palindromic Repeats (CRISPR)/CRISPR-associated (Cas) 9 loss-of-function screen (subsequently called CRISPR/Cas9 screen) in a human T-ALL cell line that carries a $STAT5B^{N642H}$ GOF mutation on both alleles. On the other hand, the upregulated T-cell cancer target gene products will be subjected to pharmacologic inhibitor treatment (**Figure 6**). The results of the CRISPR/Cas9 screen and the inhibitor treatments will be combined to identify JAK/STAT-driven cancer cell dependencies in T-ALL and might also bridge the gap to potential *in vivo* applications.

2 Materials & Methods

2.1 Materials

2.1.1 Mammalian cell cultivation

Table 1: *Cell lines used for CRISPR/Cas9 screen, transient transfection, and cytotoxicity analysis.*

Cell line	Origin	Specification
KOPT-K1 Cas9	T-ALL, male (6), transduced with LentiCas9-Blast	Suspension cells
KOPT-K1	T-ALL, male (6)	Suspension cells
Jurkat	T-ALL, male (14)	Suspension cells
HEK293T	human embryonic kidney	Adherent cells
LentiX 293T	human embryonic kidney for lentivirus production	Adherent cells
PC3	Human prostate cancer, male (64)	Adherent cells

Cultivation media – KOPT-K1 Cas9

Advanced RPMI 1640 medium (Gibco™)
with 10% (v/v) heat inactivated and sterile filtered fetal bovine serum (FBS; Gibco™)
1% (v/v) L-Glutamine (Gibco™)
1% (v/v) Penicillin-Streptomycin solution; 100x (Biowest®)
0.01 mg/ml Blasticidin (InvivoGen)

Cultivation media – KOPT-K1 and Jurkat

Advanced RPMI 1640 medium (Gibco™)
with 10% (v/v) heat inactivated and sterile FBS (Gibco™)
1% (v/v) L-Glutamine (Gibco™)
1% (v/v) Penicillin-Streptomycin solution; 100x (Biowest®)

Cultivation media – adherent cells

DMEM (1x) + GlutaMAX™ (Gibco™)

with 10% (v/v) sterile FBS (Gibco™)

1% (v/v) Penicillin-Streptomycin solution; 100x (Biowest®)

Trypsin and PBS

Trypsin-EDTA 1x in solution, sterile filtered (Biowest®)

Dulbecco's phosphate buffered saline (DPBS; Sigma®Life Science)

Cell counting

Sterile filtered trypan blue solution (Sigma®Life Science)

Neubauer chamber (Blaubrand)

2.1.2 Western blotting

1.5 M Tris-HCl

1.5 M Tris (Sigma®Life Science)

pH 8.8 (with HCl)

1 M Tris-HCl

1 M Tris (Sigma®Life Science)

pH 6.8 (with HCl)

10x Tris-buffered saline (TBS)

0.5 M Tris-HCl

pH 8.0 (with HCl)

10x Tris-glycine buffer

1.92 M Glycine (Roth®)

0.25 M Tris (Sigma®Life Science)

1x TBS-T

1x TBS

0.1% (v/v) Tween®20 (Sigma®Life Science)

1x Running buffer

0.1% (v/v) Sodium dodecyl sulfate (SDS; Roth®)

1x Tris-glycine buffer

1x Transfer buffer

20% (v/v) Methanol (Sarlab S. L.)

1x Tris-glycine buffer

6x Protein loading dye (Lämmli buffer)

0.03 mM Bromophenol blue (Sigma®Life Science)

0.259 M Dithiothreitol (DTT; Thermo Scientific™)

16% (v/v) Glycerol (Roth®)

1.6% (v/v) SDS (Roth®)

0.02 M Tris (Sigma®Life Science)

pH 6.8

Immunoprecipitation (IP) buffer

25 mM HEPES solution pH 7 (Sigma®Life Science)

25 mM Tris-HCl; pH 7.5

150 mM NaCl (Sigma®Life Science)

10 mM EDTA (AppliChem)

0.1% (v/v) Tween®20 (Sigma®Life Science)

0.5% (v/v) Nonidet® P-40 (Sigma®Life Science)

1 mM Na_3VO_4 (Aldrich Chemistry)

1 mM NaF (Sigma®Life Science)

10 µg/ml Leupeptin (Alfa Aesar)

10 µg/ml Aprotinin (Merck)

1 mM PMSF (Sigma®Life Science)

1x cOmplete™, EDTA-free protease inhibitor cocktail (Roche)

Bradford assay for protein concentration determination

5x Protein assay dye reagent concentrate (Bio-Rad)

Braun water (B. Braun Meisungen AG)

Bovine serum albumin (BSA; Sigma®Life Science)

8% SDS-running gel

8% Acrylamide mix (Roth®)

1% SDS (Roth®)

390 mM Tris-HCl; pH 8.8

0.1% Ammonium persulfate (APS; Sigma®Life Science)

0.06% TEMED (Sigma®Life Science)

5% SDS-Stacking gel

5% Acrylamide mix (Roth®)

1% SDS (Roth®)

130 mM Tris-HCl; pH 6.8

0.1% APS (Sigma®Life Science)

0.001% TEMED (Sigma®Life Science)

Blocking solution

5% Albumin Fraction V (Roth®) in TBS-T

Protein Ladder

PageRuler™ (Thermo Scientific™)

Antibodies for Western blot

Table 2: *Primary antibodies diluted in TBS-T.*

Antibody	Cat #	Company	Dilution	Size [kDa]	Host
FLAG-tag	F3165	Sigma®Life Science	1:5000		Mouse
Cas9	14697	Cell Signalling Technology	1:1000	160	Mouse
α −Tubulin	sc-32293	Santa Cruz Biotechnology	1:5000	50	Mouse

Table 3: *Secondary antibodies from LI-COR TM diluted 1:10000 in TBS-T.*

Antibody	Target	Host
IRDye® 680RD Goat anti-Mouse IgG	Anti-mouse	Goat
IRDye® 800CW Goat anti-Rabbit IgG	Anti-rabbit	Goat

2.1.3 Single guide (sg)RNA cloning

Target gene list

Table 4: *A target gene list of 46 target genes downstream of the JAK/STAT pathway was generated using Ba/F3 and TCL38 RNA seq data by Christina Wagner (University of Veterinary Medicine, Vienna).*

Gene	Protein	Key functions
ALYREF	THO complex subunit 4 (THO4)	Nuclear export of mRNA
APEX1	DNA-(apurinic or apyrimidinic site) endonuclease (APEN)	DNA repair, oxidative stress
AURKB	Aurora kinase B (AURKB)	Regulation of mitosis
BARD1	BRCA1 associated RING domain 1 (BARD1)	DNA repair
BCL2L1	B-cell lymphoma 2 (BCL2) like protein 1 (BCL-xL)	Apoptosis/ Survival
BIRC5	Baculoviral IAP repeat-containing protein 5 (Survivin)	Apoptosis/ Survival
BLM	RecQ-like DNA helicase (BLM)	DNA replication/ repair
BRCA1	Breast cancer type 1 susceptibility protein (BRCA1)	DNA repair
BUB1	Mitotic checkpoint serine/threonine-protein kinase BUB1 (hBUB1)	Regulation of mitosis
BUD31	BUD31 Homolog (BUD31)	Pre-mRNA splicing
CCNE2	G1/S-specific cyclin-E2 (CCNE2)	Cell cycle progression
CDC25A	M-phase inducer phosphatase 1 (CDC25A)	Regulation of mitosis
CDC6	Cell division control protein 6 (CDC6)	DNA replication initiation
CDC7	Cell division control protein 7 (CDC7)	DNA replication initiation
CENPE	Centromere protein E (CENP-E)	Cell division
CENPM	Centromere protein M (CENP-M)	Cell division

CENPW	Centromere protein W (CENP-W)	Cell division
CHAF1B	Chromatin assembly factor 1 subunit B (CAF-1 subunit B)	DNA replication/ repair
CHEK1	Checkpoint kinase 1 (CHK1)	Cell cycle, DNA repair
E2F1	E2F transcription factor 1 (E2F-1)	Cell cycle, DNA replication
FEN1	Flap structure-specific endonuclease 1 (FEN-1)	DNA replication/ repair
HMGB1	High mobility group box 1 (HMG-1)	DNA replication/repair
KNTC1	Kinetochore associated 1 (HsROD)	Regulation of mitosis
KPNB1	Karyopherin subunit beta 1 (Importin-90)	Nuclear protein import
MCM4	Minichromosome maintenance complex component 4 (MCM4)	DNA replication initiation
MCM5	Minichromosome maintenance complex component 5 (MCM5)	DNA replication initiation
MTHFD2	Bifunctional methylenetetrahydrofolate dehydrogenase/cyclohydrolase, mitochondria (MTHFD2)	Required for magnesium and inorganic phosphate
MYC	MYC proto-Oncogene (MYC)	Transcription factor
NDUFB6	NADH:ubiquinone oxidoreductase subunit B6 (complex I-B17)	Electron transport chain
NEK6	Serine/threonine-protein kinase Nek6 (NEK6)	Regulation of Mitosis
NUF2	Kinetochore protein Nuf2 (NUF2)	Cell division
NUP37	Nucleoporin 37 (p37)	Nuclear pore complex
PCNA	Proliferating cell nuclear antigen (PCNA)	DNA replication
PHGDH	D-3-phosphoglycerate dehydrogenase (PHGDH)	Amino acid synthesis
PSMA5	Proteasome 20S subunit alpha 5 (PSMA5)	Protein degradation

PSMB2	Proteasome 20S subunit beta 2 (PSMB2)	Protein degradation
PSMD1	Proteasome 26S subunit, non-ATPase 1 (PSMD1)	Protein degradation
RAD51	DNA repair protein RAD51 homolog 1 (RAD51)	DNA repair
RMI2	RecQ-mediated genome instability protein 2 (RMI2)	DNA repair
RPM2	Ribonuclease P protein component, mitochondrial (RPM2)	Degradation of RNA
STAT5B	Signal transducer and activator of transcription 5B (STAT5B)	Transcription factor
TFDP1	Transcription factor Dp-1 (TFDP1)	DNA replication
TYMS	Thymidylate synthetase (TS)	Nucleotide biosynthesis
UBE2N	Ubiquitin-conjugating enzyme E2 N (UBE2N)	DNA replication/ repair
VEGFA	Vascular endothelial growth factor A (VEGF-A)	Angiogenisis
YBX1	Y-box binding protein 1 (YBX1)	DNA repair, transcriptional regulation

Annealing and phosphorylation

T4 Polynucleotide Kinase (PNK; M0201L; NEB®)

10x T4 ligation buffer with ATP (B0202S; NEB®)

Restriction reaction

BsmBI (R07395; NEB®)

NEBuffer™ 3.1 (B6003S; NEB®)

Dephosphorylation

10x AP Buffer (Thermo Scientific™)

Fast AP (Thermo Scientific™)

Ligation

T4 DNA ligase (M0202M; NEB®)

10x T4 ligation buffer with ATP (B0202S; NEB®)

LentiGuide-Puro-P2A-EGFP vector for sgRNA cloning

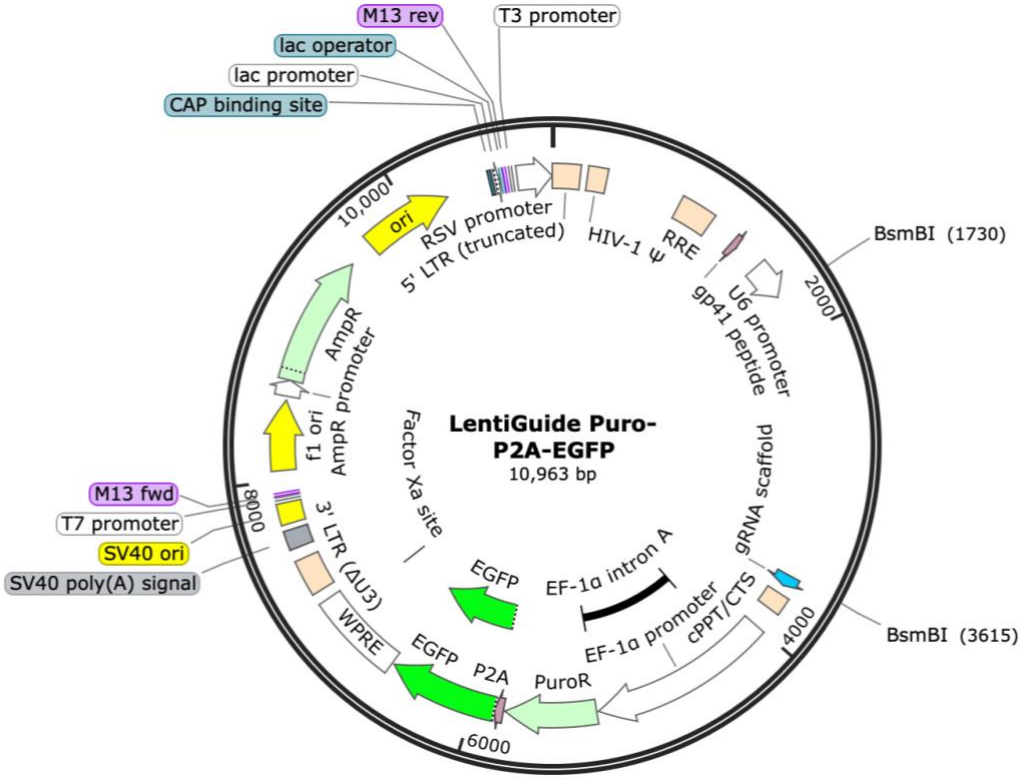

Figure 7: *Empty LentiGuide Puro-P2A-EGFP vector for sgRNA cloning (image: AddGene.com). Insert: sgRNA (supplementary,* ***Table 11****)*

LentiCas9-Blast vector

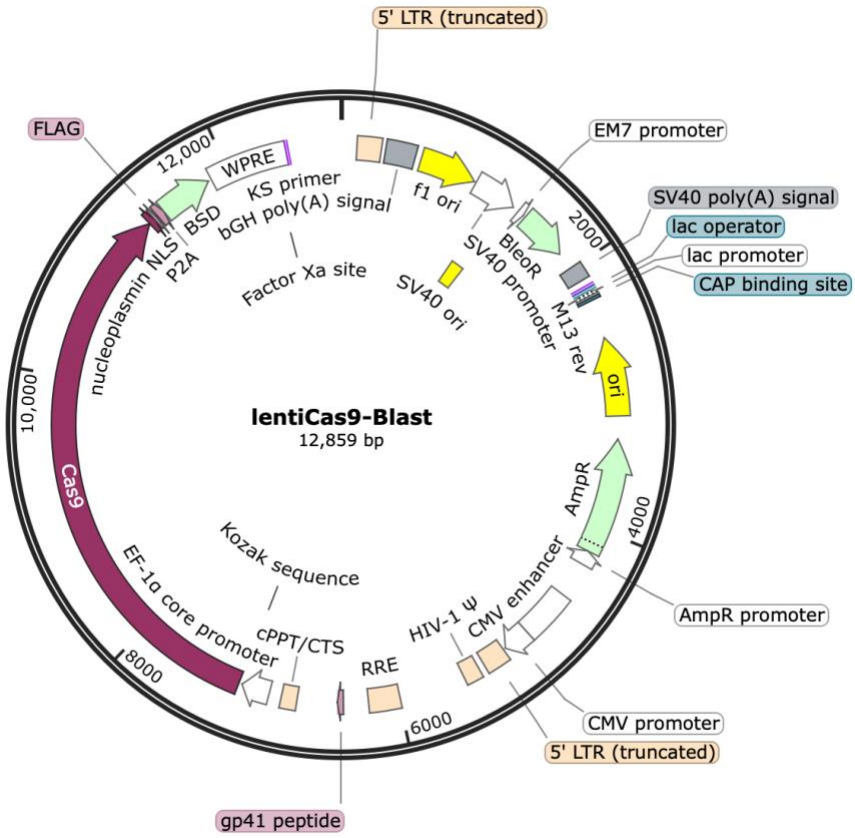

Figure 8: *LentiCas9-Blast vector (image: AddGene.com) for the generation of a KOPT-K1 Cas9 expressing cell line.*

2.1.4 Bacterial cell cultivation

Growth Medium

LB medium (Roth®)

LB plates

LB agar (Sigma®Life Science) heated until dissolved

added 100 µg/ml Carbenicillin (Roth®)

Transformation medium

SOC outgrowth medium (NEB®)

Competent *E. coli*

STBL3™ (provided by Florian Grebien, University of Veterinary Medicine, Vienna)

Plasmid preparation

High Pure Plasmid Isolation Kit (Roche) – used as instructed by the manufacturer.

2.1.5 Sequencing

Table 5: *Primer for sgRNA sequencing (designed by Christina Wagner, provided by IDT).*

Name	Target	Sequence (5' – 3')
guide_fwd1	sgRNA	GACTATCATATGCTTACCGT

2.1.6 Transient transfection

Opti-Mem™ reduced serum medium (Gibco™)

Lipofectamine®2000 reagent (Invitrogen)

PEI 2.0 (provided by Florian Grebien, University of Veterinary Medicine, Vienna)

2.1.7 Transduction

Polybrene (8 mg/ml, sterile filtered, Sigma®Life Science)

2.1.8 Cytotoxicity assay

CellTiter-Blue® Cell Viability Assay (Promega)

Table 6: *Inhibitors used for cytotoxicity assays. (source: Drugs@FDA: FDA-Approved Drugs*, 2023*)*

Name	Inhibitor	Source	FDA
AZD-4320	BCL-xL inhibitor	MedChemExpress	Not approved
Barasertib	AURKB inhibitor	MedChemExpress	Not approved
Bevacizumab	VEGF antibody	MedChemExpress	Approved
BN82002	CDC25 inhibitor	MedChemExpress	Not approved
Bortezomib	Proteasome inhibitor	MedChemExpress	Approved
Floxuridine	Antimetabolite	MedChemExpress	Approved
ML216	BLM inhibitor	MedChemExpress	Not approved
NSC697923	UBE2N inhibitor	MedChemExpress	Not approved
Olaparib	PARP inhibitor	MedChemExpress	Approved
Paclitaxel	Microtubule stabilizer	MedChemExpress	Approved
Prexasertib	CHK inhibitor	MedChemExpress	Not approved

2.2 Methods

2.2.1 Cultivation of mammalian cells

Mammalian cells (**Table 1**) were cultivated in their respective media in a density of approximately 10^6 cells/ml, counted with Trypan blue and a Neubauer chamber (Blaubrand). The cells were kept at 37°C with 5% CO_2 in a humid environment and were regularly tested for Mycoplasma with the MycoAlert™ mycoplasma detection kit (Lonza). For long-term storage at -80°C, the cells were centrifuged (300 g, 5 min) and resuspended in 1 ml freezing-medium consisting of 90% FBS (Gibco™) and 10% DMSO (Roth®). The cell suspension was transferred to cryogenic vials (Greiner bio-one) and frozen at -80°C in a controlled-rate cell-freezing container (Corning®Cool Cell®). Cells were thawed in a 37°C water bath and washed with pre-warmed fresh media (centrifugation at 300 g, 5 min) before taking them into their respective culture conditions.

2.2.2 Western blotting

2.2.2.1 Protein extraction

Adherent cells

The DMEM medium was exchanged for 5 ml cold PBS and the cells were scraped off with a cell scraper and transferred to a fresh tube. An additional 5 ml cold PBS was added to the dish to retrieve the remaining cells. After centrifugation at 300 g and 4°C for 5 min the PBS was removed. The cells were washed a second time with 1 ml PBS in 1.5 ml Eppendorf tubes. The pellets were then snap-frozen for long-term storage at -80°C. The pellets were resuspended in 30 – 100 µl IP buffer depending on the size. The samples were rotated with the STR4 rotating shaker system (Cole-Parmer®) at 4°C for 30 min and then centrifuged at 16000 g at 4°C for 15 min. The resulting lysate contained the proteins.

Suspension cells

The suspension cells were added to 5 ml cold PBS and centrifuged at 300 g and 4°C for 5 min. The supernatant was discarded, and the cells were washed a second time with cold PBS in a 1.5 ml Eppendorf tube. The remaining protein extraction was done in accordance with the protein extraction for adherent cells.

2.2.2.2 Bradford assay

The Bradford assay was done with the 5x protein assay dye reagent concentrate (Bio-Rad), diluted with Braun water (B. Braun Meisungen AG) to 1x its concentration. A standard curve was prepared containing 1 µl of IP buffer and 0 µg/ml, 1 µg/ml, 2 µg/ml, 4 µg/ml, 8 µg/ml, or 16 µg/ml BSA (Sigma®Life Science). The samples were mixed with 1 ml of diluted assay dye and 1 µl of lysate. The absorbance of each standard and sample was measured at 595 nm using the BioPhotometer plus (Eppendorf). The protein concentration was calculated with the linear equation of the BSA standard curve.

2.2.2.3 Western blot analysis

The Western blot samples were prepared by diluting the lysate with IP buffer and Lämmli buffer to a concentration of 1 – 1.5 µg/µl. The proteins were denatured at 95°C for 5 min before 20 µl of the sample was loaded onto the gel. The SDS-PAGE (sodium dodecyl sulfate-polyacrylamide gel electrophoresis) ran for 1-2 h at 150 V. The proteins were transferred from the gel to a nitrocellulose membrane. For the transfer, a 'sandwich' with the following layers was assembled: a sponge, two Whatman filter papers, the gel, a nitrocellulose membrane, two Whatman filter papers and finally a sponge again. The transfer was executed overnight at 4°C with 120 mA. The proteins were blocked with BSA (Sigma®Life Science) in TBS-T for 1 h while gently shaking. The membrane was incubated on the shaker with the primary antibody for 1 h and with the secondary antibody for 45 min in the dark. Between each antibody, the membrane was washed three times with TBS-T for 5 min. The membrane was stored in 1x TBS for scanning with the Odyssey® Imaging System.

2.2.3 CRISPR/Cas9 screen

2.2.3.1 sgRNA cloning

sgRNA annealing and phosphorylation

The 92 sgRNAs (supplementary, **Table 11**) were provided in a 96-well plate by IDT. Each well contained the forward and reverse oligomer (**Figure 9**) with the specific overhang to allow ligation with the sticky-ends of the BsmBI digestion which needed to be annealed and phosphorylated before starting the cloning process into the LentiGuide Puro-P2A-EGFP vector (**Figure 7**). Firstly, 2 µl of a master mix containing 0.4 µl 10x T4 ligation buffer with ATP (B0202S; NEB®), 0.2 µl of T4 PNK (M0201L; NEB®) and 1.4 µl of dH_20 was distributed across a 96-well plate. Secondly, 2 µl of the sgRNA was mixed with the master mix. The annealing and phosphorylation were performed with the program shown in **Table 7**. A 1:2000 dilution in dH_2O of the annealed and phosphorylated sgRNAs was prepared for the cloning process.

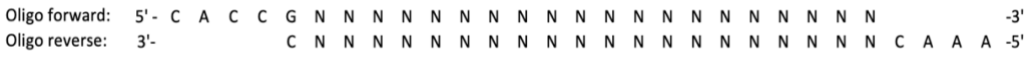

Figure 9: *Oligomer sequence for sticky-end ligation of sgRNAs with the BsmBI-digested LentiGuide Puro-P2A-EGFP vector (sgRNA sequence substituted by N).*

Table 7: *sgRNA annealing and phosphorylation program.*

Temperature	Time
37°C	30 min
95°C	5 min
25°C	0.1°C/s
4°C	∞

Ligation of sgRNA and LentiGuide Puro vector

The LentiGuide Puro-P2A-EGFP vector (**Figure 7**) was digested with BsmBI (R07395; NEB®; **Figure 10**) and dephosphorylated with Fast AP (Thermo Scientific™) according to the manufacturer's instruction by Gabriele Manhart (University of Veterinary Medicine, Vienna). For the ligation reaction, 2 µl of the 1:2000 diluted sgRNAs were mixed with 2 µl of the master mix comprised of 40 ng of digested and dephosphorylated vector, 0.4 µl of 10x T4 ligation buffer with ATP (B0202S; NEB®), 0.2 µl of T4 DNA ligase (M0202M; NEB®) and filled up with dH_2O. The ligation reaction was incubated for 20 min at room temperature. Lastly, the ligation reaction was diluted with 6 µl of dH_2O.

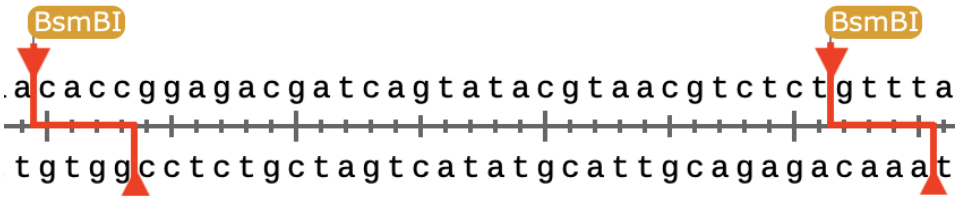

Figure 10: *BsmBI restriction site. (Source: SnapGene Viewer)*

Transformation of sgRNA-plasmid with STBL3™ competent *E. coli*

For the transformation, 10 µl of STBL3™ (kindly provided by Florian Grebien, Veterinary University of Vienna) were gently mixed with 2 µl of the ligation reaction and incubated for 5 min on ice. The heat shock was performed for 30 sec at 42°C, followed by another incubation for 1 min on ice. Pre-warmed SOC medium (30°C, 180 µl) was added for the outgrowth phase of 1 h at room temperature (not shaking). 5 µl of the transformation reaction was streaked on LB-agar plates. The plates were incubated overnight at 37°C. For the plasmid extraction, one single colony per construct was picked and two wells of a 96-deep well plate with 1.2 ml LB medium were inoculated. After overnight incubation at 37°C, the High Pure Plasmid Isolation Kit (Roche) was used to extract the plasmid according to the manufacturer's instructions. The correct integration of the sgRNA was verified by Sanger sequencing (**Table 5**) by Microsynth Austria GmbH according to the company's instructions. The sequence analysis was done with Python (Biopython package; Cock P.J. et al., 2009) and SnapGene Viewer.

2.2.3.2 Single cell clone seeding

The KOPT-K1 Cas9 cell suspension (**Table 1**) was diluted to 5 cells/ml in 30 ml RPMI to generate single cell clones (SCC). The 30 ml cell suspension was applied to a 70 µm cell strainer to separate the cells. The remaining undiluted cell suspension of approximately 10 ml was centrifuged (5 min, 300 g) and then applied to a sterile filter (0.22 µm) to gain a conditioned medium. The conditioned medium was combined with

the 30 ml cell suspension and expanded with fresh RPMI to a total volume of 60 ml. The cell suspension was mixed with 0.01 mg/ml Blasticidin (InvivoGen) to select for Cas9-positive cells. 200 µl cell suspension per well was distributed across 3 96-well plates, resulting in statistically 0.5 cells per well. The SCC were kept under continuous Blasticidin selection and transferred to bigger wells once outgrowth was visible.

2.2.3.3 Transient transfection

Transient transfection for Western blot

HEK293T cells (**Table 1**) were used for the transient transfection to determine protein expression from a plasmid via Western blot. Cells were counted with the Neubauer chamber (Blaubrand) and 2 million cells in 4 ml DMEM medium were seeded into 60 $(mm)^2$ dishes. The cells were incubated for 24 h at 37°C until a confluency of 70% was reached. Two tubes with 250 µl Opti-Mem™ (Gibco™) were prepared. 15 µl of Lipofectamine®2000 reagent (Invitrogen) were added to the first tube, followed by incubation at room temperature for 5 min. To the second tube, 5 µg of plasmid were added. The two tubes were combined (total 500 µl) and incubated again for 15 min. Meanwhile, the DMEM medium of the HEK293T cells was exchanged for 3.5 ml of fresh medium. The Opti-Mem™-mixture was added to the HEK293T cells dropwise. The dish was shaken gently and then incubated for 24 h. After 24 h the cells were harvested for a Western blot.

Transient transfection for virus production for the initial CRISPR/Cas9 screen

The initial screen was performed with positive (*AAVS1*) and negative (*RPL17*) sgRNA controls (supplementary, **Table 11**) to determine a functional KOPT-K1 Cas9 SCC. A similar protocol to the transient transfection for Western blot was followed; however, LentiX 293T cells (**Table 1**) were used and incubated for 6 h at 37°C before the plasmids were added. Two tubes for each construct with 250 µl Opti-Mem™ (Gibco™) were prepared. 10 µl of Lipofectamine®2000 reagent (Invitrogen) were added to the first tube. To the second tube, the control and packaging plasmids (**Table 8**) were

added. The medium was exchanged with 5 ml fresh RPMI medium after a 24 h incubation time at 37°C with the plasmids. The LentiX 293T cells were incubated again overnight for virus production in the RPMI medium.

Table 8: *Plasmids for the transient transfection for initial CRISPR/Cas9 screen.*

Plasmid	Amount [µg]	Function
AAVS1-LentiGuide Puro	3	Negative control
RPL17-LentiGuide Puro	3	Positive control
psPAX2	1.88	Viral packaging plasmid
pMD2g	1.1	Viral packaging plasmid

Transient transfection for virus production for the CRISPR/Cas9 screen

Approximately 4 x 10^6 cells LentiX 293T cells were cultivated in 10 ml DMEM medium in 10 $(cm)^2$ dishes overnight to a confluency of 80 – 90%. The LentiX 293T cells were harvested and resuspended again in 10 ml DMEM medium. 270 µl of this cell suspension and 1.5 ml fresh DMEM medium were seeded into one well of a 6-well plate per sgRNA-LentiGuide Puro construct (supplementary, **Table 11**). The 6-well plates were incubated overnight before the transient transfection was performed. A master mix containing 152 µl plain DMEM, 0.346 µg psPAX2 and 0.173 µg pMSD2g was prepared. In a 96-well plate, the master mix was mixed with 0.69 µg of the construct. To each construct, 3.6 µl of PEI 2.0 (kindly provided by Florian Grebien, University of Veterinary Medicine, Vienna) was added followed by a 20 min incubation time. The plasmids were added to the LentiX 293T cells for overnight incubation at 37°C. The medium was exchanged with 2 ml fresh RPMI medium and the LentiX 293T cells were incubated again overnight for virus production in the RPMI medium.

2.2.3.4 Virus harvest for the CRISPR/Cas9 screen

The transiently transduced LentiX 293T cells produce the Lentivirus; thus, the virus is

contained in the RPMI medium. The supernatant medium was transferred to a fresh tube or plate to retrieve the virus. To remove detached cells, the tube/plate was centrifuged (300 g, 5 min) and the supernatant was again transferred to a fresh tube/plate. The viral media was stored at 4°C.

2.2.3.5 Transduction for the CRISPR/Cas9 screen

KOPT-K1 Cas9 cells (**Table 1**) were transduced with Lentivirus containing the sgRNA. 1 million cells in 0.5 ml of fresh RPMI medium and 0.5 ml of the virus medium were seeded into one well of a 24-well plate. Polybrene (0.008 mg/ml final concentration; Sigma®Life Science) was added to the well to facilitate the transduction. A spinfection (75 min, 900 g) was performed followed by overnight incubation at 37°C. The plates were centrifuged (5 min, 300 g) to remove the virus supernatant. Fresh RPMI medium was added, and the cells were incubated again for 48 h until the first measurement for GFP-positive cells.

2.2.3.6 CRISPR/Cas9 screen analysis

Cell cultivation and sample preparation

The KOPT-K1 Cas9 cells were split 1:5 and measured for GFP expression every 3 - 4 days for 2 - 3 weeks. For each measurement, 150 µl of cell suspension was transferred into a U-bottom 96-well plate and washed twice with PBS. The cells were resuspended in 100 µl PBS for measurement with the IQue Screener Plus (Intellicyt, equipped with plate reader, blue (488 nm) and red (640 nm) laser).

Gating strategy and evaluation of GFP expression with the IQue Screener

The Forecyt software for the IQue Screener was used to evaluate the competition assay and determine the percentage of GFP-positive cells for each sgRNA construct. Firstly, the living cells were gated. A gate was set to focus on the singlets and lastly, the GFP-positive singlets were gated (**Figure 11**). The percentage of GFP-positive

singlets per construct was visualized as a heatmap.

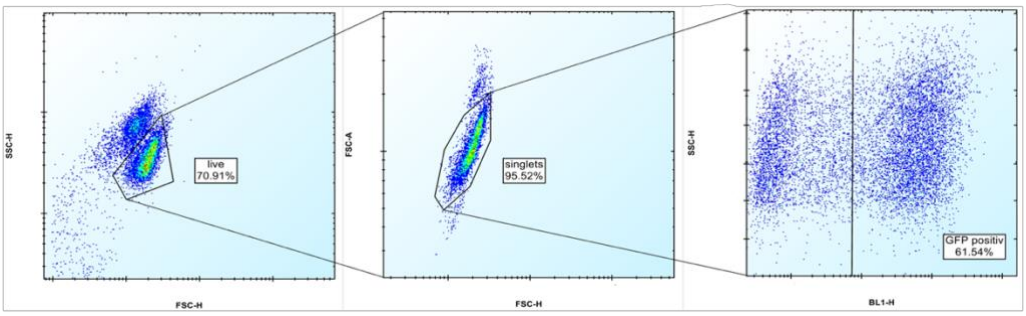

Figure 11: *Gating strategy for the evaluation of GFP percentage during the CRISPR/Cas9 screen.*

Data analysis and statistics

The data was evaluated using Microsoft Excel and an R script according to Proietti et al. 2022. The measurement 48 h after virus removal was normalized to the negative control (*AASV1* sgRNA; **Equation 2**). Each following measurement was normalized to the first measurement (**Equation 1**) and to the negative control (**Equation 2**).

Equation 1: *Normalization to day 2 (first measurement).*

$$\%GFP_{normDay2} = \frac{\%GFP_{DayX}}{\%GFP_{Day2}}$$

Equation 2: *Normalization to the negative control (AASV1).*

$$\%GFP_{sample,normDay2+normAAVS1} = \frac{\%GFP_{sample,normDay2}}{\%GFP_{AAVS1,normDay2}}$$

The normalized values were either visualized as a bar graph using Microsoft Excel or as a heatmap using R. The area under the curve (AUC) was calculated for each construct which shows the overall depletion of each construct in a condensed format.

2.2.4 Cytotoxicity

2.2.4.1 Cytotoxicity assay

Cytotoxicity assays were performed with the KOPT-K1 and Jurkat cell lines and the PC3 cell line (**Table 1**) functioning as a control. The cells were incubated for 72 h with decreasing concentrations of the inhibitor (**Table 6**) and the viability of the cells was evaluated with the CellTiter-Blue® Cell Viability Assay (Promega). The inhibitors were diluted in RPMI medium to twice the starting concentration and 100 µl were transferred to three wells (technical triplicates) of a 96-well plate. The 1:2 serial dilution was performed with RPMI medium adjusted with DMSO (Roth®) to account for the drug vehicle. One additional column of the 96-well plate was filled with 50 µl of plain RPMI medium as a negative control and another with 10 µM Bortezomib as a positive control. 1 million cells per drug were centrifuged (5 min, 300 g) and resuspended in 2 ml fresh RPMI and 50 µl of cell suspension was added to each well and incubated at 37°C.

2.2.4.2 Cytotoxicity assay analysis

The cytotoxicity assays were evaluated using 20 µl CellTiter-Blue® (Promega) diluted 1:5 in PBS per well. After a 1 – 2 h incubation time, the fluorescence was measured with the Promega Plate Reader according to the manufacturer's instructions (Promega Cooperation, 2016). The data were analysed and visualized using the GraphPad Prism 9 program.

2.2.5 Statistics

When applicable, statistics were calculated using one-way analyses of variance (ANOVA; unless otherwise stated) using the GraphPad Prism 9 software.

3 Results

3.1 CRISPR/Cas9 screen

T-ALL patients often harbour the GOF mutations STAT5B^{N642H} or JAK3^{M511I} (Pham et al., 2018; Vicente et al., 2015). Moreover, the genetically engineered GOF STAT5A^{S710F} mutation was previously shown to induce a peripheral T-cell lymphoma-like phenotype in mice (Maurer et al., 2020; Moriggl et al., 2005; Onishi et al., 1998). Ba/F3 cell lines overexpressing the aforementioned GOF mutations or the respective wt protein were previously established in our lab. The Ba/F3 cell lines are dependent on the cytokine mIL-3 and are therefore suitable for the study of the cytokine-induced JAK/STAT pathway and the transforming capacities of the GOF mutations. The Ba/F3 cell lines were used to explore the transcriptional changes induced by the GOF mutations via RNA seq. The Ba/F3 RNA seq data were overlapped with the TCL38 RNA seq data to find human T-cell cancer-relevant target genes. The target gene list was reduced by prioritizing genes that are well characterized, known to be implicated in other cancers, or have available inhibitors. In total, we selected 44 target genes and additionally two control genes (a total of 46 target genes; **Table 4**) to target with a focused CRISPR/Cas9 screen. The control genes, *MYC* and *STAT5B*, served as biological positive controls for JAK/STAT signalling specifically.

3.1.1 sgRNA cloning

Christina Wagner designed two sgRNAs for each of the 46 target genes (supplementary, **Table 11**, using the https://vbc-score.org tool) resulting in 92 unique sgRNAs. Each sgRNA has a length between 18 and 21 nucleotides and is located between a sequence (**Figure 9**) matching the restriction site of the BsmBI restriction enzyme (**Figure 10**; Shalem et al., 2014). These short sequences are necessary for the sticky-end ligation of the sgRNA into the BsmBI-digested LentiGuide Puro-P2A-EGFP vector (**Figure 7**). The sgRNAs were provided by IDT as oligomers which needed to be annealed and phosphorylated for the cloning process. Subsequently, we cloned the sgRNAs into the GFP-positive vector. The GFP marker gene will allow

monitoring of the depletion of the transduced cells during the CRISPR/Cas9 screen. We were able to clone 91 out of 92 sgRNAs successfully. However, one of the two constructs targeting *CENPW* lacked the concentration for the CRISPR/Cas9 screen. In total, 43 of 44 target genes will be covered by two independent sgRNAs and one target gene will be covered by one sgRNA during the CRISPR/Cas9 screen.

3.1.2 Transient transfection of HEK293T with the Cas9 plasmid

The target cell line of the CRISPR/Cas9 screen was the T-ALL cell line KOPT-K1 (**Table 1**). This cell line was isolated from a Japanese boy who succumbed to T-ALL at the age of seven and harbours a biallelic STAT5B^{N642H} mutation (Suske et al., 2022). The KOPT-K1 cell line is part of the TCL38 RNA seq dataset that was used to compile the target gene list for the CRISPR/Cas9 screen. This specific cell line was chosen as the target cell line because of the biallelic STAT5B^{N642H} mutation and because of its close clustering to the Ba/F3 RNA seq data. Before Christina Wagner established a stable Cas9-expressing cell line (KOPT-K1 Cas9), the Cas9 expression potential from the LentiCas9-Blast vector (**Figure 8**) was verified.

We tested the Cas9 expression potential from the plasmid by transiently transfecting HEK293T cells with the vector and detecting the Cas9 protein by Western blot. The Western blot of the transient transfection (**Figure 12 a**) shows a clear signal for the Cas9 protein (160 kDa) for the transiently transfected HEK293T cells. Thus, the Western blot confirms a functional LentiCas9-Blast vector that can be used to establish a Cas9-expressing cell line KOPT-K1 Cas9. Additionally, the Western blot validated the functionality of our Cas9 antibody and thus our tool to detect successfully transduced KOPT-K1 cells and KOPT-K1 Cas9 single cell clones (SCC).

After Christina Wagner transduced the KOPT-K1 cell line with the LentiCas9-Blast vector a Western blot was done to confirm Cas9 expression. The Western blot shows a signal for the Cas9 protein (**Figure 12 b**), indicating a successful transduction.

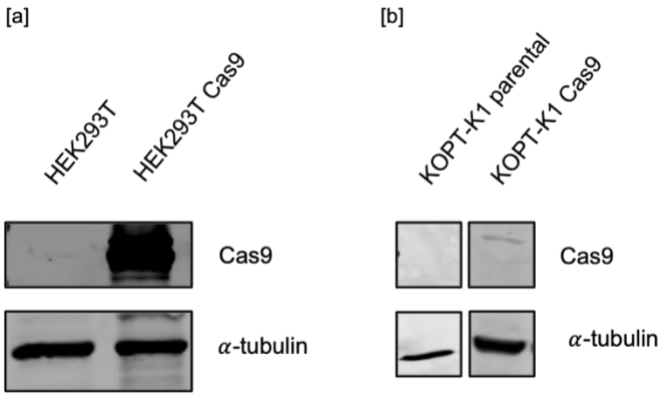

Figure 12: *(a) Western blot analysis of transiently transfected HEK293T cells with LentiCas9-Blast vector. Non-transfected HEK239T cells served as a control. (b) Western blot analysis of Cas9-transduced KOPT-K1 cells. Parental KOPT-K1 cells served as a control. Both Western blots: the Cas9 protein was detected with the Cas9 antibody and α-tubulin was used as a loading control. Experiment performed once (n=1) and represents only technical validation insight.*

3.1.3 Single cell clone seeding

We generated SCC from the KOPT-K1 Cas9 cell line (**Table 1**) to ensure the same cellular background for each Cas9 knock-out during the CRISPR/Cas9 screen. We seeded statistically 0.5 cells/well in 864 wells (9 x 96-well plates). The Cas9 protein is coupled to a Blasticidin-resistance gene to allow the selection of Cas9-positive cells. The KOPT-K1 Cas9 cells were selected with Blasticidin after the LentiCas9-Blast vector transduction to determine transduced from untransduced cells; after the selection, the transduced KOPT-K1 Cas9 cells should subsequently express Cas9 and thus the Blasticidin selection pressure was lifted. We seeded and expanded the first two rounds of SCC (3 x 96-well plates each), therefore, in RPMI medium without the addition of Blasticidin. However, the Western blot analysis of outgrown KOPT-K1 Cas9 SCC lacked Cas9 expression (data not shown). Therefore, KOPT-K1 Cas9 SCC stored at -80°C for long-term storage were thawed and re-selected with Blasticidin for 4 weeks. Meanwhile, we seeded a third round of SCC (3 x 96-well plates), which were kept under continuous Blasticidin selection pressure to assure continuous Cas9 expression. The Blasticidin re-selection of the first two rounds of SCC was survived

by 34 of over 40 KOPT-K1 Cas9 SCC (**Figure 13**, lanes 2 to 37). On the other hand, the third round of SCC seeding resulted in two additional KOPT-K1 Cas9 SCC (**Figure 13**, lanes 38 and 39). After cell expansion of all 36 KOPT-K1 Cas9 SCC under Blasticidin selection pressure, we performed a Western blot to verify the expression of Cas9 (**Figure 13**), of which 21 SCC showed a signal for the Cas9 protein. We used the results of the Western blot as a basis for selecting KOPT-K1 Cas9 SCC for the initial CRISPR/Cas9 screen. The initial CRISPR/Cas9 screen uses the positive and negative sgRNA controls (*RPL17* and *AASV1*) to validate Cas9 protein functionality and select a suitable clone for the focused CRISPR/Cas9 screen.

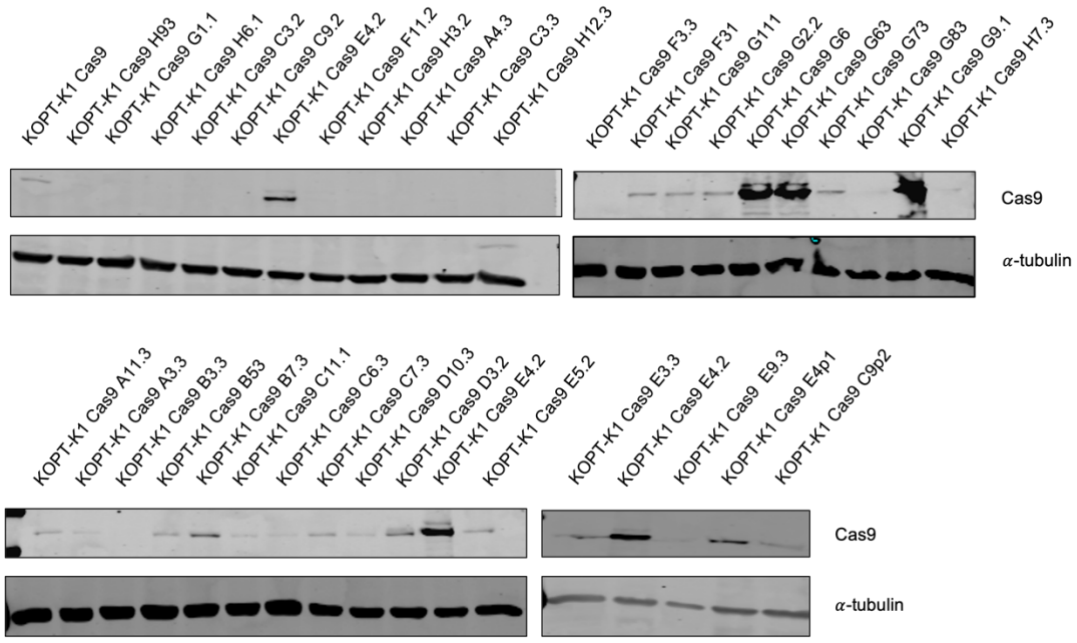

Figure 13: *Western blot analysis of 36 KOPT-K1 Cas9 SCC. The KOPT-K1 Cas9 bulk cell line was used as positive control for Cas9 expression. The Cas9 protein was detected by the Cas9 antibody and α −tubulin was used as loading control. Experiment performed once (n=1) and represents only technical validation insight.*

3.1.4 Initial CRISPR/Cas9 screen

The purpose of the initial CRISPR/Cas9 screen was to find a KOPT-K1 Cas9 SCC expressing a functional Cas9 protein. Control sgRNAs were used to determine this KOPT-K1 Cas9 SCC: a suitable SCC with a functional Cas9 protein should die with the positive control (*RPL17* sgRNA; loss of essential gene) and survive with the negative control (*AAVS1* sgRNA; loss of safe harbour locus).

We tested 21 KOPT-K1 Cas9 SCC (**Figure 13**) during the initial screen for their reaction to the control sgRNAs. We transiently transfected the LentiX 293T (**Table 1**) cells with the control sgRNA as well as two lentiviral packaging plasmids (**Table 8**) for virus production. Each KOPT-K1 Cas9 SCC was transduced separately with the positive or negative control. Two days after virus removal the first measurement for GFP expression was conducted with the IQue screener. The functionality of the Cas9 protein in the KOPT-K1 Cas9 SCC can be linked to the GFP expression percentage: The control plasmids include a GFP marker gene, and its continuous expression indicates that the sgRNA does not target an essential gene (*AAVS1*); however, its depletion indicates that the GFP-expressing cells are dying because the sgRNA target is vital (*RPL17*). The efficiency of the transduction should be above 20% GFP-positive cells on the first measurement for a reliable evaluation. This transduction efficiency was reached by nine KOPT-K1 Cas9 SCC: C6.3, D10.3, E4.2, G111, F31, G2.2, G6, G63 and G73. The presence of GFP-positive cells was monitored over 16 days with 5 measurements. Each measurement was normalized to the first measurement. **Figure 14** shows the quantification of GFP-positive cells for these nine SCC as a percentage of single cells normalized to the first measurement. The SCC G63 and G6 showed the desired trend with stable GFP expression in the negative control and decreasing GFP expression in the positive control, indicating a functional Cas9 protein. The KOPT-K1 Cas9 SCC G6 was chosen for the focused CRISPR/Cas9 screen.

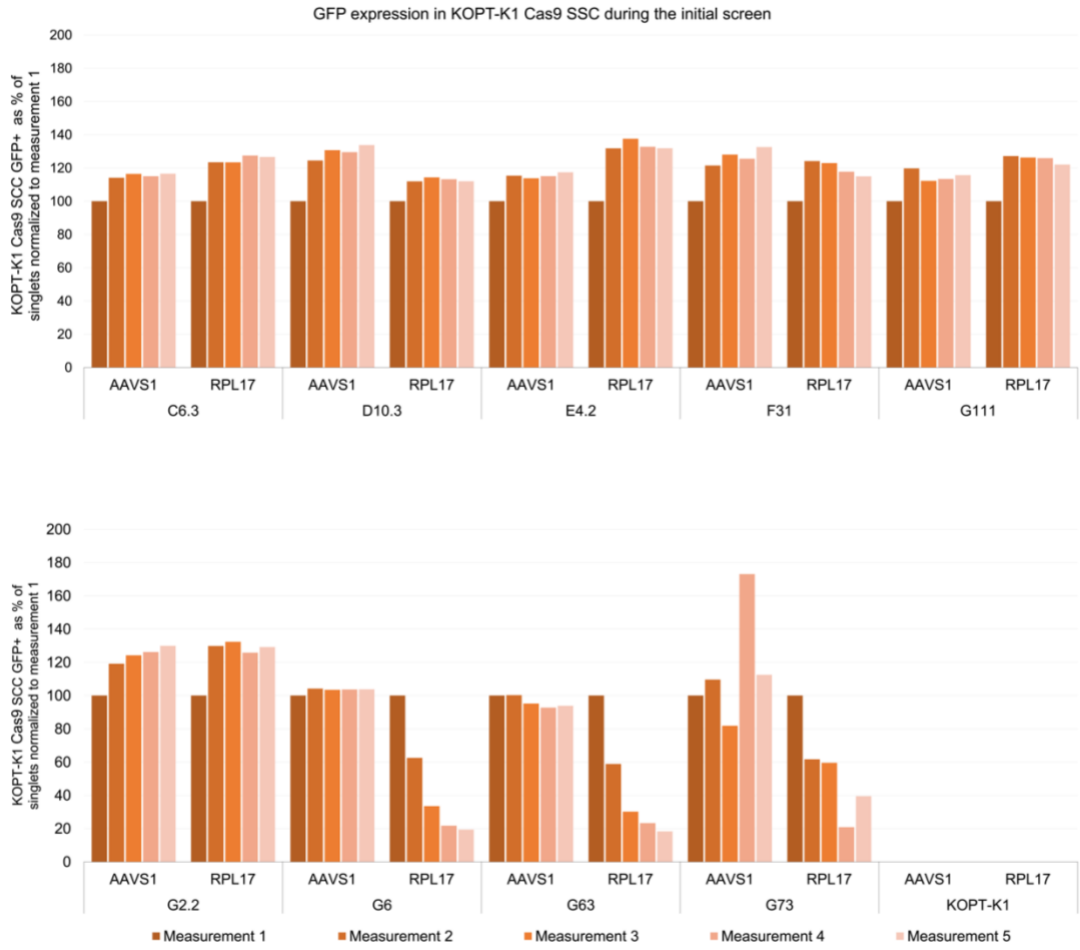

Figure 14: *An initial CRISPR/Cas9 screen with positive (RPL17 sgRNA) and negative (AASV1 sgRNA) controls to determine a suitable KOPT-K1 Cas9 SCC for the focused CRISPR/Cas9 screen. The depletion of cells due to the sgRNA knock-out was detected by monitoring the associated GFP signal with the IQue screener. The graph shows the percentage of GFP-positive cells in five measurements over 16 days normalized to the first measurement. The untransduced parental KOPT-K1 cell line was used as a GFP-negative control. Experiment was performed once (n=1) and represents only technical validation insight.*

3.1.5 Focused CRISPR/Cas9 screen

A target gene list (**Table 4**) of hyperactive JAK/STAT signalling was compiled by combining the RNA seq data of the GOF mutant Ba/F3 cell lines and the human TCL38 cell lines. The list consists of 46 target genes, where two sgRNAs were designed for each gene. We cloned 91 of 92 sgRNAs successfully thus ensuring that each gene, except one, is covered by two independent sgRNAs. The KOPT-K1 SCC G6 cells (henceforth referred to as KOPT-K1 Cas9 cells) were lentivirally transduced with the sgRNAs during the CRISPR/Cas9 screen. The GFP marker, included in the vector, indicates the survival or depletion of the cells due to the sgRNA-targeted knock-out, similar to the initial screen. Two days after virus removal, we performed the first measurement with the IQue screener to measure the initial percentage of GFP-positive cells. 13 sgRNA constructs, *BARD1, BRCA1, CENPM, CDC25, E2F1, KNTC1, MTHFD2, NUF2, PHGDH, RAD51, RMI2, TFDP1*, and *YBX1* did not reach a sufficient transduction efficiency of approximately 20% or above and were thus excluded. Therefore, the 14 target genes overall were targeted by one instead of two sgRNAs. We monitored the development of the GFP expression percentage for each construct for 20 days with seven measurements. The data evaluation was done according to the steps described by Proietti et al. 2022. The first measurement was normalized to the negative control (*AASV1* sgRNA) and each subsequent measurement was normalized to the first measurement as well as the negative control. We calculated the area under the curve (AUC) for each construct to quantify the depletion in a condensed format. The resulting heatmap (**Figure 15**) shows the sgRNA constructs leading to high depletion (low GFP expression) in red while unaffected cells are shown in blue (high GFP expression). Knock-out of the CRISPR/Cas9 screen negative control (*AASV1*) was unaffected, while the positive control (*RPL17*) showed strong depletion, validating that the selected KOPT-K1 Cas9 SCC behaved as expected with a functional Cas9 protein during the CRISPR/Cas9 screen. The positive biological controls, known members of STAT5 signalling, also depleted during the CRISPR/Cas9 screen validating our results: knock-out of *STAT5B* strongly depleted the cells and the knock-out of downstream target *MYC* also resulted in cell depletion.

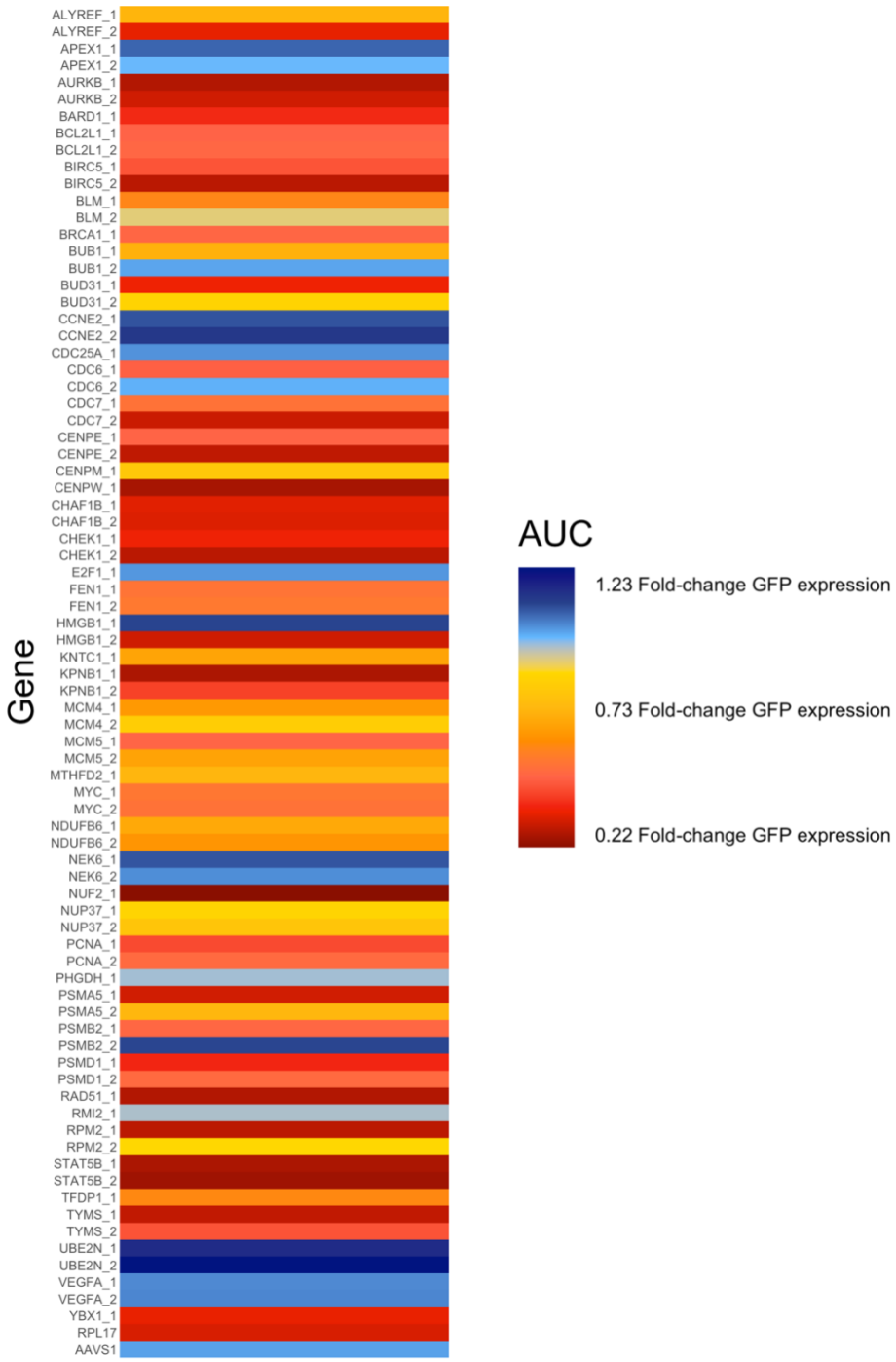

Figure 15: *The results of the CRISPR/Cas9 screen targeting 46 target genes in KOPT-K1 T-ALL cells. The depletion of cells due to the sgRNA-induced knock-out was detected by monitoring the associated GFP signal with the IQue screener over 20 days in seven measurements. Each measurement was normalized to the first measurement and to the negative control (AASV1). An area under the curve (AUC) measurement was calculated for each construct; a lower AUC (red) indicates a higher depletion due to the sgRNA-induced knock-out and a higher AUC (blue) indicates minimal impact of the gene knock-out on the cells. Experiment was performed once (n=1).*

The 18 sgRNA constructs (excluding controls *MYC* and *STAT5B*) shown in **Table 9** have an AUC in the lower third of the spectrum for either both targeting sgRNAs or one sgRNA in the cases where the gene was covered by one sgRNA.

Table 9: *The focused CRISPR/Cas9 screen of 46 target genes revealed the following 18 genes with an AUC in the lower third of the AUC spectrum for all targeting sgRNAs per gene.*

Gene	Protein	Key function
AURKB	Aurora kinase B (AURKB)	Regulation of mitosis
BARD1	BRCA1 associated RING domain 1 (BARD1)	DNA repair
BCL2L1	B-cell lymphoma 2 like protein 1 (BCL-xL)	Apoptosis/ Survival
BIRC5	Baculoviral IAP repeat-containing protein 5 (Survivin)	Apoptosis/ Survival
BRCA1	Breast cancer type 1 susceptibility protein (BRCA1)	DNA repair
CDC7	Cell division control protein 7 (CDC7)	DNA replication initiation
CENPE	Centromere protein E (CENP-E)	Cell division
CENPW	Centromere protein W (CENP-W)	Cell division
CHAF1B	Chromatin assembly factor 1 subunit B (CAF-1 subunit B)	DNA replication/ repair
CHEK1	Checkpoint kinase 1 (CHK1)	Cell cycle, DNA repair
FEN1	Flap structure-specific endonuclease 1 (FEN-1)	DNA replication/ repair
KPNB1	Karyopherin subunit beta 1 (Importin-90)	Nuclear protein import
NUF2	Kinetochore protein Nuf2 (NUF2)	Cell division
PCNA	Proliferating cell nuclear antigen (PCNA)	DNA replication

PSMD1	Proteasome 26S subunit, non-ATPase 1 (PSMD1)	Protein degradation
RAD51	DNA repair protein RAD51 homolog 1 (RAD51)	DNA repair
TYMS	Thymidylate synthetase (TS)	Nucleotide biosynthesis
YBX1	Y-box binding protein 1 (YBX1)	DNA repair, transcriptional regulation

To summarize, we selected 46 target genes of hyperactive JAK/STAT signalling in human T-cell cancers for a focused CRISPR/Cas9 screen in a T-ALL KOPT-K1 Cas9 cell line which harbours a biallelic STAT5B^{N642H} mutation. Therefore, the Cas9-expressing cell line KOPT-K1 Cas9 was generated, and SCC were seeded and selected for Cas9-functionality. The CRISPR/Cas9 screen resulted in a list of 18 genes, which led to cell depletion when knocked-out.

3.2 Cytotoxicity assay

Cytotoxicity assays use different concentrations of inhibitors to find the specific IC_{50} value which represents the inhibitor concentration needed to decrease cell viability by 50%. The IC_{50} value is unique for each inhibitor and cell line. The cytotoxicity assays were performed using the CellTiter-Blue® cell viability assay protocol. The CellTiter-Blue® reagent contains resazurin. Metabolically active, thus viable, cells reduce resazurin to resorufin. Resazurin and resorufin possess different absorbance properties and can therefore be used to measure the viability of cells (Promega Cooperation, 2016).

Due to the limited time of this study, several interesting targets were selected from the RNA seq gene list to be pharmacologically targeted using inhibitors in parallel to the CRISPR/Cas9 screen. Some inhibitors that were selected, such as the AURKB inhibitor Barasertib, inhibit single targets of the target gene list. On the other hand,

PSMA5, PSMB2, and PSMD1 are subunits of the 26S proteasome, and the entire 26S proteasome complex is inhibited by Bortezomib. Also, Floxuridine is an antimetabolite and was predicted to show an effect on the T-ALL cell line KOPT-K1 because of the upregulation of *TYMS*, which encodes for a thymidylate synthetase (TS). Furthermore, several upregulated target genes, such as *APEX1*, *BRAD1*, *BLM*, *BRACA1, CHAF1B, CHEK1, FEN1, HMGB1, RAD51, RMI2, UBE2N*, and *YBX1* show an association with DNA damage repair processes, indicating a higher dependency on these processes in human T-cell cancer compared to healthy cells. The inhibitor Olaparib targets the DNA damage repair response via the poly (ADP-ribose) polymerase (PARP) protein which is also involved in DNA damage repair. Lastly, several upregulated genes also show association with cell cycle progression, and cell division and microtubule dynamics plays an important role in these processes, which can be perturbed by the microtubule stabilizer Paclitaxel. The aim of the cytotoxicity assays was twofold: firstly, to find connections to the results of the CRISPR/Cas9 screen, and secondly, to bridge the gap to potential *in vivo* applications.

The cytotoxicity assays were performed in the T-ALL KOPT-K1 cell line which carries a biallelic $STAT5B^{N642H}$ mutation. We performed each cytotoxicity assay with 10 decreasing concentrations of each drug to plot a cell viability curve and to find the IC_{50} value for the KOPT-K1 cell line. The PC3 cell line served as a control cell line because it has neither STAT3 nor STAT5 expressed, and hence is not dependent on their signalling.

Figure 16 shows the normalized cell viability curves for each inhibitor. The KOPT-K1 T-ALL cell line was most sensitive to the proteasome inhibitor Bortezomib, the microtubule stabilizer Paclitaxel and the CHK1 inhibitor Prexasertib, indicated by their very low IC_{50} values of 2 nM. The CDC25 inhibitor BN82002, on the other hand, showed the highest IC_{50} value of 8.32 µM. We were unable to determine a concentration range that affected the T-ALL KOPT-K1 cell line for the BLM inhibitor ML216 and the VEGF antibody Bevacizumab, indicating that the cells were resistant to the targeting of these proteins.

[a]

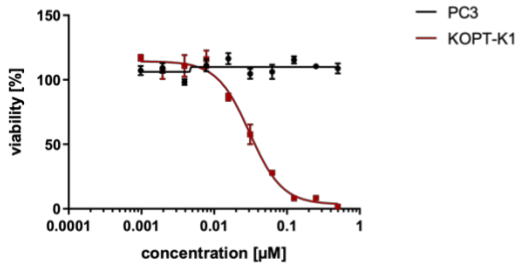
AZD-4320
PC3
KOPT-K1
viability [%]
150
100
50
0
0.0001
0.001
0.01
0.1
1
concentration [µM]

[b]

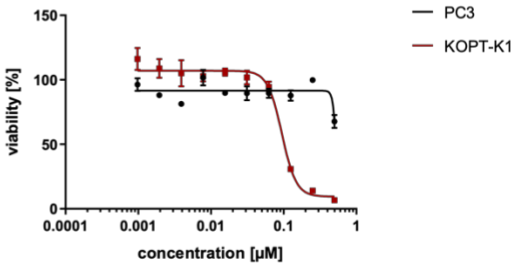
Barasertib
PC3
KOPT-K1
viability [%]
150
100
50
0
0.0001
0.001
0.01
0.1
1
concentration [µM]

[c]

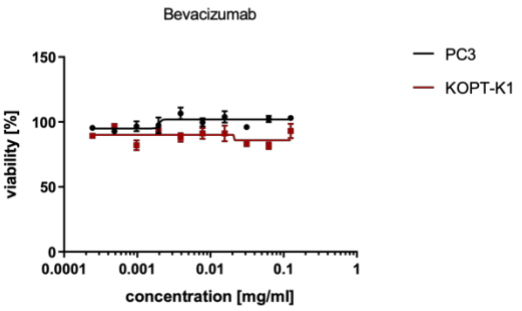
Bevacizumab
PC3
KOPT-K1
viability [%]
150
100
50
0
0.0001
0.001
0.01
0.1
1
concentration [mg/ml]

[d]

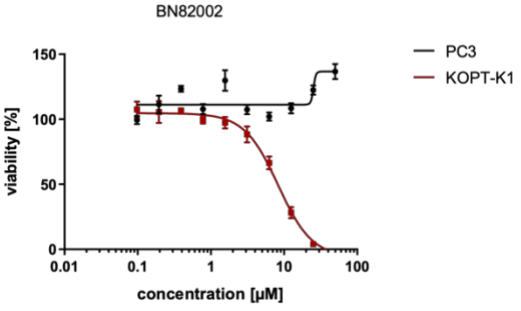
BN82002
PC3
KOPT-K1
viability [%]
150
100
50
0
0.01
0.1
1
10
100
concentration [µM]

[e]

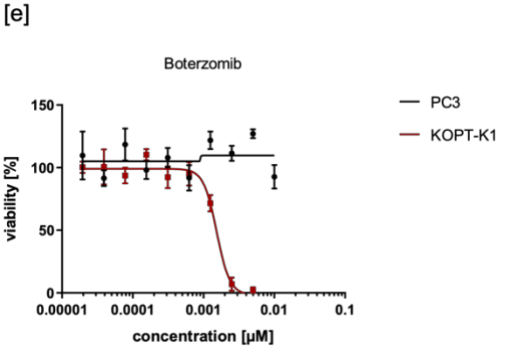
Boterzomib
PC3
KOPT-K1
viability [%]
150
100
50
0
0.00001
0.0001
0.001
0.01
0.1
concentration [µM]

[f]

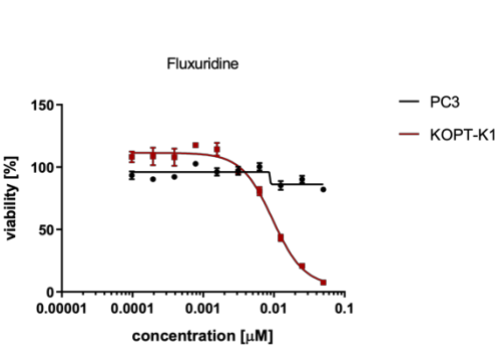
Fluxuridine
PC3
KOPT-K1
viability [%]
150
100
50
0
0.00001
0.0001
0.001
0.01
0.1
concentration [µM]

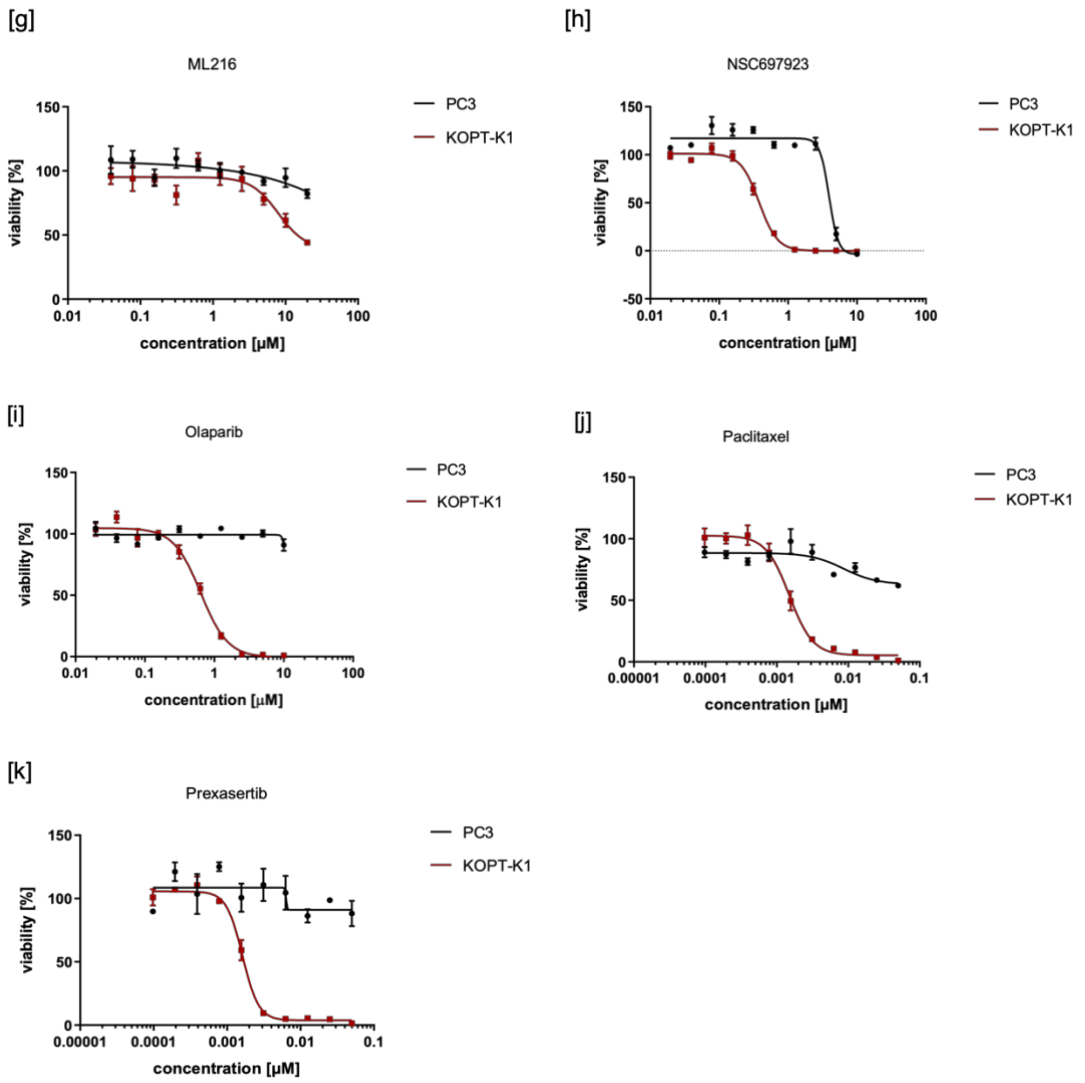

Figure 16: *Cytotoxicity assays assessing viability of KOPT-K1 T-ALL cells upon incubation with various inhibitors. (a-k) Cells were incubated with inhibitors (or DMSO vehicle control) at various concentrations for 72h, and viability was measured using a CellTiter-Blue® cell viability assay. The PC3 cell line served as a negative control. Data were plotted as mean +/- SD of technical triplicates, and IC_{50} values were obtained from the fitted curve. (a, b, e, f, i, j) Graphs are from one experiment representative of three independent experiments (n=3). (c, d, g, h) Graph is from one experiment (n = 1).*

We were able to find several links between cytotoxicity assays and the CRISPR/Cas9 screen: The target genes *AURKB, BCL2L1,* and *CHEK1* led to cell depletion during the CRISPR/Cas9 screen, moreover, inhibition of the encoded proteins also led to decreased cell viability (**Figure 16 a, b, k**), thus verifying our CRISPR/Cas9 results for those target genes. The KOPT-K1 T-ALL cell line was strongly sensitive to these three inhibitors, indicated by their low IC_{50} values (**Table 10**), which ranged between 63 - 2 nM. Additionally, the KOPT-K1 cell line showed strong sensitivity to the knock-out of the 26S proteasome subunit *PSMD1* and inhibition of the 26S proteasome complex with a low IC_{50} value of 2 nM. Likewise, knock-out of *TYMS* and treatment with the antimetabolite Floxuridine which perturbs the product of the TS protein led to decreased cell viability (IC_{50} = 10 nM). Furthermore, several of the 18 target genes leading to cell depletion during the CRISPR/Cas9 screen are associated with DNA repair processes and the PARP inhibitor Olaparib also led to decreased cell viability during cytotoxicity assays with an IC_{50} value of 635 nM. The cytotoxicity assays exposed an additional vulnerability, UBE2N, in the KOPT-K1 T-ALL cell line with an IC_{50} value of 380 nM that was not revealed during the CRISPR/Cas9 screen. Lastly, the T-ALL KOPT-K1 cell line was affected by the CDC25 inhibitor BN82002, however, the high IC_{50} value of 8.32 µM indicates that the cell line is not very sensitive to this inhibitor.

Table 10: *IC_{50} values from cytotoxicity assays were performed with the KOPT-K1 T-ALL cell line with the PC3 cell line serving as a negative control. Association of inhibitors with target genes that showed depletion during the CRISPR/Cas9 screen are indicated with either 'Hit' or 'No hit'. Assays were performed in technical triplicates and average IC_{50} values are shown. Representative of three independent experiment (n=3) except the IC_{50} value of Bevacizumab, BN82002, ML216, and NSC697923 which is representative of one experiment.*

Name	Inhibitor	KOPT-K1 IC_{50}	PC3 IC_{50}	Screen
AZD-4320	BCL-xL inhibitor	0.031 µM	> 1 µM	Hit
Barasertib	AURKB inhibitor	0.063 µM	> 1 µM	Hit
Bevacizumab	VEGF inhibitor	> 0.1 mg/ml	> 0.1 mg/ml	No hit

Bortezomib	Proteasome inhibitor	0.002 µM	> 0.01 µM	Hit
BN82002	CDC25 inhibitor	8.32 µM	> 100 µM	No hit
Floxuridine	Antimetabolite	0.01 µM	> 0.1 µM	Hit
ML216	BLM inhibitor	> 20 µM	> 20 µM	No hit
NSC697923	UBE2N inhibitor	0.38 µM	> 10 µM	No hit
Olaparib	PARP inhibitor	0.63 µM	> 10 µM	Hit
Paclitaxel	Microtubule stabilizer	0.002 µM	> 0.1 µM	Hit
Prexasertib	CHK inhibitor	0.002 µM	> 0.1 µM	Hit

To summarize, we selected 46 target genes which are upregulated in human T-cell cancers for a CRISPR/Cas9 screen in the T-ALL KOPT-K1 cell line which revealed 18 dependencies. Cytotoxicity assays, done in parallel, exposed several connections to the CRISPR/Cas9 results. The KOPT-K1 cell line was strongly sensitive to the inhibition of proteins, whose gene knock-out also led to depletion during the CRISPR/Cas9 screen: CHK1, PSMD1, TS, BCL-xL and AURKB. These key targetable vulnerabilities should be the focus of further testing and validation.

4 Discussion

Cancer development is a multi-step process in which different mutations have to accumulate in the same cell to alter pathways for cell differentiation, survival, proliferation and interaction with the environment (Hanahan, 2022; Hanahan & Weinberg, 2011). Several different mutations, chromosomal translocations or rearrangements are known to cause the hematopoietic malignancy T-ALL (Belver & Ferrando, 2016). However, many T-ALL patients exhibit mutations in the JAK/STAT pathway (Flex et al., 2008; Vainchenker & Constantinescu, 2013; Vicente et al., 2015), emphasizing the important role of this pathway in T-ALL (de Bock et al., 2018; Dorritie et al., 2014; Pham et al., 2018; Van Vlierberghe & Ferrando, 2012).

Genetic analysis of T-ALL patients found common key mutations within the JAK/STAT pathway that drive cancer progression, among them mutations in the *STAT5B* gene. The mutations in the *STAT5B* gene are predominantly located in the SH2-domain, a domain needed for the docking to a phosphorylated tyrosine on another protein (Shahmarvand et al., 2018). The STAT5B^{N642H} mutation is located in the SH2-domain and is associated with enhanced and prolonged tyrosine phosphorylation of the STAT5B TF (Bandapalli et al., 2014; de Araujo et al., 2019; Kiel et al., 2014; Nicolae et al., 2014; Rajala et al., 2013). Moreover, recent studies using mouse models showed its important role in several T-cell neoplasias (de Araujo et al., 2019; Pham et al., 2018).

The critical role of aberrant STAT5 signalling in the progression of several neoplasias has led to the investigation of possible STAT5 inhibitors for treatment (Sen et al., 2012; H. Yu & Jove, 2004; Zou et al., 2020). However, until today it was not possible to develop a STAT5 inhibitor approved for human treatment, among other things because a new cancer drug costs on average 1.5 - 3 billion Euros. Moreover, most new cancer drugs fail due to unwanted toxic side effects, poor pharmacodynamics or pharmacokinetic properties or limited tissue penetration such as reaching the bone marrow or passing the blood-brain barrier (Guan et al., 2021). Thus, currently developed STAT5 inhibitors are tool compounds to investigate targeted inhibition in

model systems. Because targeting the STAT5 TFs directly is challenging, we looked at downstream targets of hyperactive JAK/STAT signalling that might be easier to target in T-cell cancers such as T-ALL. During this thesis, such target genes previously selected based on RNA seq data were analysed with a CRISPR/Cas9 screen using the KOPT-K1 cell line which harbours a biallelic *STAT5B*^{N642H} mutation. The screen aimed to identify potential vulnerabilities that could then be targeted with inhibitors using cytotoxicity assays. We conducted the CRISPR/Cas9 screen using the two-vector system described by Shalem et al., 2014. The system requires the introduction of Cas9 and sgRNA separately with two different vectors into the KOPT-K1 target cell line.

Before the CRISPR/Cas9 screen could be performed with the introduction of sgRNAs against our selected target genes, KOPT-K1 cells with stable expression of the Cas9 protein needed to be generated. We tested the expression potential of the Cas9 gene from the vector using a transient transfection of HEK293T cells and detecting the Cas9 protein via Western blotting. The results of the Western blot showed strong expression of the Cas9 protein. Thus, this plasmid was used to introduce the Cas9 gene into the target cell line by Christina Wagner.

In order to accurately evaluate the effects of the sgRNA-induced knock-outs, the cells used for the CRISPR/Cas9 screen must have identical Cas9 functionality. Therefore, SCC were generated from the stable Cas9-expressing KOPT-K1 Cas9 cell line. The LentiCas9-Blast vector included a Blasticidin resistance gene for the selection of Cas9-positive cells. This resistance was used to ensure continued Cas9 expression during the SCC selection process. Ultimately, 21 SCC showed Cas9 expression on the Western blot.

The ongoing selection pressure of Blasticidin was necessary for the expression of Cas9 in the KOPT-K1 cell line. Initial Western blots, where the selection pressure was lifted after one initial Blasticidin selection, lacked a signal for Cas9 expression in all SCC. The need for continuous Blasticidin selection indicates that the KOPT-K1 cell

line might either lose or silence the Cas9 gene after the selection pressure is lifted. Moreover, the Cas9 signal intensity on the Western blot for the KOPT-K1 Cas9 SCC was less pronounced than the Cas9 signal for the transiently transfected HEK293T cells. Additionally, a Western blot done for the TCL38 PTCL-NOS cell line SMZ-1 transduced with the LentiCas9-Blast vector also showed a stronger signal for the Cas9 protein (supplementary, **Figure 18**). The necessity to keep the KOPT-K1 cell line under Blasticidin selection to uphold the Cas9 expression in addition to the low expression levels of the protein might indicate that the gene is silenced or lost because it imposes a metabolic burden on the KOPT-K1 Cas9 SCC. On the other hand, signalling pathways, transcription factors or specific proteins active in the KOPT-K1 cell line might also interfere with the expression of the Cas9 gene. A study in HEK293T cells by Chen et al. also showed that Cas9 expression changes the inherent gene expression of the cell and should thus be considered when performing a CRISPR/Cas9 screen (L. Chen et al., 2020).

Cas9 expression within the SCC was validated by Western blot, but still the expressed Cas9 protein may lack its intended function because unknown cellular factors or spontaneous mutations might interfere. An initial screen to test the functionality of the Cas9 protein in the 21 Cas9-expressing KOPT-K1 Cas9 SCC with the positive (*RPL17* sgRNA) and negative (*AAVS1* sgRNA) controls was thus crucial. The initial screen revealed two functional KOPT-K1 Cas9 SCC; SCC G6 was chosen for the implementation of the focused CRISPR/Cas9 screen.

We cloned and transduced the sgRNAs matching the 46 pre-selected target genes into the KOPT-K1 cell lines during the CRISPR/Cas9 screen. The sgRNA leads the Cas9 endonuclease to the target gene, leading to a double-strand break and subsequent knock-out of the gene (Shalem et al., 2014). The GFP-marker gene of the LentiGuide vector allowed the monitoring of transduced cells during the screening and thus the evaluation of the effect of the knock-out. We monitored cell depletion due to sgRNA-induced knock-out and illustrated the results in a condensed format by calculating the AUC over seven measurements. 20 genes showed an AUC in the

lower third of the AUC spectrum indicating strong depletion. The control genes *MYC* and *STAT5B*, which are direct members or downstream effectors of the JAK/STAT pathway and are considered essential in T-cell lines, were among these 20 genes, , which confirmed the technical success of the screen (Hennighausen & Robinson, 2008; Lord et al., 2000; Nozais et al., 2021).

In parallel to the CRISPR/Cas9 screen, we selected several targets from the target gene list for pharmacological inhibitor treatment via cytotoxicity assays. The T-ALL KOPT-K1 cell line was strongly sensitive (IC_{50} < 63 nM) to the inhibitors of the proteins associated with the genes *AURKB, BCL2L1, PMSD1, CHEK1*, and *TYMS,* in line with the results of the CRISPR/Cas9 screen, identifying these factors as key dependencies (**Figure 17**, marked in orange). Additionally, vulnerabilities in DNA damage repair processes and microtubule dynamics were revealed, indicated by the sensitivity of the T-ALL cell line KOPT-K1 to Olaparib (IC_{50} = 635 nM) and Paclitaxel (IC_{50} = 2 nM). Two additional potential dependencies, CDC25A and UBE2N, were uncovered by cytotoxicity assays that were not revealed by the CRISPR/Cas9 screen. However, the T-ALL KOPT-K1 cell line showed a low sensitivity (IC_{50} = 8.32 µM) to the CDC25 inhibitor BN82002 and thus this target is not considered a key vulnerability. The sensitivity of the KOPT-K1 cell line to the UBE2N inhibitor NSC697923 (IC_{50} = 380 nM), but not to the genetic knock-out of this gene, might be due to off-target effects of the drug.

The findings of the CRISPR/Cas9 screen and the cytotoxicity assays as well as found connections between the results are summarized in **Figure 17**. Genes depicted in orange in **Figure 17** are considered key dependencies and will be further discussed in the following paragraphs.

Knock-out of the *BCL2L1* gene showed cell depletion during the CRISPR/Cas9 screen. Inhibition of the protein BCL-xL, a member of the B-cell lymphoma-2 (BCL2) protein family, with the inhibitor AZD-4320 revealed an IC_{50} of 31 nM in the KOPT-K1 cell line. Accordingly, ChIP seq data (unpublished, GEO database repository

accession numbers GSE218858 and GSE219155) showing the STAT5B binding sites for several T-ALL cell lines (KOPT-K1, Loucy, SUP-T13 and Jurkat) revealed STAT5 binding to the *BCL2L1* locus for the two T-ALL cell lines KOPT-K1 and SUP-T13. STAT5B promoting BCL-xL expression was previously established thus supporting our results (De Groot et al., 2000; Lord et al., 2000). The BCL2 family has a role in controlling the mitochondrial membrane potential as well as apoptosis. The family includes pro- and anti-apoptotic members and BCL-xL belongs to the latter part of the family (Chipuk et al., 2010). Avoiding apoptosis is one of the hallmarks of cancer described by Hanahan & Weinberg, 2011; hence, the anti-apoptotic BCL-xL is often highly expressed in T-ALL and several other forms of leukaemia (Feng et al., 2010; Majid et al., 2008; Otake et al., 2007; Vaux et al., 1988). AZD-4320 is a small molecular inhibitor of BCL2 and BCL-xL and induced cell death in several hematopoietic cancer cell lines such as ALL and AML cell lines (Balachander et al., 2020). Female C.B-17 SCID mice implanted subcutaneously with T-ALL MOLT-4 cells by Balachander et al. also showed that the inhibitor leads to cancer regression. However, the inhibitor seems to also have an effect on platelets leading to thrombocytopenia (Balachander et al., 2020). Also, another BCL-2 family inhibitor Navitoclax showed a pharmacological effect on circulating platelets leading to thrombocytopenia, indicating an important role of BCL-xL in platelet survival (W. H. Wilson et al., 2010; Zhang et al., 2007). Therefore, BCL-xL represents a promising target in T-ALL. However, neither AZD-4320 nor Navitoclax are currently approved for clinical use.

The 26S proteasome complex mediates the degradation of ubiquitinated cellular proteins and thus supports cellular homeostasis. Two sub-complexes, the 20S core particle and the 19S regulatory particle, constitute the 26S proteasome (Livneh et al., 2016). The initial target gene list contained several components of the 26S proteasome complex: *PSMA5*, *PSMB2*, and *PSMD1*. However, during the CRISPR/Cas9 screen, only the knock-out of *PSMD1* led to cell depletion. The *PSMD1* gene encodes the PSMD1 protein, a non-ATPase subunit of the 19S regulatory particle, while proteins PSMA5 and PSMB2 are part of the 20S core particle. The 19S

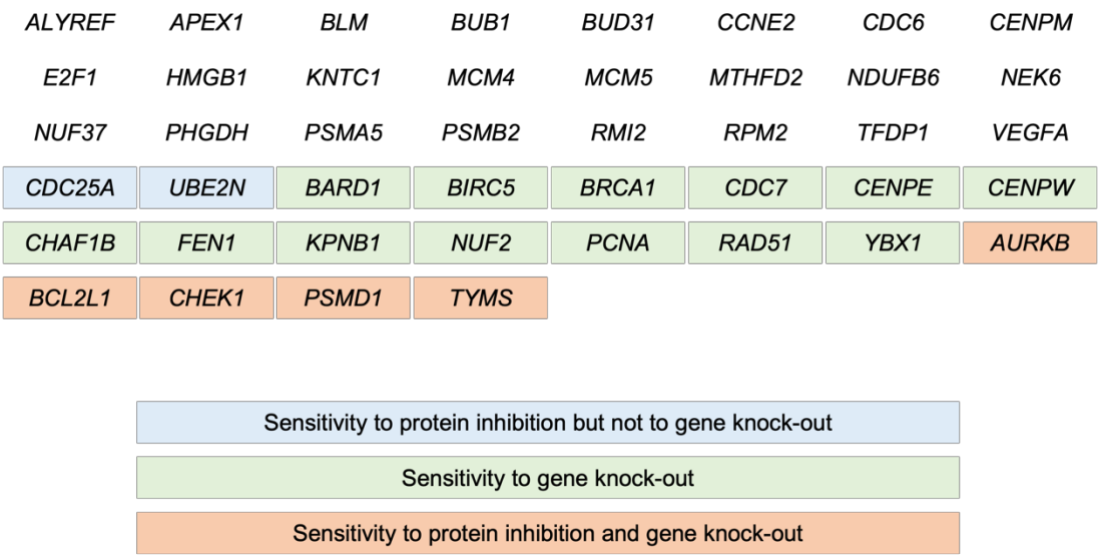

Figure 17: *Summary of results and connections of CRISPR/Cas9 screen and cytotoxicity assays using the T-ALL KOPT-K1 cell line.*

regulatory particle regulates the identification, binding, de-ubiquitination, unfolding, and protein translocation to the proteolytic chamber of the 20S core particle (Livneh et al., 2016). The results of the CRISPR/Cas9 screen suggest that the non-ATPase subunit PSMD1 of the 19S regulatory particle is essential for proteasome function; but the loss of two core particle subunits, PSMA5 and PSMB2, can be compensated. Additionally, the T-ALL cell line KOPT-K1 showed strong sensitivity to the inhibition of the 26S proteasomal complex with Bortezomib. Bortezomib is a dipeptide boronic acid derivative and can bind to a subunit of the 20S core particle to inhibit its activity. The anti-cancer mechanism of Bortezomib is yet unknown, but, one theory states that through the inhibition of the proteasome the inhibitory protein IκB, which is located in the cytoplasm, might not be degraded and thus, Bortezomib might help to suppress the NF-κB signalling pathway, which results in the downregulation of anti-apoptotic targets such as BCL-xL (Adams, 2004; D. Chen et al., 2011). A study in CML patients also identified upregulation of PSMD1 and demonstrated that knock-out of the *PSMD1* gene led to decreased viability of CML cells, supporting our results of PSMD1 upregulation in the TCL38 data set and the CRISPR/Cas9 screen in T-ALL cells. Apart from upregulated PSMD1, the CML cells also showed an NF-κB signature, and the

team of Bencomo-Alvarez suggested that PSMD1 and PSMD3 stabilize NF-κB protein expression in CML (Bencomo-Alvarez et al., 2021). Also, an aCGH analysis on SNK-6 and extranodal NK-cell lymphoma (NK-YS) cell lines also revealed a REL amplification on chromosome 2, enhancing NF-κB expression (Pölöske et al.; manuscript in preparation). Further studies to analyse REL amplification or IκB deletion in the KOPT-K1 cell line could reveal relevant insight into the NF- κB signature of this T-ALL cell line. Moreover, further studies must be done to uncover the mechanism of Bortezomib and the role of NF-κB, PSMD1 and PSMD3 and their connection to BCL-xL in T-ALL.

The *TYMS* gene encodes for the thymidylate synthase (TS) protein. TS is needed for the synthesis of deoxythymidine monophosphate (dTMP) from deoxyuridine monophosphate (dUMP), one of the basic building blocks of DNA. *De novo* DNA synthesis during cell division and DNA damage repair relies on the availability of dTMP (Berg et al., 2008). Knock-out of the *TYMS* gene led to cell depletion during the CRISPR/Cas9 screen. Also, the treatment of T-ALL KOPT-K1 cells with the antimetabolite Floxuridine led to decreased cell viability. Rapidly dividing cells need an abundance of dTMP; however, Floxuridine, a pyrimidine analogue, generates an imbalance in favour of dUMP which stalls DNA synthesis (Ewald et al., 2008; Huehls et al., 2011). Floxuridine is FDA-approved, however, it is used to treat metastatic liver cancers (Power & Kemeny, 2009). The antimetabolite Methotrexate also inhibits the synthesis of purines and pyrimidines and thus also inhibits TS. Methotrexate is currently used to treat cancers such as ALL but also as an immunosuppressive drug for long-term use in rheumatoid arthritis or systemic lupus erythematosus (Berg et al., 2008; Cipriani et al., 2014). However, Methotrexate treatment leads to severe side effects. Floxuridine might pose as an alternative to Methotrexate in the treatment of T-ALL, but, further studies are needed to determine the *in vivo* effects of Floxuridine on T-ALL cells and toxic side effects.

Knock-out of the *AURKB* gene caused depletion of the transduced cells during the CRISPR/Cas9 screen and the results of the inhibitor Barasertib (IC_{50} = 63 nM)

validated the importance of the kinase for the survival of the cells. Additionally, the microtubule stabilizer Paclitaxel (IC_{50} = 2 nM) acts downstream of AURKB, impairing correct chromosomal movement. AURKB is a serine/threonine kinase associated with the mitotic centromeres. It was shown that AURKB kinase activity is required for the localization of the mitotic centromere-associated kinesin (MCAK) to the centromere. MCAK regulates the depolymerisation of microtubules and is thus necessary for chromatin movement (Andrews et al., 2004; Gorbsky, 2004; Lan et al., 2004). The inhibitor Paclitaxel reduces the concentration of tubulin subunits needed for assembly but increases the percentage of subunits that are assembled. Microtubules assembled in the presence of Paclitaxel are protected from disassembly and thus lead to impaired chromosomal movement during mitosis (Schiff & Horwitz, 1980; Waters et al., 1998; Weaver, 2014). Mitotic checkpoints recognise the missegregation of the chromosomes, leading to mitotic arrest (Foley & Kapoor, 2013; Waters et al., 1998). Paclitaxel is FDA-approved for several forms of solid cancers such as breast cancer (M. Liu et al., 2022). However, Paclitaxel is only used off-label to treat lymphomas and leukaemias (Weaver, 2014).

We also targeted AURKB directly with the selective AURKB inhibitor Barasertib. A study by Yang et al. showed inhibition of cell proliferation and increased apoptosis in AML and ALL cell lines on account of Barasertib (Yang et al., 2007), supporting our results of the CRISPR/Cas9 screen and cytotoxicity assays with the T-ALL cell line KOPT-K1. Research by Jiang et al. found that AURKB phosphorylates MYC, preventing its proteasomal degradation. Further, MYC activates *AURKB* transcription, creating a positive feedback loop. MYC is a proto-oncogene often downregulated by post-translational modifications leading to its rapid degradation after being induced by several oncogenic TF including the STAT family members. MYC is encoded by three different genes (*MYC, MYCL, MYCN*) and these are often amplified in T-ALL and other hematopoietic cancers and the positive feedback loop stabilizes this deregulation of MYC (Jiang et al., 2020; Sanchez-Martin & Ferrando, 2017). MYC expression is increased by STAT5 signalling as it binds to the super-enhancer regions of the *MYC* gene (Pinz et al., 2016). Pinz et al. showed that in transformed Ba/F3 cells

the BET protein bromodomain-containing protein 2 (BRD2), a STAT5 co-factor, also localizes to the super-enhancer of the *MYC* gene which leads to the transcription of the gene (Pinz et al., 2016). *MYC* is thus a known downstream target of STAT5 and was therefore included in our target gene list as a control, and its knock-out also lead to depletion during the CRISPR/Cas9 screen (Lord et al., 2000). A hyperactive JAK/STAT pathway thus might increase MYC transcription, feeding into the positive feedback loop of MYC and AURKB. Pham et al. concluded that a mouse model expressing the GOF STAT5B^{N642H} develops a T-cell malignancy with continuous and enhanced levels of STAT5B^{N642H} tyrosine phosphorylation in transformed CD8^{+} T-cells. A DNA methylome analysis demonstrated decreased DNA methylation of possible EZH2-binding sites in STAT5B^{N642H}-transgenic mice, leading to changes in gene expression. The aurora kinase genes, especially *AURKB*, were among the differently methylated genes, resulting in AURKB enrichment in these cells (Pham et al., 2018). There are conflicting reports on the interaction of STAT5 and EZH2: on the one hand, STAT5 was reported to be essential for EZH2 recruitment to repress Ig κ-chain (*Igk)* transcription in progenitor B-cells but on the other hand, it was reported that EZH2 and STAT5 compete for binding sites and lastly, Pham et al. did not find a direct interaction between STAT5B^{N642H} and EZH2 (Katerndahl et al., 2017; Mandal et al., 2011; Pham et al., 2018; Yoo et al., 2015). The DNA methylome changes should be further investigated in T-ALL cell lines also due to the results of an aCGH analysis on SNK-6 and extranodal NK-YS cell lines that revealed an amplification of the DNA methyltransferase genes DNMT3A on chromosome 2 and DNMT3B on chromosome 20 (Pölöske et al.; manuscript in preparation). While we targeted AURKB with the selective AURKB inhibitor Barasertib, Pham et al. showed that T-cells harbouring the STAT5B^{N642H} mutation are also sensitive to the dual-specific JAK and Aurora kinase inhibitor AT9283 (Pham et al., 2018). Deregulation of AURKB and its association with MYC was also found in several different cancer types such as B-cell lymphoma and small-cell lung cancer (Den Hollander et al., 2010; Helfrich et al., 2016). Hence, cancers with MYC and JAK/STAT pathway deregulation, especially due to the STAT5B^{N642H} mutation, might be targetable by AUKRB inhibition with Barasertib or Paclitaxel.

The knock-out of the *CHEK1* gene led to the depletion of cells during the CRISPR/Cas9 screen. *CHEK1* encodes the CHK1 protein, a checkpoint kinase that can prevent cell cycle progression in the event of DNA damage (Flaggs et al., 1997; Q. Liu et al., 2000). The results of the CRISPR/Cas9 screen were validated by inhibiting the CHK1 protein with Prexasertib (IC_{50} = 2 nM). CHK1 is activated through phosphorylation by either the ATM or ATR kinase in response to DNA damage (Gatei et al., 2003; Q. Liu et al., 2000; Zhao & Piwnica-Worms, 2001). The kinases ATM and ATR are also able to activate BRCA1 to promote homologous repair of DNA damage (Foo et al., 2021). BRCA1 itself can again activate CHK1, creating a regulatory loop (Sato et al., 2012; Yarden et al., 2002). Moreover, activated CHK1 phosphorylates the phosphatase CDC25, which leads to mitotic arrest (Furnari et al., 1997, 1999). The *CDC25A* gene was also screened during the CRISPR/Cas9 screen but its knock-out did not affect cell survival and the KOPT-K1 cell line showed low sensitivity to the inhibition of the CDC25 protein with the inhibitor BN82002. This suggests that other pathways downstream of CHK1 are essential or compensate for the lack of CDC25A. In addition to BRCA1, CHK1 also shows a connection to AURKB. A study by Zachos et al. showed that CHK1-deficient cells fail the CHK1 spindle checkpoint which results in decreased AURKB activity. Further, CHK1 can phosphorylate AURKB, increasing its *in vitro* activity. The team of Zachos suggested that CHK1 checkpoint signalling is needed for AURKB regulation (Zachos et al., 2007). Cell depletion due to either *AURKB* or *CHEK1* knock-out suggests a central function of these two proteins, supported by their connection to each other but also to various other target genes of this screen such as MYC and the BRCA1/BARD1 complex.

The knock-out of either gene, *BRCA1* or *BARD1*, also led to cell depletion during the CRISPR/Cas9 screen. The BRCA1-associated ring domain protein 1 (BARD1) interacts with BRCA1 via its RING finger domain (Wu et al., 1996). The BRCA1/BARD1 complex is, among other processes, involved in DNA damage repair (Joukov et al., 2006; Westermark et al., 2003). The BRCA1/BARD1 complex joins with the recombinase RAD51 to promote homologous repair in the case of DNA

damage (Daley et al., 2014; Scully et al., 1997). RAD51 was also included in our target gene list and its knock-out also induced depletion during the CRISPR/Cas9 screen, indicating the importance of the BRCA1/BARD1/RAD51 complex for cell survival. It was also previously shown that STAT5 regulates TP53, the most frequently deleted or point-mutated (TP53*) tumour suppressor, via BRCA1, BARD1, and nucleophosmin (NPM1; Ren et al., 2016), connecting these genes to STAT5B hyperactivation. In myeloproliferative neoplasm (MPN), continuously active STAT5 can recruit normal but also mutated TP53, leading to a pathologic gene expression (Girardot et al., 2015). Mukhopadhyay et al. also showed that TP53 regulates STAT5A (Mukhopadhyay et al., 2016). While Fritsche et al. showed that TP53 represses cytokine-induced STAT5-mediated transcription (Fritsche et al., 1998). Due to limited time, we were unable to pharmacologically inhibit the BRCA1, BARD1, or RAD51 proteins specifically to verify the CRISPR/Cas9 screen on the protein level. However, we inhibited DNA damage repair processes with the PARP inhibitor Olaparib because, like *BRACA1*, *BARD1* and *RAD51*, several upregulated target genes showed association with DNA repair. The treatment of T-ALL KOPT-K1 cells with Olaparib led to decreased cell viability. In CML, high BCR-ABL1-dependent STAT5 activation has been linked to the production of reactive oxygen species (ROS), which induce DNA damage (Warsch et al., 2012). Thus, hyperactivation due to the STAT5B^{N642H} mutation might increase ROS production leading to severe genomic instability. To counteract the genomic instability, the cancer cells might upregulate proteins associated with the DNA damage repair pathways. However, inhibition with the PARP inhibitor Olaparib might tip this balance leading to cell death. Further studies must be conducted to determine the ROS levels in the T-ALL KOPT-K1 cell line as well as the specific influence of the STAT5B^{N642H} mutation on ROS production. Furthermore, the effect of protein inhibition of targets associated with DNA damage repair, *BARD1*, *BRACA1, CHAF1B, FEN1, RAD51, and YBX1* should be examined in more depth.

Moreover, the target genes, *BIRC5, CDC7 CENPE, CENPW, KPNB1, NUF2,* and *PCNA*, which also showed depletion during the CRISPR/Cas9 screen must be further tested for the effects of protein inhibition in the T-ALL cell line KOPT-K1 to verify

additional key dependencies. Especially, survivin (BIRC5), NUF2 and CENP-E might be potential vulnerabilities because these genes also show a connection to AURKB, forming an axis that could be further explored.

AURKB autophosphorylates itself to associate with the inner centromere protein (INCENP; Yasui et al., 2004). AURKB and INCENP are part of the chromosomal passenger complex (CPC) which also includes survivin. This complex orchestrates several processes including chromosome alignment, segregation, and histone modification (Gassmann et al., 2004; Vader et al., 2006; Wheatley et al., 2001). Survivin and AURKB bind different domains of INCENP, and the coincidental binding of both proteins stimulates a stronger activity of AURKB (Bolton et al., 2002). Thus, loss of survivin might result in a lower AURKB activity, leading to incorrect chromatin segregation during mitosis and to mitotic arrest. Moreover, survivin belongs to the inhibitor of apoptosis (IAP) family and is often highly expressed in transformed cells (Ambrosini et al., 1997); evading apoptosis is an important hallmark of cancer according to Hanahan & Weinbrg (Hanahan & Weinberg, 2011). Even though survivin presents as a promising target, therapeutic targeting of this protein has been challenging because the protein lacks deep 'pockets' to accommodate small-molecule inhibitors (Dang et al., 2017; Wheatley & Altieri, 2019). Nevertheless, indirect inhibition of survivin is possible with YM155 and further studies have to be conducted to investigate the effect of this inhibitor on the KOPT-K1 cell line (Rauch et al., 2014; Wheatley & Altieri, 2019).

The *NUF2* gene encodes the kinetochore protein NUF2 and the kinetochore protein complex is required for correct microtubule binding and chromosome movement during mitosis (Fukagawa, 2004). NUF2 is responsible for the stable attachment of microtubules and the localization of the centromere-associated protein E (CENP-E) to the kinetochore (DeLuca et al., 2002; D. Liu et al., 2007). CENP-E is a microtubule-based kinesin motor protein and is responsible for the movement of mono-oriented sister chromatids along the kinetochore fibres of already bioriented sister chromatid pairs (Kapoor et al., 2006). Its deletion leads to failed mitotic checkpoint signalling

(Mao et al., 2003, 2005; Yen et al., 1991). Currently, inhibitors for neither CENP-E nor NUF2 are available. Nonetheless, while CENP-E is not yet therapeutically targetable, there is a connection between CENP-E and the targetable AURKB. CENP-E and AURKB and the CPC participate in chromosome orientation and movement. AURKB phosphorylates kinetochore-associated factors to dissemble erroneously oriented kinetochore-microtubule fibres (Tanaka et al., 2002). Studies by Maia et al. showed that CENP-E and AURKB cooperate for chromosome biorientation, and anaphase start (Maia et al., 2010). Thus, the AURKB-CENP-E axis may be affected by either Barasertib or the microtubule stabilizer Paclitaxel.

In summary, we tested 46 target genes during this CRISPR/Cas9 screen in the T-ALL cell line KOPT-K1 which harbours the GOF mutation $STAT5B^{N642H}$. The screen aimed to identify potential targets downstream of hyperactive JAK/STAT signalling that could then be targeted with inhibitors. During this thesis, five key vulnerabilities – AURKB, BCL-xL, CHK1, PDSM1, and TS – were identified in the T-ALL KOPT-K1 cell line, leading to decreased cell viability due to gene knock-out or protein inhibition. Further studies are needed to determine if treatment with Barasertib, Paclitaxel, AZD-4320, Prexasertib, or Floxuridine also leads to T-ALL regression *in vivo* but also to decreased cell viability in other human T-cell cancers with hyperactive JAK/STAT signalling. Additionally, the CRISPR/Cas9 screen revealed dependencies on genes involved in DNA damage repair pathways, and the PARP inhibitor Olaparib led to decreased cell viability. Lastly, several of the genes that led to cell depletion during the CRISPR/Cas9 screen also show an association with AURKB; some are currently not targetable and could be affected by AURKB inhibition. However, genes involved in DNA damage response and the network around AURKB need to be further characterized and studied in T-ALL.

5 Bibliography

Abbas, A. K., Lichtman, A. H., & Pillai, S. (2021). *Cellular and Molecular Immunology* (10th ed.). Elsevier.

Adams, J. (2004). The proteasome: A suitable antineoplastic target. In *Nature Reviews Cancer* (Vol. 4, Issue 5, pp. 349–360). Nature Publishing Group. https://doi.org/10.1038/nrc1361

Aifantis, I., Raetz, E., & Buonamici, S. (2008). Molecular pathogenesis of T-cell leukaemia and lymphoma. In *Nature Reviews Immunology* (Vol. 8, Issue 5, pp. 380–390). Nature Publishing Group. https://doi.org/10.1038/nri2304

Ambrosini, G., Adida, C., & Altieri, D. C. (1997). A novel anti-apoptosis gene, survivin, expressed in cancer and lymphoma. *Nature Medicine*, *3*(8), 917–921. https://doi.org/10.1038/nm0897-917

Andrews, P. D., Ovechkina, Y., Morrice, N., Wagenbach, M., Duncan, K., Wordeman, L., & Swedlow, J. R. (2004). Aurora B regulates MCAK at the mitotic centromere. *Developmental Cell*, *6*(2), 253–268. https://doi.org/10.1016/S1534-5807(04)00025-5

Awasthi, N., Liongue, C., & Ward, A. C. (2021). STAT proteins: a kaleidoscope of canonical and non-canonical functions in immunity and cancer. In *Journal of Hematology and Oncology* (Vol. 14, Issue 1, pp. 1–17). BioMed Central. https://doi.org/10.1186/s13045-021-01214-y

Balachander, S. B., Criscione, S. W., Byth, K. F., Cidado, J., Adam, A., Lewis, P., Macintyre, T., Wen, S., Lawson, D., Burke, K., Lubinski, T., Tyner, J. W., Kurtz, S. E., McWeeney, S. K., Varnes, J., Diebold, R. B., Gero, T., Ioannidis, S., Hennessy, E. J., … Gibbons, F. D. (2020). AZD4320, a dual inhibitor of bcl-2 and bcl-xl, induces tumor regression in hematologic cancer models without dose-limiting thrombocytopenia. *Clinical Cancer Research*, *26*(24), 6535–6549. https://doi.org/10.1158/1078-0432.CCR-20-0863

Bandapalli, O. R., Schuessele, S., Kunz, J. B., Rausch, T., Stütz, A. M., Tal, N., Geron, I., Gershman, N., Izraeli, S., Eilers, J., Vaezipour, N., Kirschner-Schwabe, R., Hof, J., von Stackelberg, A., Schrappe, M., Stanulla, M., Zimmermann, M., Koehler, R., Avigad, S., … Kulozik, A. E. (2014). The activating STAT5B N642H mutation is a common abnormality in pediatric T-cell acute lymphoblastic leukemia and confers a higher risk of relapse. *Haematologica*, *99*(10), e188–e192. https://doi.org/10.3324/HAEMATOL.2014.104992

Bar-Natan, M., Nelson, E. A., Xiang, M., & Frank, D. A. (2012). STAT signaling in the pathogenesis and treatment of myeloid malignancies. *JAK-STAT*, *1*(2), 55–64. https://doi.org/10.4161/jkst.20006

Belver, L., & Ferrando, A. (2016). The genetics and mechanisms of T cell acute lymphoblastic leukaemia. In *Nature Reviews Cancer* (Vol. 16, Issue 8, pp. 494–507). Nature Publishing Group. https://doi.org/10.1038/nrc.2016.63

Bencomo-Alvarez, A. E., Rubio, A. J., Olivas, I. M., Gonzalez, M. A., Ellwood, R., Fiol, C. R., Eide, C. A., Lara, J. J., Barreto-Vargas, C., Jave-Suarez, L. F., Nteliopoulos, G., Reid, A. G., Milojkovic, D., Druker, B. J., Apperley, J., Khorashad, J. S., & Eiring, A. M. (2021). Proteasome 26S subunit, non-ATPases 1 (PSMD1) and 3 (PSMD3), play an oncogenic role in chronic myeloid leukemia by stabilizing nuclear factor-kappa B. *Oncogene*, *40*(15), 2697–2710. https://doi.org/10.1038/s41388-021-01732-6

Berg, J. M., Tymoczko, J. L., & Stryer, L. (2008). Biochemistry. In *WH Freeman: New York.*

Bhattacharya, S., Eckner, R., Grossman, S., Oldread, E., Arany, Z., D'Andrea, A., & Livingston, D. M. (1996). Cooperation of Stat2 and p300/CBP in signalling induced by interferon- α. *Nature*, *383*(6598), 344–347. https://doi.org/10.1038/383344a0

Bolton, M. A., Lan, W., Powers, S. E., McCleland, M. L., Kuang, J., & Stukenberg, P. T. (2002). Aurora B kinase exists in a complex with survivin and INCENP and its kinase activity is stimulated by survivin binding and phosphorylation. *Molecular Biology of the Cell*, *13*(9), 3064–3077. https://doi.org/10.1091/mbc.E02-02-0092

Bousoik, E., & Montazeri Aliabadi, H. (2018). "Do We Know Jack" About JAK? A Closer Look at JAK/STAT Signaling Pathway. In *Frontiers in Oncology* (Vol. 8, p. 287). Frontiers Media S.A. https://doi.org/10.3389/fonc.2018.00287

Brachet-Botineau, M., Polomski, M., Neubauer, H. A., Juen, L., Hédou, D., Viaud-Massuard, M. C., Prié, G., & Gouilleux, F. (2020). Pharmacological inhibition of oncogenic STAT3 and STAT5 signaling in hematopoietic cancers. *Cancers*, *12*(1), 1–48. https://doi.org/10.3390/cancers12010240

Buratovic, M. A., & Jackson-Grusby, L. (2016). *Salem Health: Cancer*. GREY HOUSE PUBLISHING MLA 9th Edition (Modern Language Assoc.) Buratovich, Michael A., and Laurie Jackson-Grusby. Cancer. Salem Press, 2016. APA 7th Edition (American Psychological Assoc.) Buratovich, M. A., & Jackson-Grusby, L.

(2016). Cancer: Vol. Secon.

Burchill, M. A., Goetz, C. A., Prlic, M., O'Neil, J. J., Harmon, I. R., Bensinger, S. J., Turka, L. A., Brennan, P., Jameson, S. C., & Farrar, M. A. (2003). Distinct Effects of STAT5 Activation on CD4+ and CD8+ T Cell Homeostasis: Development of CD4+CD25+ Regulatory T Cells versus CD8+ Memory T Cells. *The Journal of Immunology*, *171*(11), 5853–5864. https://doi.org/10.4049/jimmunol.171.11.5853

Caldenhoven, E., Van Dijk, T. B., Solari, R., Armstrong, J., Raaijmakers, J. A. M., Lammers, J. W. J., Koenderman, L., & De Groot, R. P. (1996). STAT3β, a splice variant of transcription factor STAT3, is a dominant negative regulator of transcription. *Journal of Biological Chemistry*, *271*(22), 13221–13227. https://doi.org/10.1074/jbc.271.22.13221

Chen, D., Frezza, M., Schmitt, S., Kanwar, J., & P. Dou, Q. (2011). Bortezomib as the First Proteasome Inhibitor Anticancer Drug: Current Status and Future Perspectives. *Current Cancer Drug Targets*, *11*(3), 239–253. https://doi.org/10.2174/156800911794519752

Chen, L., Zhang, H., Zhang, L., Li, W., Fan, F., Wu, X., Wu, X., & Lin, J. (2020). Cas9 Protein Triggers Differential Expression of Inherent Genes Especially NGFR Expression in 293T Cells. *Cellular and Molecular Bioengineering*, *13*(1), 61–72. https://doi.org/10.1007/s12195-019-00606-y

Chen, Y., Wen, R., Yang, S., Schuman, J., Zhang, E. E., Yi, T., Feng, G. S., & Wang, D. (2003). Identification of Shp-2 as a Stat5A phosphatase. *Journal of Biological Chemistry*, *278*(19), 16520–16527. https://doi.org/10.1074/jbc.M210572200

Chipuk, J. E., Moldoveanu, T., Llambi, F., Parsons, M. J., & Green, D. R. (2010). The BCL-2 Family Reunion. In *Molecular Cell* (Vol. 37, Issue 3, pp. 299–310). NIH Public Access. https://doi.org/10.1016/j.molcel.2010.01.025

Cho, S. S., Bacon, C. M., Sudarshan, C., Rees, R. C., Finbloom, D., Pine, R., & O'Shea, J. J. (1996). Activation of STAT4 by IL-12 and IFN-alpha: evidence for the involvement of ligand-induced tyrosine and serine phosphorylation. *The Journal of Immunology*, *157*(11), 4781–4789. https://doi.org/10.4049/jimmunol.157.11.4781

Choudhary, C., Brandts, C., Schwable, J., Tickenbrock, L., Sargin, B., Ueker, A., Böhmer, F. D., Berdel, W. E., Müller-Tidow, C., & Serve, H. (2007). Activation mechanisms of STAT5 by oncogenic Flt3-ITD. *Blood*, *110*(1), 370–374.

https://doi.org/10.1182/blood-2006-05-024018

Cipriani, P., Ruscitti, P., Carubbi, F., Liakouli, V., & Giacomelli, R. (2014). Methotrexate: An old new drug in autoimmune disease. In *Expert Review of Clinical Immunology* (Vol. 10, Issue 11, pp. 1519–1530). Taylor & Francis. https://doi.org/10.1586/1744666X.2014.962996

Cock, P. J. (2009). Biopython: freely available Python tools for computational molecular biology and bioinformatics. *Bioinformatics*, *25*(11), 1422–1423.

Daley, J. M., Gaines, W. A., Kwon, Y., & Sung, P. (2014). Regulation of DNA pairing in homologous recombination. *Cold Spring Harbor Perspectives in Biology*, *6*(11), 1–15. https://doi.org/10.1101/cshperspect.a017954

Dang, C. V., Reddy, E. P., Shokat, K. M., & Soucek, L. (2017). Drugging the "undruggable" cancer targets. In *Nature Reviews Cancer* (Vol. 17, Issue 8, pp. 502–508). Nature Publishing Group. https://doi.org/10.1038/nrc.2017.36

de Araujo, E. D., Erdogan, F., Neubauer, H. A., Meneksedag-Erol, D., Manaswiyoungkul, P., Eram, M. S., Seo, H. S., Qadree, A. K., Israelian, J., Orlova, A., Suske, T., Pham, H. T. T., Boersma, A., Tangermann, S., Kenner, L., Rülicke, T., Dong, A., Ravichandran, M., Brown, P. J., … Gunning, P. T. (2019). Structural and functional consequences of the STAT5BN642H driver mutation. *Nature Communications*, *10*(1), 1–15. https://doi.org/10.1038/s41467-019-10422-7

de Bock, C. E., Demeyer, S., Degryse, S., Verbeke, D., Sweron, B., Gielen, O., Vandepoel, R., Vicente, C., Bempt, M. Vanden, Dagklis, A., Geerdens, E., Bornschein, S., Gijsbers, R., Soulier, J., Meijerink, J. P., Heinäniemi, M., Teppo, S., Bouvy-Liivrand, M., Lohi, O., … Cools, J. (2018). HOXA9 cooperates with activated JAK/STAT signaling to drive leukemia development. *Cancer Discovery*, *8*(5), 616–631. https://doi.org/10.1158/2159-8290.CD-17-0583

De Groot, R. P., Raaijmakers, J. A. M., Lammers, J. W. J., & Koenderman, L. (2000). STAT5-dependent cyclinD1 and bcl-xL expression in Bcr-Abl-transformed cells. *Molecular Cell Biology Research Communications*, *3*(5), 299–305. https://doi.org/10.1006/mcbr.2000.0231

Degryse, S., Bornschein, S., De Bock, C. E., Leroy, E., Bempt, M. Vanden, Demeyer, S., Jacobs, K., Geerdens, E., Gielen, O., Soulier, J., Harrison, C. J., Constantinescu, S. N., & Cools, J. (2018). Mutant JAK3 signaling is increased by loss of wild-type JAK3 or by acquisition of secondary JAK3 mutations in T-

ALL. *Blood*, *131*(4), 421–425. https://doi.org/10.1182/blood-2017-07-797597

Delgoffe, G. M., & Vignali, D. A. A. (2013a). STAT heterodimers in immunity: A mixed message or a unique signal? *JAK-STAT*, *2*(1), e23060. https://doi.org/10.4161/JKST.23060

Delgoffe, G. M., & Vignali, D. A. A. (2013b). STAT heterodimers in immunity: A mixed message or a unique signal? *JAK-STAT*, *2*(1), e23060. https://doi.org/10.4161/jkst.23060

DeLuca, J. G., Moree, B., Hickey, J. M., Kilmartin, J. V., & Salmon, E. D. (2002). hNuf2 inhibition blocks stable kinetochore–microtubule attachment and induces mitotic cell death in HeLa cells. *Journal of Cell Biology*, *159*(4), 549–555. https://doi.org/10.1083/JCB.200208159

Den Hollander, J., Rimpi, S., Doherty, J. R., Rudelius, M., Buck, A., Hoellein, A., Kremer, M., Graf, N., Scheerer, M., Hall, M. A., Goga, A., Von Bubnoff, N., Duyster, J., Peschel, C., Cleveland, J. L., Nilsson, J. A., & Keller, U. (2010). Aurora kinases A and B are up-regulated by Myc and are essential for maintenance of the malignant state. *Blood*, *116*(9), 1498–1505. https://doi.org/10.1182/blood-2009-11-251074

Dorritie, K. A., McCubrey, J. A., & Johnson, D. E. (2014). STAT transcription factors in hematopoiesis and leukemogenesis: Opportunities for therapeutic intervention. In *Leukemia* (Vol. 28, Issue 2, pp. 248–257). Nature Publishing Group. https://doi.org/10.1038/leu.2013.192

Drugs@FDA: FDA-Approved Drugs. (2023). Fda. https://www.accessdata.fda.gov/scripts/cder/daf/index.cfm

Ewald, B., Sampath, D., & Plunkett, W. (2008). Nucleoside analogs: Molecular mechanisms signaling cell death. In *Oncogene* (Vol. 27, Issue 50, pp. 6522–6537). Nature Publishing Group. https://doi.org/10.1038/onc.2008.316

Fattizzo, B., Rosa, J., Giannotta, J. A., Baldini, L., & Fracchiolla, N. S. (2020). The Physiopathology of T- Cell Acute Lymphoblastic Leukemia: Focus on Molecular Aspects. In *Frontiers in Oncology* (Vol. 10, p. 273). Frontiers Media SA. https://doi.org/10.3389/fonc.2020.00273

Flex, E., Petrangeli, V., Stella, L., Chiaretti, S., Hornakova, T., Knoops, L., Ariola, C., Fodale, V., Clappier, E., Paoloni, F., Martinelli, S., Fragale, A., Sanchez, M., Tavolaro, S., Messina, M., Cazzaniga, G., Camera, A., Pizzolo, G., Tornesello, A., … Tartaglia, M. (2008). Somatically acquired JAK1 mutations in adult acute

lymphoblastic leukemia. *Journal of Experimental Medicine*, *205*(4), 751–758. https://doi.org/10.1084/jem.20072182

Foley, E. A., & Kapoor, T. M. (2013). Microtubule attachment and spindle assembly checkpoint signalling at the kinetochore. In *Nature Reviews Molecular Cell Biology* (Vol. 14, Issue 1, pp. 25–37). Nat Rev Mol Cell Biol. https://doi.org/10.1038/nrm3494

Foo, T. K., Vincelli, G., Huselid, E., Her, J., Zheng, H., Simhadri, S., Wang, M., Huo, Y., Li, T., Yu, X., Li, H., Zhao, W., Bunting, S. F., & Xia, B. (2021). Atr/atm-mediated phosphorylation of brca1 t1394 promotes homologous recombinational repair and g2-m checkpoint maintenance. *Cancer Research*, *81*(18), 4676–4684. https://doi.org/10.1158/0008-5472.CAN-20-2723

Fritsche, M., Mundt, M., Merkle, C., Jähne, R., & Groner, B. (1998). P53 suppresses cytokine induced, Stat5 mediated activation of transcription. *Molecular and Cellular Endocrinology*, *143*(1–2), 143–154. https://doi.org/10.1016/S0303-7207(98)00140-3

Furnari, B., Blasina, A., Boddy, M. N., McGowan, C. H., & Russell, P. (1999). Cdc25 inhibited in vivo and in vitro by checkpoint kinases Cds1 and Chk1. *Molecular Biology of the Cell*, *10*(4), 833–845. https://doi.org/10.1091/mbc.10.4.833

Furnari, B., Rhind, N., & Russell, P. (1997). Cdc25 mitotic inducer targeted by Chk1 DNA damage checkpoint kinase. *Science*, *277*(5331), 1495–1497. https://doi.org/10.1126/science.277.5331.1495

Gatei, M., Sloper, K., Sörensen, C., Syljuäsen, R., Falck, J., Hobson, K., Savage, K., Lukas, J., Zhou, B. B., Bartek, J., & Khanna, K. K. (2003). Ataxia-telangiectasia-mutated (ATM) and NBS1-dependent phosphorylation of Chk1 on Ser-317 in response to ionizing radiation. *Journal of Biological Chemistry*, *278*(17), 14806–14811. https://doi.org/10.1074/jbc.M210862200

Girardot, M., Pecquet, C., Chachoua, I., Van Hees, J., Guibert, S., Ferrant, A., Knoops, L., Baxter, E. J., Beer, P. A., Giraudier, S., Moriggl, R., Vainchenker, W., Green, A. R., & Constantinescu, S. N. (2015). Persistent STAT5 activation in myeloid neoplasms recruits p53 into gene regulation. *Oncogene*, *34*(10), 1323–1332. https://doi.org/10.1038/onc.2014.60

Gorbsky, G. J. (2004). Mitosis: MCAK under the Aura of Aurora B. In *Current Biology* (Vol. 14, Issue 9, pp. R346–R348). Cell Press. https://doi.org/10.1016/j.cub.2004.04.022

Guan, Z., Lan, H., Cai, X., Zhang, Y., Liang, A., & Li, J. (2021). Blood–Brain Barrier, Cell Junctions, and Tumor Microenvironment in Brain Metastases, the Biological Prospects and Dilemma in Therapies. In *Frontiers in Cell and Developmental Biology* (Vol. 9, p. 2159). Frontiers Media S.A. https://doi.org/10.3389/fcell.2021.722917

Hanahan, D. (2022). Hallmarks of Cancer: New Dimensions. *Cancer Discovery*, *12*(1), 31–46. https://doi.org/10.1158/2159-8290.CD-21-1059

Hanahan, D., & Weinberg, R. A. (2011). Hallmarks of cancer: The next generation. *Cell*, *144*(5), 646–674. https://doi.org/10.1016/j.cell.2011.02.013

Haspel, R. L., Salditt-Georgieff, M., & Darnell, J. E. (1996). The rapid inactivation of nuclear tyrosine phosphorylated Stat1 depends upon a protein tyrosine phosphatase. *EMBO Journal*, *15*(22), 6262–6268. https://doi.org/10.1002/j.1460-2075.1996.tb01016.x

Helfrich, B. A., Kim, J., Gao, D., Chan, D. C., Zhang, Z., Tan, A. C., & Bunn, P. A. (2016). Barasertib (AZD1152), a small molecule Aurora B inhibitor, inhibits the growth of SCLC cell lines in vitro and in vivo. *Molecular Cancer Therapeutics*, *15*(10), 2314–2322. https://doi.org/10.1158/1535-7163.MCT-16-0298

Hennighausen, L., & Robinson, G. W. (2008). Interpretation of cytokine signaling through the transcription factors STAT5A and STAT5B. *Genes and Development*, *22*(6), 711–721. https://doi.org/10.1101/gad.1643908

Heppler, L. N., & Frank, D. A. (2017). Targeting Oncogenic Transcription Factors: Therapeutic Implications of Endogenous STAT Inhibitors. In *Trends in Cancer* (Vol. 3, Issue 12, pp. 816–827). NIH Public Access. https://doi.org/10.1016/j.trecan.2017.10.004

Hermiston, M. L., Xu, Z., & Weiss, A. (2003). CD45: A critical regulator of signaling thresholds in immune cells. In *Annual Review of Immunology* (Vol. 21, pp. 107–137). Annu Rev Immunol. https://doi.org/10.1146/annurev.immunol.21.120601.140946

Hoelbl, A., Kovacic, B., Kerenyi, M. A., Simma, O., Warsch, W., Cui, Y., Beug, H., Hennighausen, L., Moriggl, R., & Sexl, V. (2006). Clarifying the role of Stat5 in lymphoid development and Abelson-induced transformation. *Blood*, *107*(12), 4898–4906. https://doi.org/10.1182/blood-2005-09-3596

Hoelbl, A., Schuster, C., Kovacic, B., Zhu, B., Wickre, M., Hoelzl, M. A., Fajmann, S., Grebien, F., Warsch, W., Stengl, G., Hennighausen, L., Poli, V., Beug, H.,

Moriggl, R., & Sexl, V. (2010). Stat5 is indispensable for the maintenance of Bcr/Abl-positive leukaemia. *EMBO Molecular Medicine*, *2*(3), 98–110. https://doi.org/10.1002/emmm.201000062

Hoelzer, D., Thiel, E., Arnold, R., Beck, J., Beelen, D. W., Bornhäuser, M., Bunjes, D., Ditz, D., Dührsen, U., Finke, J., Horst, H. A., Kobbe, G., Kolb, H. J., Kreuzer, K. A., Kröger, N., Lipp, T., Schaich, M., Schmid, M., Schwartz, S., … Gökbuget, N. (2009). Successful Subtype Oriented Treatment Strategies in Adult T-All; Results of 744 Patients Treated in Three Consecutive GMALL Studies. *Blood*, *114*(22), 324–324. https://doi.org/10.1182/blood.v114.22.324.324

Horvath, C. M., & Darnell, J. E. (1997). The state of the STATs: Recent developments in the study of signal transduction to the nucleus. *Current Opinion in Cell Biology*, *9*(2), 233–239. https://doi.org/10.1016/S0955-0674(97)80067-1

Hsiao, W. Y., Lin, Y. C., Liao, F. H., Chan, Y. C., & Huang, C. Y. (2015). Dual-specificity phosphatase 4 regulates STAT5 protein stability and helper T cell polarization. *PLoS ONE*, *10*(12). https://doi.org/10.1371/journal.pone.0145880

Huang, E. Y., Gallegos, A. M., Richards, S. M., Lehar, S. M., & Bevan, M. J. (2003). Surface Expression of Notch1 on Thymocytes: Correlation with the Double-Negative to Double-Positive Transition. *The Journal of Immunology*, *171*(5), 2296–2304. https://doi.org/10.4049/jimmunol.171.5.2296

Huang, M., Qian, F., Hu, Y., Ang, C., Li, Z., & Wen, Z. (2002). Chromatin-remodelling factor BRG1 selectively activates a subset of interferon-α-inducible genes. *Nature Cell Biology*, *4*(10), 774–781. https://doi.org/10.1038/ncb855

Huehls, A. M., Wagner, J. M., Huntoon, C. J., Geng, L., Erlichman, C., Patel, A. G., Kaufmann, S. H., & Karnitz, L. M. (2011). Poly(ADP-ribose) polymerase inhibition synergizes with 5-fluorodeoxyuridine but not 5-fluorouracil in ovarian cancer cells. *Cancer Research*, *71*(14), 4944–4954. https://doi.org/10.1158/0008-5472.CAN-11-0814

Imada, K., & Leonard, W. J. (2000). The Jak-STAT pathway. In *Molecular Immunology* (Vol. 37, Issues 1–2, pp. 1–11). Mol Immunol. https://doi.org/10.1016/S0161-5890(00)00018-3

Jiang, J., Wang, J., Yue, M., Cai, X., Wang, T., Wu, C., Su, H., Wang, Y., Han, M., Zhang, Y., Zhu, X., Jiang, P., Li, P., Sun, Y., Xiao, W., Feng, H., Qing, G., & Liu, H. (2020). Direct Phosphorylation and Stabilization of MYC by Aurora B Kinase Promote T-cell Leukemogenesis. *Cancer Cell*, *37*(2), 200-215.e5.

https://doi.org/10.1016/j.ccell.2020.01.001

Joukov, V., Groen, A. C., Prokhorova, T., Gerson, R., White, E., Rodriguez, A., Walter, J. C., & Livingston, D. M. (2006). The BRCA1/BARD1 heterodimer modulates ran-dependent mitotic spindle assembly. *Cell*, *127*(3), 539–552. https://doi.org/10.1016/j.cell.2006.08.053

Kanai, T., Seki, S., Jenks, J. A., Kohli, A., Kawli, T., Martin, D. P., Snyder, M., Bacchetta, R., & Nadeau, K. C. (2014). Identification of STAT5A and STAT5B Target Genes in Human T Cells. *PLoS ONE*, *9*(1), 86790. https://doi.org/10.1371/JOURNAL.PONE.0086790

Kapoor, T. M., Lampson, M. A., Hergert, P., Cameron, L., Cimini, D., Salmon, E. D., McEwen, B. F., & Khodjakov, A. (2006). Chromosomes can congress to the metaphase plate before biorientation. *Science*, *311*(5759), 388–391. https://doi.org/10.1126/science.1122142

Katerndahl, C. D. S., Heltemes-Harris, L. M., Willette, M. J. L., Henzler, C. M., Frietze, S., Yang, R., Schjerven, H., Silverstein, K. A. T., Ramsey, L. B., Hubbard, G., Wells, A. D., Kuiper, R. P., Scheijen, B., Van Leeuwen, F. N., Müschen, M., Kornblau, S. M., & Farrar, M. A. (2017). Antagonism of B cell enhancer networks by STAT5 drives leukemia and poor patient survival. *Nature Immunology*, *18*(6), 694–704. https://doi.org/10.1038/ni.3716

Kiel, M. J., Velusamy, T., Rolland, D., Sahasrabuddhe, A. A., Chung, F., Bailey, N. G., Schrader, A., Li, B., Li, J. Z., Ozel, A. B., Betz, B. L., Miranda, R. N., Medeiros, L. J., Zhao, L., Herling, M., Lim, M. S., & Elenitoba-Johnson, K. S. J. (2014). Integrated genomic sequencing reveals mutational landscape of T-cell prolymphocytic leukemia. *Blood*, *124*(9), 1460. https://doi.org/10.1182/blood-2014-03-559542

Kim, B. R., Ha, J., Kang, E., & Cho, S. (2020). Regulation of signal transducer and activator of transcription 3 activation by dual-specificity phosphatase 3. *BMB Reports*, *53*(6), 335–340. https://doi.org/10.5483/BMBRep.2020.53.6.054

Kim, M., Morales, L. D., Jang, I. S., Cho, Y. Y., & Kim, D. J. (2018). Protein tyrosine phosphatases as potential regulators of STAT3 signaling. In *International Journal of Molecular Sciences* (Vol. 19, Issue 9). Multidisciplinary Digital Publishing Institute (MDPI). https://doi.org/10.3390/ijms19092708

Kim, T. K., & Maniatis, T. (1996). Regulation of interferon-γ-activated STAT1 by the ubiquitin-proteasome pathway. *Science*, *273*(5282), 1717–1719.

https://doi.org/10.1126/science.273.5282.1717

Kim, W., Bird, G. H., Neff, T., Guo, G., Kerenyi, M. A., Walensky, L. D., & Orkin, S. H. (2013). Targeted disruption of the EZH2-EED complex inhibits EZH2-dependent cancer. *Nature Chemical Biology*, *9*(10), 643–650. https://doi.org/10.1038/nchembio.1331

Koch, U., Fiorini, E., Benedito, R., Besseyrias, V., Schuster-Gossler, K., Pierres, M., Manley, N. R., Duarte, A., MacDonald, H. R., & Radtke, F. (2008). Delta-like 4 is the essential, nonredundant ligand for Notchl during thymic T cell lineage commitment. *Journal of Experimental Medicine*, *205*(11), 2515–2523. https://doi.org/10.1084/jem.20080829

Kollmann, S., Grundschober, E., Maurer, B., Warsch, W., Grausenburger, R., Edlinger, L., Huuhtanen, J., Lagger, S., Hennighausen, L., Valent, P., Decker, T., Strobl, B., Mueller, M., Mustjoki, S., Hoelbl-Kovacic, A., & Sexl, V. (2019). Twins with different personalities: STAT5B—but not STAT5A—has a key role in BCR/ABL-induced leukemia. *Leukemia*, *33*(7), 1583–1597. https://doi.org/10.1038/s41375-018-0369-5

Kontro, M., Kuusanmäki, H., Eldfors, S., Pemovska, T., Rajala, H. L. M., Edgren, H., Ellonen, P., Lagström, S., Lundán, T., Kallioniemi, O., Mustjoki, S., Porkka, K., & Heckman, C. (2013). Novel Activating STAT5B Mutations As Drivers Of T-ALL. *Blood*, *122*(21), 3863–3863. https://doi.org/10.1182/blood.v122.21.3863.3863

Kroeze, E., Loeffen, J. L. C., Poort, V. M., & Meijerink, J. P. P. (2020). T-cell lymphoblastic lymphoma and leukemia: Different diseases from a common premalignant progenitor? In *Blood Advances* (Vol. 4, Issue 14, pp. 3466–3473). American Society of Hematology. https://doi.org/10.1182/bloodadvances.2020001822

Lan, W., Zhang, X., Kline-Smith, S. L., Rosasco, S. E., Barrett-Wilt, G. A., Shabanowitz, J., Hunt, D. F., Walczak, C. E., & Stukenberg, P. T. (2004). Aurora B phosphorylates centromeric MCAK and regulates its localization and microtubule depolymerization activity. *Current Biology*, *14*(4), 273–286. https://doi.org/10.1016/S0960-9822(04)00064-8

Leonard, W. J., & O'Shea, J. J. (1998). Jaks and STATs: Biological implications. In *Annual Review of Immunology* (Vol. 16, pp. 293–322). Annu Rev Immunol. https://doi.org/10.1146/annurev.immunol.16.1.293

Lew, D. J., Decker, T., Strehlow, I., & Darnell, J. E. (1991). Overlapping elements in

the guanylate-binding protein gene promoter mediate transcriptional induction by alpha and gamma interferons. *Molecular and Cellular Biology*, *11*(1), 182–191. https://doi.org/10.1128/mcb.11.1.182-191.1991

Liu, D., Ding, X., Du, J., Cai, X., Huang, Y., Ward, T., Shaw, A., Yang, Y., Hu, R., Jin, C., & Yao, X. (2007). Human NUF2 interacts with centromere-associated protein E and is essential for a stable spindle microtubule-kinetochore attachment. *Journal of Biological Chemistry*, *282*(29), 21415–21424. https://doi.org/10.1074/jbc.M609026200

Liu, M., Li, Y., Zhang, C., & Zhang, Q. (2022). Role of aurora kinase B in regulating resistance to paclitaxel in breast cancer cells. *Human Cell*, *35*(2), 678–693. https://doi.org/10.1007/s13577-022-00675-8

Liu, Q., Guntuku, S., Cui, X. S., Matsuoka, S., Cortez, D., Tamai, K., Luo, G., Carattini-Rivera, S., DeMayo, F., Bradley, A., Donehower, L. A., & Elledge, S. J. (2000). Chk1 is an essential kinase that is regulated by Atr and required for the G2/M DNA damage checkpoint. *Genes and Development*, *14*(12), 1448–1459. https://doi.org/10.1101/gad.14.12.1448

Liu, X., Robinson, G. W., Wagner, K. U., Garrett, L., Wynshaw-Boris, A., & Hennighausen, L. (1997). Stat5a is mandatory for adult mammary gland development and lactogenesis. *Genes and Development*, *11*(2), 179–186. https://doi.org/10.1101/gad.11.2.179

Livneh, I., Cohen-Kaplan, V., Cohen-Rosenzweig, C., Avni, N., & Ciechanover, A. (2016). The life cycle of the 26S proteasome: From birth, through regulation and function, and onto its death. In *Cell Research* (Vol. 26, Issue 8, pp. 869–885). Nature Publishing Group. https://doi.org/10.1038/cr.2016.86

Lord, J. D., McIntosh, B. C., Greenberg, P. D., & Nelson, B. H. (2000). The IL-2 Receptor Promotes Lymphocyte Proliferation and Induction of the c- myc, bcl-2, and bcl-x Genes Through the trans- Activation Domain of Stat5. *The Journal of Immunology*, *164*(5), 2533–2541. https://doi.org/10.4049/jimmunol.164.5.2533

Maia, A. F., Feijão, T., Vromans, M. J. M., Sunkel, C. E., & Lens, S. M. A. (2010). Aurora B kinase cooperates with CENP-E to promote timely anaphase onset. *Chromosoma*, *119*(4), 405–413. https://doi.org/10.1007/s00412-010-0265-x

Mandal, M., Powers, S. E., Maienschein-Cline, M., Bartom, E. T., Hamel, K. M., Kee, B. L., Dinner, A. R., & Clark, M. R. (2011). Epigenetic repression of the Igk locus by STAT5-mediated recruitment of the histone methyltransferase Ezh2. *Nature*

Immunology, *12*(12), 1212–1220. https://doi.org/10.1038/ni.2136

Mao, Y., Abrieu, A., & Cleveland, D. W. (2003). Activating and silencing the mitotic checkpoint through CENP-E-dependent activation/inactivation of BubR1. *Cell*, *114*(1), 87–98. https://doi.org/10.1016/S0092-8674(03)00475-6

Mao, Y., Desai, A., & Cleveland, D. W. (2005). Microtubule capture by CENP-E silences BubR1-dependent mitotic checkpoint signaling. *Journal of Cell Biology*, *170*(6), 873–880. https://doi.org/10.1083/jcb.200505040

Maurer, B., Nivarthi, H., Wingelhofer, B., Pham, H. T. T., Schlederer, M., Suske, T., Grausenburger, R., Schiefer, A. I., Prchal-Murphy, M., Chen, D., Winkler, S., Merkel, O., Kornauth, C., Hofbauer, M., Hochgatterer, B., Hoermann, G., Hoelbl-Kovacic, A., Prochazkova, J., Lobello, C., … Moriggl, R. (2020). High activation of STAT5A drives peripheral T-cell lymphoma and leukemia. *Haematologica*, *105*(2), 435–447. https://doi.org/10.3324/haematol.2019.216986

Mikita, T., Daniel, C., Wu, P., & Schindler, U. (1998). Mutational analysis of the STAT6 SH2 domain. *Journal of Biological Chemistry*, *273*(28), 17634–17642. https://doi.org/10.1074/jbc.273.28.17634

Min, X., Ungureanu, D., Maxwell, S., Hammarén, H., Thibault, S., Hillert, E. K., Ayres, M., Greenfield, B., Eksterowicz, J., Gabel, C., Walker, N., Silvennoinen, O., & Wang, Z. (2015). Structural and functional characterization of the JH2 pseudokinase domain of JAK family tyrosine kinase 2 (TYK2). *Journal of Biological Chemistry*, *290*(45), 27261–27270. https://doi.org/10.1074/jbc.M115.672048

Mitchell, T. J., & John, S. (2005). Signal transducer and activator of transcription (STAT) signalling and T-cell lymphomas. In *Immunology* (Vol. 114, Issue 3, pp. 301–312). Wiley-Blackwell. https://doi.org/10.1111/j.1365-2567.2005.02091.x

Miyazaki, T., Kawahara, A., Fujii, H., Nakagawa, Y., Minami, Y., Liu, Z. J., Oishi, I., Silvennoinen, O., Witthuhn, B. A., Ihle, J. N., & Taniguchi, T. (1994). Functional activation of Jak1 and Jak3 by selective association with IL-2 receptor subunits. *Science*, *266*(5187), 1045–1047. https://doi.org/10.1126/science.7973659

Möricke, A., Zimmermann, M., Valsecchi, M. G., Stanulla, M., Biondi, A., Mann, G., Locatelli, F., Cazzaniga, G., Niggli, F., Aricò, M., Bartram, C. R., Attarbaschi, A., Silvestri, D., Beier, R., Basso, G., Ratei, R., Kulozik, A. E., Lo Nigro, L., Kremens, B., … Schrappe, M. (2016). Dexamethasone vs prednisone in induction treatment of pediatric ALL: results of the randomized trial AIEOP-BFM ALL 2000.

Blood, *127*(17), 2101–2112. https://doi.org/10.1182/blood-2015-09-670729

Moriggl, R., Sexl, V., Kenner, L., Duntsch, C., Stangl, K., Gingras, S., Hoffmeyer, A., Bauer, A., Piekorz, R., Wang, D., Bunting, K. D., Wagner, E. F., Sonneck, K., Valent, P., Ihle, J. N., & Beug, H. (2005). Stat5 tetramer formation is associated with leukemogenesis. *Cancer Cell*, *7*(1), 87–99. https://doi.org/10.1016/j.ccr.2004.12.010

Moriggl, R., Topham, D. J., Teglund, S., Sexl, V., McKay, C., Wang, D., Hoffmeyer, A., Van Deursen, J., Sangster, M. Y., Bunting, K. D., Grosveld, G. C., & Ihle, J. N. (1999). Stat5 is required for IL-2-induced cell cycle progression of peripheral T cells. *Immunity*, *10*(2), 249–259. https://doi.org/10.1016/S1074-7613(00)80025-4

Mukhopadhyay, U. K., Cass, J., Raptis, L., Craig, A. W., Bourdeau, V., Varma, S., SenGupta, S., Elliott, B. E., & Ferbeyre, G. (2016). STAT5A is regulated by DNA damage via the tumor suppressor p53. *Cytokine*, *82*, 70–79. https://doi.org/10.1016/j.cyto.2016.01.013

Nakao, M., Yokota, S., Iwai, T., Kaneko, H., Horiike, S., Kashima, K., Sonoda, Y., Fujimoto, T., & Misawa, S. (1996). Internal tandem duplication of the flt3 gene found in acute myeloid leukemia. *Leukemia*, *10*(12), 1911–1918. https://europepmc.org/article/med/8946930/reload=0

Nicolae, A., Xi, L., Pittaluga, S., Abdullaev, Z., Pack, S., Chen, J., Waldmann, T., Jaffe, E., & Raffeld, M. (2014). Frequent STAT5B mutations in γδ hepatosplenic T-cell lymphomas. *Leukemia*, *28*(11), 2244–2248. https://doi.org/10.1038/leu.2014.200.

Nosaka, T., Kawashima, T., Misawa, K., Ikuta, K., Mui, A. L. F., & Kitamura, T. (1999). STAT5 as a molecular regulator of proliferation, differentiation and apoptosis in hematopoietic cells. *EMBO Journal*, *18*(17), 4754–4765. https://doi.org/10.1093/emboj/18.17.4754

Nozais, M., Loosveld, M., Pankaew, S., Grosjean, C., Gentil, N., Quessada, J., Nadel, B., Mionnet, C., Potier, D., & Payet-Bornet, D. (2021). MYC deficiency impairs the development of effector/memory T lymphocytes. *IScience*, *24*(7), 102761. https://doi.org/10.1016/j.isci.2021.102761

Onishi, M., Nosaka, T., Misawa, K., Mui, A. L.-F., Gorman, D., McMahon, M., Miyajima, A., & Kitamura, T. (1998). Identification and Characterization of a Constitutively Active STAT5 Mutant That Promotes Cell Proliferation. *Molecular*

and Cellular Biology, *18*(7), 3871–3879. https://doi.org/10.1128/MCB.18.7.3871

Palomero, T., Wei, K. L., Odom, D. T., Sulis, M. L., Real, P. J., Margolin, A., Barnes, K. C., O'Neil, J., Neuberg, D., Weng, A. P., Aster, J. C., Sigaux, F., Soulier, J., Look, A. T., Young, R. A., Califano, A., & Ferrando, A. A. (2006). NOTCH1 directly regulates c-MYC and activates a feed-forward-loop transcriptional network promoting leukemic cell growth. *Proceedings of the National Academy of Sciences of the United States of America*, *103*(48), 18261–18266. https://doi.org/10.1073/pnas.0606108103

Pham, H. T. T., Maurer, B., Prchal-Murphy, M., Grausenburger, R., Grundschober, E., Javaheri, T., Nivarthi, H., Boersma, A., Kolbe, T., Elabd, M., Halbritter, F., Pencik, J., Kazemi, Z., Grebien, F., Hengstschläger, M., Kenner, L., Kubicek, S., Farlik, M., Bock, C., … Moriggl, R. (2018). STAT5B N642H is a driver mutation for T cell neoplasia. *Journal of Clinical Investigation*, *128*(1), 387–401. https://doi.org/10.1172/JCI94509

Pinz, S., Unser, S., & Rascle, A. (2016). Signal transducer and activator of transcription STAT5 is recruited to c-Myc super-enhancer. *BMC Molecular Biology*, *17*(1). https://doi.org/10.1186/s12867-016-0063-y

Power, D. G., & Kemeny, N. E. (2009). The role of floxuridine in metastatic liver disease. *Molecular Cancer Therapeutics*, *8*(5), 1015–1025. https://doi.org/10.1158/1535-7163.MCT-08-0709

Proietti, L., Manhart, G., Heyes, E., Troester, S., & Grebien, F. (2022). Arrayed CRISPR/Cas9 Screening for the Functional Validation of Cancer Genetic Dependencies. *BIO-PROTOCOL*, *12*(24), 1–15. https://doi.org/10.21769/BioProtoc.4577

Qi, W., Chan, H. M., Teng, L., Li, L., Chuai, S., Zhang, R., Zeng, J., Li, M., Fan, H., Lin, Y., Gu, J., Ardayfio, O., Zhang, J. H., Yan, X., Fang, J., Mi, Y., Zhang, M., Zhou, T., Feng, G., … Li, E. (2012). Selective inhibition of Ezh2 by a small molecule inhibitor blocks tumor cells proliferation. *Proceedings of the National Academy of Sciences of the United States of America*, *109*(52), 21360–21365. https://doi.org/10.1073/pnas.1210371110

Raetz, E. A., & Teachey, D. T. (2016). T-cell acute lymphoblastic leukemia. *Hematology (United States)*, *2016*(1), 580–588. https://doi.org/10.1182/asheducation-2016.1.580

Rajala, H. L. M., Eldfors, S., Kuusanmäki, H., van Adrichem, A. J., Olson, T.,

Lagström, S., Andersson, E. I., Jerez, A., Clemente, M. J., Yan, Y., Zhang, D., Awwad, A., Ellonen, P., Kallioniemi, O., Wennerberg, K., Porkka, K., Maciejewski, J. P., Loughran, T. P., Heckman, C., & Mustjoki, S. (2013). Discovery of somatic STAT5b mutations in large granular lymphocytic leukemia. *Blood*, *121*(22), 4541–4550. https://doi.org/10.1182/blood-2012-12-474577

Rane, S. G., & Reddy, E. P. (2000). Janus kinases: Components of multiple signaling pathways. *Oncogene*, *19*(49), 5662–5679. https://doi.org/10.1038/sj.onc.1203925

Rauch, A., Hennig, D., Schäfer, C., Wirth, M., Marx, C., Heinzel, T., Schneider, G., & Krämer, O. H. (2014). Survivin and YM155: How faithful is the liaison? In *Biochimica et Biophysica Acta - Reviews on Cancer* (Vol. 1845, Issue 2, pp. 202–220). Elsevier. https://doi.org/10.1016/j.bbcan.2014.01.003

Rawlings, J. S., Rosler, K. M., & Harrison, D. A. (2004). The JAK/STAT signaling pathway. *Journal of Cell Science*, *117*(Pt 8), 1281–1283. https://doi.org/10.1242/JCS.00963

Ren, Z., Aerts, J. L., Vandenplas, H., Wang, J. A., Gorbenko, O., Chen, J. P., Giron, P., Heirman, C., Goyvaerts, C., Zacksenhaus, E., Minden, M. D., Stambolic, V., Breckpot, K., & De Grève, J. (2016). Phosphorylated STAT5 regulates p53 expression via BRCA1/BARD1-NPM1 and MDM2. *Cell Death and Disease*, *7*(12), e2560–e2560. https://doi.org/10.1038/cddis.2016.430

Ross, S. H., & Cantrell, D. A. (2018). Signaling and Function of Interleukin-2 in T Lymphocytes. *Annual Review of Immunology*, *36*, 411–433. https://doi.org/10.1146/annurev-immunol-042617-053352

Russell, S. M., Johnston, J. A., Noguchi, M., Kawamura, M., Bacon, C. M., Friedmann, M., Berg, M., McVicar, D. W., Witthuhn, B. A., Silvennoinen, O., Goldman, A. S., Schmalstieg, F. C., Ihle, J. N., O'Shea, J. J., & Leonard, W. J. (1994). Interaction of IL-2R beta and gamma c chains with Jak1 and Jak3: implications for XSCID and XCID. *Science (New York, N.Y.)*, *266*(5187), 1042–1045. https://doi.org/10.1126/SCIENCE.7973658

Ryser, S., Dizin, E., Jefford, C. E., Delaval, B., Gagos, S., Christodoulidou, A., Krause, K.-H., Birnbaum, D., & Irminger-Finger, I. (2009). Distinct roles of BARD1 isoforms in mitosis: full-length BARD1 mediates Aurora B degradation, cancer-associated BARD1beta scaffolds Aurora B and BRCA2. *Cancer Research*, *69*(3), 1125–1134. https://doi.org/10.1158/0008-5472.CAN-08-2134

Saharinen, P., Takaluoma, K., & Silvennoinen, O. (2000). Regulation of the Jak2 tyrosine kinase by its pseudokinase domain. *Molecular and Cellular Biology*, *20*(10), 3387–3395. https://doi.org/10.1128/MCB.20.10.3387-3395.2000

Sato, K., Sundaramoorthy, E., Rajendra, E., Hattori, H., Jeyasekharan, A. D., Ayoub, N., Schiess, R., Aebersold, R., Nishikawa, H., Sedukhina, A. S., Wada, H., Ohta, T., & Venkitaraman, A. R. (2012). A DNA-damage selective role for BRCA1 E3 ligase in claspin ubiquitylation, CHK1 activation, and DNA repair. *Current Biology*, *22*(18), 1659–1666. https://doi.org/10.1016/j.cub.2012.07.034

Schaller-Schönitz, M., Barzan, D., Williamson, A. J. K., Griffiths, J. R., Dallmann, I., Battmer, K., Ganser, A., Whetton, A. D., Scherr, M., & Eder, M. (2014). BCR-ABL affects STAT5A and STAT5B differentially. *PLoS ONE*, *9*(5), e97243. https://doi.org/10.1371/journal.pone.0097243

Schiff, P. B., & Horwitz, S. B. (1980). Taxol stabilizes microtubules in mouse fibroblast cells. *Proceedings of the National Academy of Sciences of the United States of America*, *77*(3 I), 1561–1565. https://doi.org/10.1073/pnas.77.3.1561

Scully, R., Chen, J., Ochs, R. L., Keegan, K., Hoekstra, M., Feunteun, J., & Livingston, D. M. (1997). Dynamic changes of BRCA1 subnuclear location and phosphorylation state are initiated by DNA damage. *Cell*, *90*(3), 425–435. https://doi.org/10.1016/S0092-8674(00)80503-6

Sen, M., Thomas, S. M., Kim, S., Yeh, J. I., Ferris, R. L., Johnson, J. T., Duvvuri, U., Lee, J., Sahu, N., Joyce, S., Freilino, M. L., Shi, H., Li, C., Ly, D., Rapireddy, S., Etter, J. P., Li, P.-K., Wang, L., Chiosea, S., … Grandis, J. R. (2012). First-in-Human Trial of a STAT3 Decoy Oligonucleotide in Head and Neck Tumors: Implications for Cancer Therapy. *Cancer Discovery*, *2*(8), 694–705. https://doi.org/10.1158/2159-8290.CD-12-0191

Shahmarvand, N., Nagy, A., Shahryari, J., & Ohgami, R. S. (2018). Mutations in the signal transducer and activator of transcription family of genes in cancer. *Cancer Science*, *109*(4), 926–933. https://doi.org/10.1111/cas.13525

Shalem, O., Sanjana, N. E., Hartenian, E., Shi, X., Scott, D. A., Mikkelsen, T. S., Heckl, D., Ebert, B. L., Root, D. E., Doench, J. G., & Zhang, F. (2014). Genome-Scale CRISPR-Cas9 Knockout Screening in Human Cells. *Science*, *343*(6166), 84–87. https://doi.org/10.1126/science.1247005

Shiraz, P., Jehangir, W., & Agrawal, V. (2021). T-cell acute lymphoblastic leukemia—current concepts in molecular biology and management. In *Biomedicines* (Vol.

9, Issue 11). Multidisciplinary Digital Publishing Institute (MDPI). https://doi.org/10.3390/biomedicines9111621

Suske, T., Sorger, H., Ruge, F., Prutsch, N., Zimmerman, M. W., Eder, T., Maurer, B., Wagner, C., Schönefeldt, S., Spirk, K., Pichler, A., Pemovska, T., Schweicker, C., Pölöske, D., Jungherz, D., Müller, T. A., Aung, M. M. K., Pham, H. T. T., Zimmel, K., … Moriggl, R. (2022). STAT5 Gain-of-Function Variants Promote Precursor T-Cell Receptor Activation to Drive T-Cell Acute Lymphoblastic Leukemia. *BioRxiv*, *13*, 2022.12.21.519945. https://doi.org/10.1101/2022.12.21.519945

Tanaka, T. U., Rachidi, N., Janke, C., Pereira, G., Galova, M., Schiebel, E., Stark, M. J. R., & Nasmyth, K. (2002). Evidence that the Ipl1-Sli15 (Aurora Kinase-INCENP) complex promotes chromosome bi-orientation by altering kinetochore-spindle pole connections. *Cell*, *108*(3), 317–329. https://doi.org/10.1016/S0092-8674(02)00633-5

Udy, G. B., Towers, R. P., Snell, R. G., Wilkins, R. J., Park, S. H., Ram, P. A., Waxman, D. J., & Davey, H. W. (1997). Requirement of STAT5b for sexual dimorphism of body growth rates and liver gene expression. *Proceedings of the National Academy of Sciences of the United States of America*, *94*(14), 7239–7244. https://doi.org/10.1073/pnas.94.14.7239

Ungureanu, D., Wu, J., Pekkala, T., Niranjan, Y., Young, C., Jensen, O. N., Xu, C. F., Neubert, T. A., Skoda, R. C., Hubbard, S. R., & Silvennoinen, O. (2011). The pseudokinase domain of JAK2 is a dual-specificity protein kinase that negatively regulates cytokine signaling. *Nature Structural and Molecular Biology*, *18*(9), 971–976. https://doi.org/10.1038/nsmb.2099

Vainchenker, W., & Constantinescu, S. N. (2013). JAK/STAT signaling in hematological malignancies. In *Oncogene* (Vol. 32, Issue 21, pp. 2601–2613). Nature Publishing Group. https://doi.org/10.1038/onc.2012.347

Van Vlierberghe, P., & Ferrando, A. (2012). The molecular basis of T cell acute lymphoblastic leukemia. *Journal of Clinical Investigation*, *122*(10), 3398–3406. https://doi.org/10.1172/JCI61269

Varghese, M. T., & Alsubait, S. (2022, November 7). *T-Cell Lymphoma*. StatPearls; StatPearls Publishing. https://www.ncbi.nlm.nih.gov/books/NBK564354/

Vicente, C., Schwab, C., Broux, M., Geerdens, E., Degryse, S., Demeyer, S., Lahortiga, I., Elliott, A., Chilton, L., La Starza, R., Mecucci, C., Vandenberghe,

P., Goulden, N., Vora, A., Moorman, A. V., Soulier, J., Harrison, C. J., Clappier, E., & Cools, J. (2015). Targeted sequencing identifies associations between IL7R-JAK mutations and epigenetic modulators in T-cell acute lymphoblastic leukemia. *Haematologica*, *100*(10), 1301–1310. https://doi.org/10.3324/haematol.2015.130179

Villarino, A., Laurence, A., Robinson, G. W., Bonelli, M., Dema, B., Afzali, B., Shih, H. Y., Sun, H. W., Brooks, S. R., Hennighausen, L., Kanno, Y., & O'Shea, J. J. (2016). Signal transducer and activator of transcription 5 (STAT5) paralog dose governs T cell effector and regulatory functions. *ELife*, *5*(MARCH2016). https://doi.org/10.7554/eLife.08384

Wang, D., Stravopodis, D., Teglund, S., Kitazawa, J., & Ihle, J. N. (1996). Naturally occurring dominant negative variants of Stat5. *Molecular and Cellular Biology*, *16*(11), 6141–6148. https://doi.org/10.1128/mcb.16.11.6141

Wang, R., Dillon, C. P., Shi, L. Z., Milasta, S., Carter, R., Finkelstein, D., McCormick, L. L., Fitzgerald, P., Chi, H., Munger, J., & Green, D. R. (2011). The transcription factor Myc controls metabolic reprogramming upon T lymphocyte activation. *Immunity*, *35*(6), 871. https://doi.org/10.1016/J.IMMUNI.2011.09.021

Warsch, W., Grundschober, E., Berger, A., Gille, L., Cerny-Reiterer, S., Tigan, A. S., Hoelbl-Kovacic, A., Valent, P., Moriggl, R., & Sexl, V. (2012). STAT5 triggers BCR-ABL1 mutation by mediating ROS production in chronic myeloid leukaemia. *Oncotarget*, *3*(12), 1669–1687. https://doi.org/10.18632/oncotarget.806

Waters, J. C., Chen, R. H., Murray, A. W., & Salmon, E. D. (1998). Localization of Mad2 to kinetochores depends on microtubule attachment, not tension. *Journal of Cell Biology*, *141*(5), 1181–1191. https://doi.org/10.1083/jcb.141.5.1181

Weaver, B. A. (2014). How Taxol/paclitaxel kills cancer cells. *Molecular Biology of the Cell*, *25*(18), 2677. https://doi.org/10.1091/MBC.E14-04-0916

Wen, Z., Zhong, Z., & Darnell, J. E. (1995). Maximal activation of transcription by statl and stat3 requires both tyrosine and serine phosphorylation. *Cell*, *82*(2), 241–250. https://doi.org/10.1016/0092-8674(95)90311-9

Weng, A. P., Ferrando, A. A., Lee, W., Morris IV, J. P., Silverman, L. B., Sanchez-Irizarry, C., Blacklow, S. C., Look, A. T., & Aster, J. C. (2004). Activating mutations of NOTCH1 in human T cell acute lymphoblastic leukemia. *Science*, *306*(5694), 269–271. https://doi.org/10.1126/SCIENCE.1102160/SUPPL_FILE/WENG_SOM.PDF

Westermark, U. K., Reyngold, M., Olshen, A. B., Baer, R., Jasin, M., & Moynahan, M. E. (2003). BARD1 participates with BRCA1 in homology-directed repair of chromosome breaks. *Molecular and Cellular Biology*, *23*(21), 7926–7936. https://doi.org/10.1128/MCB.23.21.7926-7936.2003

Wheatley, S. P., & Altieri, D. C. (2019). Survivin at a glance. *Journal of Cell Science*, *132*(7). https://doi.org/10.1242/jcs.223826

Wilson, A., Murphy, M. J., Oskarsson, T., Kaloulis, K., Bettess, M. D., Oser, G. M., Pasche, A. C., Knabenhans, C., MacDonald, H. R., & Trumpp, A. (2004). c-Myc controls the balance between hematopoietic stem cell self-renewal and differentiation. *Genes & Development*, *18*(22), 2747–2763. https://doi.org/10.1101/GAD.313104

Wilson, W. H., O'Connor, O. A., Czuczman, M. S., LaCasce, A. S., Gerecitano, J. F., Leonard, J. P., Tulpule, A., Dunleavy, K., Xiong, H., Chiu, Y. L., Cui, Y., Busman, T., Elmore, S. W., Rosenberg, S. H., Krivoshik, A. P., Enschede, S. H., & Humerickhouse, R. A. (2010). Navitoclax, a targeted high-affinity inhibitor of BCL-2, in lymphoid malignancies: A phase 1 dose-escalation study of safety, pharmacokinetics, pharmacodynamics, and antitumour activity. *The Lancet Oncology*, *11*(12), 1149–1159. https://doi.org/10.1016/S1470-2045(10)70261-8

Wu, L. C., Wang, Z. W., Tsan, J. T., Spillman, M. A., Phung, A., Xu, X. L., Yang, M. C. W., Hwang, L. Y., Bowcock, A. M., & Baer, R. (1996). Identification of a RING protein that can interact in vivo with the BRCA1 gene product. *Nature Genetics*, *14*(4), 430–440. https://doi.org/10.1038/ng1296-430

Yan, J., Li, B., Lin, B., Lee, P. T., Chung, T. H., Tan, J., Bi, C., Lee, X. T., Selvarajan, V., Ng, S. B., Yang, H., Yu, Q., & Chng, W. J. (2016). EZH2 phosphorylation by JAK3 mediates a switch to noncanonical function in natural killer/T-cell lymphoma. *Blood*, *128*(7), 948–958. https://doi.org/10.1182/blood-2016-01-690701

Yang, J., Ikezoe, T., Nishioka, C., Tasaka, T., Taniguchi, A., Kuwayama, Y., Komatsu, N., Bandobashi, K., Togitani, K., Koeffler, H. P., Taguchi, H., & Yokoyama, A. (2007). AZD1152, a novel and selective aurora B kinase inhibitor, induces growth arrest, apoptosis, and sensitization for tubulin depolymerizing agent or topoisomerase II inhibitor in human acute leukemia cells in vitro and in vivo. *Blood*, *110*(6), 2034–2040. https://doi.org/10.1182/blood-2007-02-073700

Yarden, R. I., Pardo-Reoyo, S., Sgagias, M., Cowan, K. H., & Brody, L. C. (2002).

BRCA1 regulates the G2/M checkpoint by activating Chk1 kinase upon DNA damage. *Nature Genetics*, *30*(3), 285–289. https://doi.org/10.1038/ng837

Yasui, Y., Urano, T., Kawajiri, A., Nagata, K. I., Tatsuka, M., Saya, H., Furukawa, K., Takahashi, T., Izawa, I., & Inagaki, M. (2004). Autophosphorylation of a Newly Identified Site of Aurora-B Is Indispensable for Cytokinesis. *Journal of Biological Chemistry*, *279*(13), 12997–13003. https://doi.org/10.1074/jbc.M311128200

Yen, T. J., Compton, D. A., Wise, D., Zinkowski, R. P., Brinkley, B. R., Earnshaw, W. C., & Cleveland, D. W. (1991). CENP-E, a novel human centromere-associated protein required for progression from metaphase to anaphase. *EMBO Journal*, *10*(5), 1245–1254. https://doi.org/10.1002/j.1460-2075.1991.tb08066.x

Yoo, K. H., Oh, S., Kang, K., Hensel, T., Robinson, G. W., & Hennighausen, L. (2015). Loss of EZH2 results in precocious mammary gland development and activation of STAT5-dependent genes. *Nucleic Acids Research*, *43*(18), 8774–8789. https://doi.org/10.1093/nar/gkv776

Yu, C. L., Jin, Y. J., & Burakoff, S. J. (2000). Cytosolic tyrosine dephosphorylation of STAT5. Potential role of SHP-2 in STAT5 regulation. *Journal of Biological Chemistry*, *275*(1), 599–604. https://doi.org/10.1074/jbc.275.1.599

Yu, H., & Jove, R. (2004). The STATs of cancer — new molecular targets come of age. *Nature Reviews Cancer 2004 4:2*, *4*(2), 97–105. https://doi.org/10.1038/nrc1275

Zachos, G., Black, E. J., Walker, M., Scott, M. T., Vagnarelli, P., Earnshaw, W. C., & Gillespie, D. A. F. (2007). Chk1 Is Required for Spindle Checkpoint Function. *Developmental Cell*, *12*(2), 247–260. https://doi.org/10.1016/j.devcel.2007.01.003

Zhang, H., Nimmer, P. M., Tahir, S. K., Chen, J., Fryer, R. M., Hahn, K. R., Iciek, L. A., Morgan, S. J., Nasarre, M. C., Nelson, R., Preusser, L. C., Reinhart, G. A., Smith, M. L., Rosenberg, S. H., Elmore, S. W., & Tse, C. (2007). Bcl-2 family proteins are essential for platelet survival. *Cell Death and Differentiation*, *14*(5), 943–951. https://doi.org/10.1038/sj.cdd.4402081

Zhao, H., & Piwnica-Worms, H. (2001). ATR-Mediated Checkpoint Pathways Regulate Phosphorylation and Activation of Human Chk1. *Molecular and Cellular Biology*, *21*(13), 4129–4139. https://doi.org/10.1128/mcb.21.13.4129-4139.2001

Zou, S., Tong, Q., Liu, B., Huang, W., Tian, Y., & Fu, X. (2020). Targeting STAT3 in Cancer Immunotherapy. *Molecular Cancer 2020 19:1*, *19*(1), 1–19.

https://doi.org/10.1186/S12943-020-01258-7

6 Supplementary

Table 11: *sgRNAs used for the CRISPR/Cas9 screen (designed by Christina Wagner and provided by IDT).*

Gene	Name	Sequence (5' – 3')
ALYREF	ALYREF_1_f	CAC CGT GAA TTT GGA ACG CTG AAG A
	ALYREF_1_r	AAA CTC TTC AGC GTT CCA AAT TCA C
	ALYREF_2_f	CAC CGT GAC AAG CTG AAT GTT CAT G
	ALYREF_2_r	AAA CCA TGA ACA TTC AGC TTG TCA C
BCL2L1	BCL2L1_1_f	CAC CGC AGG CGA CGA GTT TGA ACT G
	BCL2L1_1_r	AAA CCA GTT CAA ACT CGT CGC CTG C
	BUB1_2_f	CAC CGG AAA CTC AAA AAA TTG ATG G
	BUB1_2_r	AAA CCC ATC AAT TTT TTG AGT TTC C
BUB1	BUB1_1_f	CAC CGC GCC CAG GCA ATG TAC AGA G
	BUB1_1_r	AAA CCT CTG TAC ATT GCC TGG GCG C
	BUB1_2_f	CAC CGG AAA CTC AAA AAA TTG ATG G
	BUB1_2_r	CAC CGG AAA CTC AAA AAA TTG ATG G
CDC6	CDC6_1_f	CAC CGA TAG CGT GTA CAA TAC ATC C
	CDC6_1_r	AAA CGG ATG TAT TGT ACA CGC TAT C
	CDC6_2_f	CAC CGA ATA GCT GGG AAT ACA GCC T
	CDC6_2_r	AAA CAG GCT GTA TTC CCA GCT ATT C
CENPW	CENPW_1_f	CAC CGA TAA AGC GGA AGG CTC CCC G
	CENPW_1_r	AAA CCG GGG AGC CTT CCG CTT TAT C
	CENPW_2_f	CAC CGA CTC GCT TTA GAA AGC CAC G
	CENPW_2_r	AAA CCG TGG CTT TCT AAA GCG AGT C
E2F2	E2F1_1_f	CAC CGA AGG TCC TGA CAC GTC ACG T
	E2F1_1_r	AAA CAC GTG ACG TGT CAG GAC CTT C
	E2F1_2_f	CAC CGG ACA TCA CCA ACG TCC TTG A
	E2F1_2_r	AAA CCA GTG TAG TTG TTC GAG ATA C
KPNB1	KPNB1_1_f	CAC CGA GCT CCT AGA GAC TAC AGA C
	KPNB1_1_r	AAA CGT CTG TAG TCT CTA GGA GCT C

	KPNB1_2_f	CAC CGT ATC TCG AAC AAC TAC ACT G
	KPNB1_2_r	AAA CCA GTG TAG TTG TTC GAG ATA C
MYC	MYC_1_f	CAC CGG AAG GGT GTG ACC GCA ACG T
	MYC_1_r	AAA CAC GTT GCG GTC ACA CCC TTC C
	MYC_2_f	CAC CGC GAG GGG TCG ATG CAC TCT G
	MYC_2_r	AAA CCA GAG TGC ATC GAC CCC TCG C
NUP37	NUP37_1_f	CAC CGT GCC ATT AAT GTC AGC ACA C
	NUP37_1_r	AAA CGT GTG CTG ACA TTA ATG GCA C
	NUP37_2_f	CAC CGT GAG TGA CGA TCA CAC CTG C
	NUP37_2_r	AAA CGC AGG TGT GAT CGT CAC TCA C
PSMA5	PSMA5_1_f	CAC CGG TAG AGA TTG ATG CTC ACA T
	PSMA5_1_r	AAA CAT GTG AGC ATC AAT CTC TAC C
	PSMA5_2_f	CAC CGT GAG TGA CGA TCA CAC CTG C
	PSMA5_2_r	AAA CCA ATG TTT GTT GCA TTC AGC C
RMI2	RMI2_1_f	CAC CGT GGA GGT AGA AGA TTT ACA C
	RMI2_1_r	AAA CGT GTA AAT CTT CTA CCT CCA C
	RMI2_2_f	CAC CGG CAT TAC CTG GGA CTA GAC A
	RMI2_2_r	AAA CTG TCT AGT CCC AGG TAA TGC C
TYMS	TYMS_1_f	CAC CGC GAT GTT GAA AGG CAC ACC G
	TYMS_1_r	AAA CCG GTG TGC CTT TCA ACA TCG C
	TYMS_2_f	CAC CGT GCC CTC TGC CAG TTC TAT G
	TYMS_2_r	AAA CCA TAG AAC TGG CAG AGG GCA C
APEX1	APEX1_1_f	CAC CGT GCC GTA AGA AAC TTT GAG T
	APEX1_1_r	AAA CAC TCA AAG TTT CTT ACG GCA C
	APEX1_2_f	CAC CGT TGA AGG CAC AGT ATA TCT G
	APEX1_2_r	AAA CCA GAT ATA CTG TGC CTT CAA C
BIRC5	BIRC5_1_f	CAC CGG GGC AGT CTC ACC CGC TCC G
	BIRC5_1_r	AAA CCG GAG CGG GTG AGA CTG CCC C
	BIRC5_2_f	CAC CGA GTT CTT GAA TGT AGA GAT G
	BIRC5_2_r	AAA CCA TCT CTA CAT TCA AGA ACT C
BUD31	BUD31_1_f	CAC CGA GAG GAA AGT GGA ATC TCT G

	BUD31_1_r	AAA CCA GAG ATT CCA CTT TCC TCT C
	BUD31_2_f	CAC CGA AAG AGG TCG AAG ATG TAG C
	BUD31_2_r	AAA CGC TAC ATC TTC GAC CTC TTT C
CDC7	CDC7_1_f	CAC CGT GAA CTT CAG TGC CTA ACA G
	CDC7_1_r	AAA CCT GTT AGG CAC TGA AGT TCA C
	CDC7_2_f	CAC CGG GCC AAA CCA AAG TCT ACC A
	CDC7_2_r	AAA CTG GTA GAC TTT GGT TTG GCC C
CHAF1B	CHAF1B_1_f	CAC CGG CTG AAC AAG GAG AAC TGG A
	CHAF1B_1_r	AAA CTC CAG TTC TCC TTG TTC AGC C
	CHAF1B_2_f	CAC CGG ATG GCT GTG TTA TCC ACA G
	CHAF1B_2_r	AAA CCT GTG GAT AAC ACA GCC ATC C
FEN1	FEN1_1_f	CAC CGG AAC TGA TAA ATG CTC ATA G
	FEN1_1_r	AAA CCT ATG AGC ATT TAT CAG TTC C
	FEN1_2_f	CAC CGT GAG GAG CGA ATC CGC AGT G
	FEN1_2_r	AAA CCA CTG CGG ATT CGC TCC TCA C
MCM4	MCM4_1_f	CAC CGG ATG TTC TAA GAT TGA GTC A
	MCM4_1_r	AAA CTG ACT CAA TCT TAG AAC ATC C
	MCM4_2_f	CAC CGG GTA TGC AGA AAC CAT TCC C
	MCM4_2_r	AAA CGG GAA TGG TTT CTG CAT ACC C
NDUFB6	NDUFB6_1_f	CAC CGG CTG AGA AGG CGA TGG CTG A
	NDUFB6_1_r	AAA CTC AGC CAT CGC CTT CTC AGC C
	NDUFB6_2_f	CAC CGT GCG AGA GCT GAG AAG GCG A
	NDUFB6_2_r	AAA CTC GCC TTC TCA GCT CTC GCA C
PSMB2	PSMB2_1_f	CAC CGA TGA TTC GAA CAC TGA AGG T
	PSMB2_1_r	AAA CAC CTT CAG TGT TCG AAT CAT C
	PSMB2_2_f	CAC CGG CTG TAT TAC ATG GAC TAC C
	PSMB2_2_r	AAA CGG TAG TCC ATG TAA TAC AGC C
RPM2	RRM2_1_f	CAC CGT GCA AAG AAA GCC AGA ACA T
	RRM2_1_r	AAA CAT GTT CTG GCT TTC TTT GCA C
	RRM2_2_f	CAC CGT GGC CAG CAA GAC CGC GAG G
	RRM2_2_r	AAA CCC TCG CGG TCT TGC TGG CCA C

UBE2N	UBE2N_1_f	CAC CGT TCT GTC TAC AGC TAG AGC A
	UBE2N_1_r	AAA CTG CTC TAG CTG TAG ACA GAA C
	UBE2N_2_f	CAC CGT GTG GTC ATT GCT GGC CCT C
	UBE2N_2_r	AAA CGA GGG CCA GCA ATG ACC ACA C
AURKB	AURKB_1_f	CAC CGA GGC CAC CAT ACC TCA GGG A
	AURKB_1_r	AAA CTC CCT GAG GTA TGG TGG CCT C
	AURKB_2_f	CAC CGC AGG CCA CCA TAC CTC AGG G
	AURKB_2_r	AAA CCC CTG AGG TAT GGT GGC CTG C
BLM	BLM_1_f	CAC CGA GTG ACC CCA GGA GAA ACA C
	BLM_1_r	AAA CGT GTT TCT CCT GGG GTC ACT C
	BLM_2_f	CAC CGG TAG TCA GTA AAC AGT CCC C
	BLM_2_r	AAA CGG GGA CTG TTT ACT GAC TAC C
CCNE2	CCNE2_1_f	CAC CGA GAA GTA TGG ACC TCA TCT G
	CCNE2_1_r	AAA CCA GAT GAG GTC CAT ACT TCT C
	CCNE2_2_f	CAC CGG TCC TGT AAC AAT CAT CTC C
	CCNE2_2_r	AAA CGG AGA TGA TTG TTA CAG GAC C
CENPE	CENPE_1_f	CAC CGG CCA CAG AGT AAA TCT GTA A
	CENPE_1_r	AAA CTT ACA GAT TTA CTC TGT GGC C
	CENPE_2_f	CAC CGT CAT TTG GGA GTT ATA CCC A
	CENPE_2_r	AAA CTG GGT ATA ACT CCC AAA TGA C
CHEK1	CHEK1_1_f	CAC CGT GGG ACT TGG TGC AAA CCC T
	CHEK1_1_r	AAA CAG GGT TTG CAC CAA GTC CCA C
	CHEK1_2_f	CAC CGT GGT ATT GGA ATA ACT CAC A
	CHEK1_2_r	AAA CTG TGA GTT ATT CCA ATA CCA C
HMGB1	HMGB1_1_f	CAC CGG ATA CTC ACG GAG GCC TCT T
	HMGB1_1_r	AAA CAA GAG GCC TCC GTG AGT ATC C
	HMGB1_2_f	CAC CGG GAG ATC CTA AGA AGC CGA G
	HMGB1_2_r	AAA CCT CGG CTT CTT AGG ATC TCC C
MCM5	MCM5_1_f	CAC CGG GAG CCC CCA AAG AGC AGG C
	MCM5_1_r	AAA CGC CTG CTC TTT GGG GGC TCC C
	MCM5_2_f	CAC CGG ATG CGA GAA GAT GAC CGT G

	MCM5_2_r	AAA CCA CGG TCA TCT TCT CGC ATC C
NEK6	NEK6_1_f	CAC CGA GGC CGA GGA CAG TTC AGC G
	NEK6_1_r	AAA CCG CTG AAC TGT CCT CGG CCT C
	NEK6_2_f	CAC CGG GCG AGG CAG GAC TGT GTC A
	NEK6_2_r	AAA CTG ACA CAG TCC TGC CTC GCC C
PCNA	PCNA_1_f	CAC CGA TGT CTG CAG ATG TAC CCC T
	PCNA_1_r	AAA CAG GGG TAC ATC TGC AGA CAT C
	PCNA_2_f	CAC CGA GTT GTA GAG TAT AAA ATT G
	PCNA_2_r	AAA CCA ATT TTA TAC TCT ACA ACT C
PSMD1	PSMD1_1_f	CAC CGG GGC AGC AGT AGA ATC ACT T
	PSMD1_1_r	AAA CAA GTG ATT CTA CTG CTG CCC C
	PSMD1_2_f	CAC CGA CAA CAA AGA GAC AAC ACT T
	PSMD1_2_r	AAA CAA GTG TTG TCT CTT TGT TGT C
STAT5B	STAT5B_1_f	CAC CGG TTC ATT GTA CAA TAT ATG G
	STAT5B_1_r	AAA CCC ATA TAT TGT ACA ATG AAC C
	STAT5B_2_f	CAC CGA GCA TTG TCC CAG AGA ACA G
	STAT5B_2_r	AAA CCT GTT CTC TGG GAC AAT GCT C
VEGFA	VEGFA_1_f	CAC CGG GAG GGC AGA ATC ATC ACG A
	VEGFA_1_r	AAA CTC GTG ATG ATT CTG CCC TCC C
	VEGFA_2_f	CAC CGA GCA CAA CAA ATG TGA ATG C
	VEGFA_2_r	AAA CGC ATT CAC ATT TGT TGT GCT C
BARD1	BARD1_1_f	CAC CGA GCT GCT GCG CTG CTC GCG T
	BARD1_1_r	AAA CAC GCG AGC AGC GCA GCA GCT C
	BARD1_2_f	CAC CGG TCG AGC GCG GCG CGA CTG T
	BARD1_2_r	AAA CAC AGT CGC GCC GCG CTC GAC C
BRACA1	BRCA1_1_f	CAC CGG CTG CAC AAC CAC AAT TGG G
	BRCA1_1_r	AAA CCC CAA TTG TGG TTG TGC AGC C
	BRCA1_2_f	CAC CGG TCA ATG GAA GAA ACC ACC A
	BRCA1_2_r	AAA CTG GTG GTT TCT TCC ATT GAC C
CDC25A	CDC25A_1_f	CAC CGA TAC GAG GGA GGC CAC ATC A
	CDC25A_1_f	AAA CTG ATG TGG CCT CCC TCG TAT C

	CDC25A_2_f	CAC CGC GAT ACC CAT ATG AAT ACG A
	CDC25A_2_f	AAA CTC GTA TTC ATA TGG GTA TCG C
CENPM	CENPM_1_f	CAC CGG GGG TGG GCA GTA ACA GGC G
	CENPM_1_r	AAA CCG CCT GTT ACT GCC CAC CCC C
	CENPM_2_f	CAC CGA ACA CGA TCA GGT CAA TTC G
	CENPM_2_r	AAA CCG AAT TGA CCT GAT CGT GTT C
KNTC1	KNTC1_1_f	CAC CGG ATG GAG GGA ATA AGC TCT G
	KNTC1_1_r	AAA CCA GAG CTT ATT CCC TCC ATC C
	KNTC1_2_f	CAC CGG TTG ACT ATA GAG AGT AAG C
	KNTC1_2_r	AAA CGC TTA CTC TCT ATA GTC AAC C
MTHFD2	MTHFD2_1_f	CAC CGG GGG CGC ATG AAC GTC CCG G
	MTHFD2_1_r	AAA CCC GGG ACG TTC ATG CGC CCC C
	MTHFD2_2_f	CAC CGG CTG GAA GGT CAA AAA ACG T
	MTHFD2_2_r	AAA CAC GTT TTT TGA CCT TCC AGC C
NUF2	NUF2_1_f	CAC CGG CTT TGG AGA AAT ACC ACG A
	NUF2_1_r	AAA CTC GTG GTA TTT CTC CAA AGC C
	NUF2_2_f	CAC CGT AGA AGC AAA ACG GAC AAG T
	NUF2_2_r	AAA CAC TTG TCC GTT TTG CTT CTA C
PHGDH	PHGDH_1_f	CAC CGG AAG GGG AAA TCT CTC ACG G
	PHGDH_1_r	AAA CCC GTG AGA GAT TTC CCC TTC C
	PHGDH_2_f	CAC CGA GTG CCG CAG AAC TCA CTT G
	PHGDH_2_r	AAA CCA AGT GAG TTC TGC GGC ACT C
RAD51	RAD51_1_f	CAC CGG TAG TCT GTT CTG TAA AGG G
	RAD51_1_r	AAA CCC CTT TAC AGA ACA GAC TAC C
	RAD51_2_f	CAC CGG TCG AGG TGA GCT TTC AGC C
	RAD51_2_r	AAA CGG CTG AAA GCT CAC CTC GAC C
TFDP1	TFDP1_1_f	CAC CGG GAC ACC GGA GTC TCC ACC C
	TFDP1_1_r	AAA CGG GTG GAG ACT CCG GTG TCC C
	TFDP1_2_f	CAC CGG CTC TGG AGC CAT ACG TGA C
	TFDP1_2_r	AAA CGT CAC GTA TGG CTC CAG AGC C
YBX1	YBX1_1_f	CAC CGG GAT CGG AGA GTG CTC CCG A

	YBX1_1_r	AAA CTC GGG AGC ACT CTC CGA TCC C
	YBX1_2_f	CAC CGG GAC CAT ACC TGC GGA ATC G
	YBX1_2_r	AAA CCG ATT CCG CAG GTA TGG TCC C
AAVS1		CTC CGG AAA GAG CAT CCT
RPL17		TAC CAT TCC GAC GTT ACA A

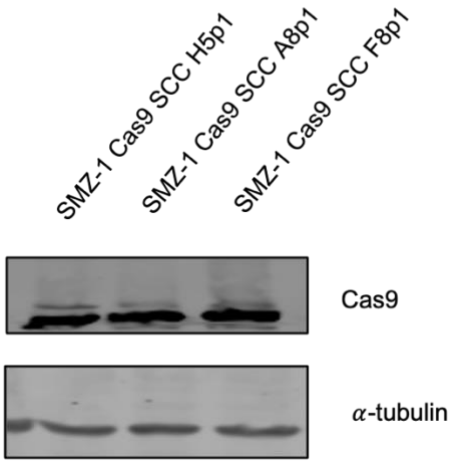

Figure 18: *Western blot analysis of SMZ-1 Cas9 SCC. The SCC show Cas9 expression. The Cas9 protein was detected by the Cas9 antibody and α −tubulin was used as loading control.*

7 Appendix

7.1 Table of figures

7.2 Table of tables

7.3 Abstract

T-cell acute lymphoblastic leukaemia (T-ALL) is a rare form of cancer and is found especially in children. T-ALL arises from the maturational arrest of precursor T-cells and their proliferation. The JAK3/STAT5-axis has an important role in the proliferation of T-cells and its deregulation is found in T-ALL patients. The gain of function (GOF) mutation *STAT5B*^{N642H} has been implicated with the hyperactivation of the protein, leading to CD8^{+} T-cell lymphoma and leukaemia in mouse models. We used a focused CRISPR/Cas9 loss-of-function screen to find hyperactive JAK/STAT-induced genes, essential for the oncogenicity of T-ALL. In parallel, we inhibited several of the encoded proteins with inhibitors. The results of the CRISPR/Cas9 screen and cytotoxicity assays were compared to find key dependencies. The screen and cytotoxicity assays were performed with the T-ALL cell line KOPT-K1 harbouring the STAT5B^{N642H} mutation. 46 target genes were covered in the CRISPR/Cas9 screen and 91 of 92 sgRNAs were successfully cloned. The functionality of Cas9-expression was determined in an initial screen with KOPT-K1 Cas9 single cell clones. The CRISPR/Cas9 screen revealed 18 of 46 target genes, whose knock-out led to strong cell depletion. Comparison with the results of the cytotoxicity assays verified five key dependencies – AURKB, BCL-xL, CHK1, PSMD1, and TS – in the T-ALL KOPT-K1 cell line. Additionally, the KOPT-K1 cell line was sensitive to inhibition of microtubule dynamics and DNA damage repair processes. Further validation is needed to determine the effects of protein inhibition on the remaining 13 target genes that were revealed during the CRISPR/Cas9 screen.

7.4 Zusammenfassung

Akute lymphoblastische T-Zell-Leukämie (T-ALL) ist eine seltene Krebsart und tritt insbesondere bei Kindern auf. T-ALL entsteht durch die Proliferation von Vorläufer-T-Zellen, deren Entwicklung vorläufig abgebrochen wurde. Der JAK3/STAT5 Signalweg spielt dabei eine wichtige Rolle, da er maßgeblich bei der Proliferation von T-Zellen beteiligt ist und daher kann eine Deregulierung zu Krankheit und Krebs führen. Die Gain-of-Function (GOF)-Mutation $STAT5B^{N642H}$ wurde mit der Hyperaktivierung des STAT5B-Proteins in Verbindung gebracht und führte in Mausmodellen zu CD8+ T-Zell-Lymphom und Leukämie. Wir haben einen fokussierten CRISPR/Cas9 loss-of-function Screen durchgeführt, um hyperaktive JAK/STAT-induzierte Gene zu finden, die für die Onkogenität von T-Zellen essenziell sind. Parallel dazu hemmten wir mehrere der codierten Proteine mit Inhibitoren. Die Ergebnisse des CRISPR/Cas9 Screens und der Cytotoxicity Assays wurden verglichen, um Abhängigkeiten aufzudecken. Der Screen und die Cytotoxicity Assays wurden mit der T-ALL-Zelllinie KOPT-K1 durchgeführt, die ein biallelische $STAT5B^{N642H}$-Mutation trägt. Der CRISPR/Cas9 Screen deckte 46 Zielgene ab und 91 der 92 sgRNAs wurden erfolgreich kloniert. Die Funktionalität des Cas9-Proteins wurde in einem ersten Screening mit zuvor generierten KOPT-K1 Cas9-Einzelzellklonen bestimmt. Der CRISPR/Cas9 Screen zeigte 18 von 46 Zielgenen auf, deren Knock-out zum Zelltod führte. Ein Vergleich mit den Ergebnissen der Cytotoxicity Assays bestätigte fünf Abhängigkeiten – AURKB, BCL-xL, CHK1, PSMD1, TS – in der T-ALL KOPT-K1-Zelllinie. Darüber hinaus war die KOPT-K1-Zelllinie empfindlich gegenüber der Hemmung von Mikrotubuli-Dynamik und DNA-Reparaturprozessen. Eine weitere Validierung ist erforderlich, um die Auswirkungen der Proteinhemmung der verbleibenden 13 Zielgene zu bestimmen, die während des CRISPR/Cas9 Screens aufgedeckt wurden.